Ph.D Dissertation

Organic sedimentological studies on the Miocene turbidites and Holocene paleotsunami deposits of Hokkaido, Japan

(北海道の新第三系タービダイトおよび古津波堆積物の有機堆積学的研究)

Hiroyasu Asahi

Department of Natural History Sciences, Graduate School of Science, Hokkaido University

March 2023

Abstract

Event deposits are deposits formed by tsunamis and floods, and are known as the only proxies recorded depositional processes of past disasters. Sedimentological analysis has been traditionally used to study event deposits, contributing to the estimation of tsunami inundation areas and the probability of occurrence. On the other hand, some event deposits are destroyed or lost after deposition, and have been difficult to identify event deposits. So the development of new research methods that could contrast and complement sedimentological methods has recently attracted attention. In the present study, I conducted organic geochemical analysis of tsunami and event deposits with focus on degraded organic molecules to evaluate the sedimentological process of event deposits and establish proxy could be identified past-event deposits.

Tsunami deposit is mainly characterized by mixture of marine sand and sedimentary structures formed by huge tsunami flow. In many cases, however, sedimentological information recorded as the structure of tsunami deposit was erased by erosion and disturbance during the post-depositional processes. In the present study, we performed organic geochemical analyses using biomarker and kerogen of the peat sediment cores from the Akkeshi and Kiritappu areas, eastern Hokkaido, Japan to evaluate the sedimentological and geochemical features of the paleo-tsunami deposits. In kerogen analysis, terrestrial plant fragments are mainly observed in all sand layers, indicating the redeposition of peat-derived matter by tsunami. However, the inner organic lining of foraminifera and the marine dinocyst could be identified in the tsunami layers. These reults can be direct evidences of paleo-tsunami. In steroid biomarkers, stanols could be detected in all samples of the Akkeshi and Kiritappu cores. The stanol conversion reaction from biosterol is thought to occur by microbial reduction in the sediment–water interface and anoxic water column of marine and lacustrine environments. Therefore, the stanol/sterol ratio can be used as redox indicator. We found that the C27 stanol/sterol (cholestanol/cholesterol) ratios are clearly higher than those of C29 in the sand layers of both Akkeshi and Kiritappu cores. The higher C27 stanol/sterol ratios suggest the contribution of marine compounds deposited under more reduced condition in the tsunami layer. However, some sand layers do not show this trend, and they can be considered event deposits of other origin.

In the middle Miocene of central Hokkaido, island-arc collision resulted in the formation of narrow foreland basins, Ishikari and Hidaka basins, extending about 400 km north-south and several tens of kilometers wide. Previous studies (Kawakami, 2013) have shown that a number of turbidite beds, Kawabata Formation, containing large amounts of terrestrial organic matter derived from higher plants have been identified. This suggested that a sedimentary system in which terrestrial organic matter was directly transported from the land to the deepseafloor was prevalent in the Ishikari Basin. In the present study, we conducted sedimentological and organic geochemical analyses on turbidites of the Abetsu Formation deposited in the Hidaka Basin to reconstruct sedimentary processes that occurred in the Hidaka Basin in the middle Miocene. In the Hobetsu area of Mukawa-city, south-central Hokkaido, sand and mud alternations deposited in the Hidaka Basin during the middle to late Miocene are widely distributed. The upper part of the Abetsu Formation (coarse-grained and

sandstone/mudstone alternation) and the Nibutani Formation (fine-grained sandstone alternation) are exposed at the Horokanbe-sawa River. We analyzed two thin, fine-grained turbiditic sequences collected from the upper part of the Abetsu Formation. These are mainly composed of three units from the lower part: massive sandstone part, organic lamination part, and mudstone part. For organic geochemical analysis, the turbiditic sequences were divided into units about 1 cm thick, focusing on the changes in sedimentary structure. Diterpenoids gymnosperm components), triterpenoids (angiosperm components), and des-A terpenoids (angiosperm components generated by microbial degradation under anoxic conditions) were detected as major biomarkers in the turbidites from the Abetsu Formation. The concentrations of diterpenoids and des-A terpenoids nearly constant throughout the sequences, whereas the triterpenoids significantly vary, and especially, concentrated in the from the top of the massive sandstone to the lamination section. These results suggests that the turbulent flow-forming turbidites in the Abetsu Formation contained large amounts of components originated from angiosperms. In the Kawabata Formation, the des-A terpenoids were remarkably abundant rather than triterpenoids and diterpenoids in the turbidites (Furota et al., 2014). These differences indicate that the terrigenous matter in the turbidites of the Abetsu Formation was transported from different type land area and/or different source vegetation to the deep sea. The terrestrial/marine organic matter ratio using steroid (sterane) composition was evaluated in the turbidite sequence. The sterane index shows a high proportion of terrestrial organic matter over the massive sandstone and lamination part, with a rapid shift to marine organic matter in the mudstone part. This trend is observed in the both Abetsu turbidites, but some sequences having a higher contribution of marine organic matter throughout the sequence. Such trends were also confirmed by the pristane/phytane index (Pr/Ph), which indicates the redox condition and contribution of terrestrial organic matter.

Aliphatic and aromatic degraded triterpenoids (TTs) including des-A and des-E TTs were investigated in the turbidite and hemipelagic mudstones from the Miocene Kawabata Formation (Ishikari basin) and Abetsu and Nibutani formations (Hodaka basin), south-central Hokkaido, Japan. The des-A TTs, having the carbon skeletons of oleanane, ursane, and lupane, are derived from angiosperm, and the des-E TTs, having the carbon skeletons of hopane, are bacterial origin. These compounds are thought to be formed by the microbial degradation under dysoxic and anoxic conditions. We found that the concentrations and relative abundances per TOC of total degraded TTs, especially des-A TTs, were remarkably higher in the Kawabata Formation, and significantly contained in the Abetsu and Nibutani formations. These results clearly indicate that the huge amounts of the des-A TTs were possibly transported and deposited in the Ishikari basin during the deposition of the Kawabata Formation of the late Miocene. The degraded TTs/TOC ratios are correlated with the values of the aquatic macrophyte n-alkane proxy (Paq) in the Kawabata and Abetsu formations. The higher Paq values are interpreted to be high contribution of aquatic and submerge/floating macrophytes, and moreover, were commonly observed in lake and pond environments. Thus, large amounts of the degraded TTs were possibly produced by biodegradation of the transported angiospermous TTs in the dysoxic or anoxic environments such as ponds and wetlands. Furthermore, it is presumed that the organic matter deposited in the Ishikari basin was transported from wetland or marsh areas of the paleo-Hidaka Island. The class distributions

of the aliphatic and aromatic degraded TTs varied in the samples from these formations. In the Kawabata Formation, the des-A lupanes are detected as major compounds, but the des-A oleananes are the most major compounds in aliphatic degraded TTs in the Abetsu and Nibutani formations. The higher relative abundances of the des-A lupanes in the only Ishikari basin (Kawabata Formation) suggest that the TTs had been supplied from mountain forest areas, where lupenoid-producing woody plant taxa might be spread. Meanwhile, the des-A lupanes are less abundant in the Abetsu and Nibutani formations, suggesting no or less supply of TTs from the mountain forest areas in the Hidaka basin.

According to these studies, we believe that the degraded organic molecules formed under anoxic environments are important markers. The anoxic environments are distributed in only a limited range of natural environments and the composition of degraded organic molecules vary by location to setting. It could be pointed out that degraded organic molecules are highly useful in event deposit studies, especially in estimating the sources of event flows and reconstructing transport processes.

Contents

Chapter.1 Evaluation for sedimentological processes of tsunami deposits by biomarker and kerogen analyses of peat sediments from the Akkeshi and Hamanaka area, eastern Hokkaido, Japan.

1.1. Introduction

When Tohoku earthquake emerged in Japan on March 11, 2011, the blackish seawater struck coastal areas a huge tsunami, and formed thick tsunami deposits on land. The brackish water was producted by containing sediments and organic matter of seafloor eroded by huge tsunami. Usually, the organic molecules deposited in seafloor were decomposed by specific reaction under dysoxic or anoxic condition (Wakeham 1989), hense, these molecules might be the proxy of tsunami identification. Traditionally, identification of tsunami deposits is conducted by sedimentological method (sediment structure, grain size, and composition of lithofacies). Although sedimentological data is still the most important and fundamental proxy in recent years, several problems could not be solved by sedimentological proxies were pointed. This indicates the possibility of preservation of marine-derived heterotopic organic matter in tsunami deposits, which raises the possibility of a new tsunami deposits identification proxy based on geochemical methods. Firstly thin sediment and the sediment collapsed sedimentological structure by bioturbation and rainwater is difficult to identify tsunami deposits, because of these sediments were not preserve sedimentological data recorded phenomenon of disaster. Furthermore, the tsunami inundation estimated by survey of tsunami deposits might be underestimated because extent of tsunami deposits may be smaller than the inundation area (Chagué-Goff et al., 2012),

According to the problems, new proxy development using geochemical methods is attracting attention and several studies have been reported (Chagué-Goff et al., 2017). In Sinozaki et al.(2015) reported dinosterol, a biomarker of dinoflagellates known as marine algae was detected in the uppermost mud layer of the 2011 Tohoku-oki tsunami deposits, and proposed as a marker for tsunami deposits.

In another study of 2011 Tohoku-Oki tsunami deposits, TAR using short-chain-alkane (C15, C16, C17) from marine algae, aquatic plant n-alkane indicator (Paq), and PAHs emitted by human activities transported from urban and rural areas are also reported to be useful for identifying tsunami deposits and estimation of the inundation area of huge tsunami(Bellanova et al., 2020, 2021; Konechnaya et al., 2022). The organic geochemical analysis of paleo-tsunami deposits conducted in Mediterranean paleo-tsunami deposits of the Turkish coastal region, eastern Mediterranean reported tsunami deposits contains n-alkane, fatty acids and C28 steroid derived from diatom and other algae(Alpar et al., 2012). Pr/Ph and TAR have been also proposed as proxies of tsunami deposits according to organic geochemical analysis of paleo-tsunami deposit in the northwestern Greek coastal region(Mathes-Schmidt et al., 2013).

However, organic geochemical features common to several tsunami deposits or tsunami deposits from different sites have been rarely found in previous studies and are not useful as proxies. This suggests different tsunami sources and local geographical factors may influence the composition of organic matter preserved in tsunami deposits. Therefore, there have been reported marine biomarkers are difficult to detect because of tsunami deposits contained significantly terrestrial plant OM derived from redeposition of terrestrial sediments and (Shinozaki et al., 2016). According to these previous studies, it is necessary to analyze different biomarkers to evaluate marine sediment transported by huge tsunami and develop organic geochemical proxies. While, biomarker have potential as paleoenvironmental indicators (vegetation, redox and degradation). Huge tsunamis

destroy terrestrial environment and changed onshore environment dramaticall, paleoenvironment indicators of biomarker might be recorded the impact of past huge tsunamis. In the eastern of Hokkaido, tsunami deposits emerged by great underthrust earthquakes were deposited in large area, many studies of paleo-tsunami were conducted. The huge tsunami forming tsunami deposits are known to occur at intervals of about 500 years in the Kuril Trench, are distributed over a distance of about 200 km(Nanayama et al., 2003, 2007). In Akkeshi area, eastern Hokkaido, nine tsunami layers have been identified over the past 3000 years(Soeda et al., 2003), suggesting the past tsunami records are preserved in the peatland. Especially in the Akkeshi area, the percentage of marine or blackish diatoms tends to increase in the sand layers, and these sand layers are considered to be tsunami deposits(Soeda et al., 2003). In previous studies, eastern Hokkaido, nine large tsunami deposits from the past 4000 years were found in Hamanaka area, eastern Hokkaido (Nanayama et al.,2003;2007). According to these previous studies, earstern Hokkaido is an ideal field for studies of tsunami deposits because tsunami deposits are preserved very well. In this study, peat cores containing tsunami deposits in the eastern Hokkaido region were used to examine tsunami deposit identification indices.

1.2. Sample

1.2.1. Study area

We studied sediment cores in a natural coastal wetland of Akkeshi and Hamanaka on the Pacific coast of Hokkaido, Japan in August 2016(Fig.1; 43.0N 144.5E). These wetlands were thought to be rarely struck by typhoons and no large flooding events because of no rivers nearby. These wetland mainly deposited peat sediments formed by local terrestrial plants. Tsunami deposits are mainly composed of coarse to fine sand, which is easily visible in peat cores.

These peat cores narrowly containing tsunami deposits were sampled on August 23-24, 2016 as part of a joint project between the Geological Survey of Japan, Hokkaido Research Institute (Hokkaido Research Institute), Niigata University, and Hokkaido University. Dr. Gentaro Kawakami, Dr. Keiichi Hayashi, and Yoshihiro Kase of the Hokkaido Research Institute, Associate Professor Yasuhiro Takashimizu and Associate Professor Atsushi Urabe of Niigata University, and Dr. Satoshi Furota of Hokkaido University (now at the Research Institute of Industrial Science and Technology) were involved in the sampling. The sand layers and tephra in the peat core are based on data provided by Mr. Kase.

1.2.2. Akkeshi Core (Akkeshi town)

The Akkeshi core sample was sampled on August 23, 2016 at Akkeshi-town, Akkeshi-gun, Hokkaido (43.0N, 144.5E). The sampling site is located at an elevation of 5 m above ground level and 1.8 km from the coastline. The Akkeshi core was sampled at a location where there are no rivers in the surrounding area and flood sediments were not might reached in sampling site. The total length of the sedimentary core is about 3 m. The lower part of the core consists of muddy layer, and the upper 1.5 m consists of peat. The peat layers are interbedded with sand and tephra layers, and two tephra layers and six sand layers have been identified. The two tephra layers have been identified from previous study (Nakamura et al.,2016), the upper tephra layer is Ta-a (A.D.1739 Mt. Tarumae eruption), the lower tephra layer is B-Tm (about 1000 years ago Mt. Baitou) from

Korea. The upper five sand layers in the Akkeshi core are considered to have been formed by tsunamis, based on comparisons with previous tsunami sediment surveys conducted in the Akkeshi area. On the other hand, the lowest sand layer is in contact with the marine mud layer below and has clearly fewer plant fragments than the other five layers. Hence, the lowest sand layer is thought to have been formed during the transition of the sample site from the coastal bottom to the land. In the Akkeshi peat core used in this study, layers A, B, and C may represent the 17th and 12th centuries, respectively. However, taking into consideration the contrast in depositional depth with volcanic tephra and the rate of peat deposition, layers A and C are assumed to be the 17th and 12th century tsunami deposits in this study.

1.2.3. Hamanaka core (Hamanaka town)

Hamanaka core samples were taken on August 24, 2016 at Hamanaka-town, Akkeshi-gun, Hokkaido (43.1N, 145.0E). It was sampled by a joint team of Niigata University, the Geological Research Institute of Hokkaido General Research Organization, and Hokkaido University. The sampling site is located at an elevation of 4 m above sea level and 4.2 km from the coastline. According to the "Tsunami inundation maps for the Pacific coast of Hokkai" prepared by the Geological Survey of Japan, AIST in 2004, this site is within the limit of tsunami inundation. The total core length is 2.5m, and consists mainly of peat deposits at all depths. Sand and tephra layers were intercalated between the Hamanaka core. Four sand layers and one sand patch were identified. These sand layers may be tsunami deposits. However, since the area is within the tsunami inundation limit based on the past paleo-tsunami history and there are terraces in the background, landslides and soil runoff due to rainwater may have been the cause.

Two tephra layers have been identified, the upper tephra layer is Ta-a (1739 Mt. Tarumae eruption), and the tephra layer found directly below the Ta-a tephra is estimated to be Ko-c2 (1694 Hokkaido eruption) (Nakamura et al., 2016).

1.3. Method

1.3.1. Biomarker analysis

1.3.1.1. lipid extraction

Lipids were extracted from sediment samples with dichloromethane (DCM) and methanol (MeOH) as described by Sawada (2006). Free organic molecule compounds were extracted with MeOH, MeOH/DCM (1/1, v/v) and DCM. d62-Tria-contane was added to extraction as internal standard for quantifying biomarkers. The extracts were dried in a rotary evaporator and redissolved in hexane. The hexane extract was passed through a silica gel column (95% activated), and aliphatic hydrocarbon fraction was collected. This fraction was analyzed by gas chromatography-mass spectrometry (GC-MS).

1.3.1.2. Gas chromatography-mass spectrometry (GC-MS)

Identification and quantification of the lipid fraction was carried out by GC-MS. The GC-MS was conducted with a Hewlett Packard 6890 attached to a DB-5HT column (30 m × 0.25 mm i.d., J&W Scientific) directly coupled to Hewlett Packard XL MSD quadrupole mass spectrometer (electon voltage, 70 eV; emission current,

350 μA; mass range, m/z 50 – 550 in 2.91 s). The GC oven was programmed at 4ºC/min from 50ºC (4 min) to 310ºC (held 17.50 min). Individual compound was identified on the basis of mass spectra and relative retention times Quantification of the compounds was made from the individual base peaks (e.g. m/z 57 for n-alkanes) determined from the authentic standards and previous literatures.

1.3.2. Kerogen analysis

1.3.2.1. Kerogen separation

Whole rock samples were crushed to a 'rice'-sized (diameter 2 – 5 mm) grain in an agate mortar as described by Sawada et al (2012). Crushed rock samples (5 to 10 g) were extracted with ultrasonication, by successive treatment with methanol and dichloromethane. Thereafter, residues were treated sequentially in a water bath shaker as follows: HCl 6 M (100 ml, 60℃, 12 h), HCl 12 M / HF 46 % (1/1 v/v) (100 ml, 60℃, 24 h), HCl 6 M (100 ml, 60℃, 4 h). After each treatment, the supernatant was removed after centrifugation (3000 rpm, 10 min). The residue, kerogen, was sequentially washed with HCl 6 M (x 2) and distilled water (x 5), and was recovered and freeze-dried under vacuum.

1.3.2.2. Palynofacies analysis

Palynofacies analysis was carried out as described by Sawada(2006). Briefly, wet residual particles obtained after HCl / HF treatment were siphoned and dropped onto non-fluorescent slides, and were then mounted in permanent slides for microscopic examination. Organic matter composition of kerogen was determined under an Olympus BX41 reflected light fluorescent microscope with an Olympus ULH100HG mercury lamp, a DM400 dichroic mirror containing a 330–385-nm excitation filter; and 420-nm–long pass barrier filter at the Department of Natural History Sciences, Hokkaido University. The light emitted was observed at × 200 magnification.

1.3.3. Elemental analysis (Total organic carbon contents)

Powdered sediment samples were acidified with 3M HCl to remove carbonate. After this treatment, these samples were dried on hot plate for 6 hours. Dry samples were analyzed for total organic carbon (TOC) content by a J-Science Micro Corder JM10 at the Global Facility Center, Hokkaido University.

1.4. Result

1.4.1 Kerogen analysis and Elemental analysis (Akkeshi core)

In palynomorph analysis, sand layers contain amounts of land plant debris, indicates erosion and redeposition of land by huge tsunami. But, we examined the identification of a foraminifera linings in sand layers 2 and 3(Fig.1.4.1. a,b) and dinocyst generated by dinoflagellates in sand layer 4(Fig.1.4.1 c,d) indicates transportation from marine. Foraminifera lining derived of inner structure of foraminifera, mainly observed of benthic foraminifera(Stancliffe and Matsuoka, 1991) is able to preserve in acid soil calcareous crust dissolution. The tsunami layer from Okushiri island of western Hokkaido also detected foraminifera linings and dinocysts, they consider proof of huge tsunami(Kase et al., 2016). Hence, the foraminifera linings and dinocysts detected in

Akkeshi tsunami layers also give evidence transported marine organism particles from seafloor by huge tsunami. The TOC values range 3.5-43.0% in peat sediments, while range 0.42- 10.0% in sand layers (Table.1). Although there is a tendency for the sand layer to show lower values, both the sand layers and peat sediments show large fluctuations, suggesting environmental factors at the time. The mud lower parts of Akkeshi core show lower TOC value (0.54%), the contribution of marine sediments transported by tsunami to the amount of TOC in the tsunami deposits is considered to be low.

1.4.2. Biomarker analysis: aliphatic fraction

1.4.2.1. *n*-alkane composition

Hydrocarbons (n-alkane and hopanoids) dominantly were detected in peat sediments and sand layers. Fig.1.4.2. shows mass fragmentograms of m/z 57(n-alkanes) and m/z 66(internal standard: tetracosane) of tsunami layer, pre- and post- tsunami deposit. The distributions of n-alkanes were dominated by long-chain homologues with odd carbon-numbers such as C23, C25, C27, and C29. Long-chain *n*-alkanes have been known to be derived from higher plant wax. *n*-alkane compositions also indicate erosion and redeposition of land soil by huge tsunami.

1.4.2.2. Aliphatic biomarker indices (Paq, CPI, ββ-hopane ratio)

Paq were ranging from 0.2 to 0.7 (Table 2, Fig. 5c) in Akkeshi sediment, it indicates the contribution of aquatic plants fluctuate during periods of peat formation(Ficken et al., 2000). The sand layers show various value (0.32-0.61), which might be influence by terrestrial environment and upstream route of tsunami. Although the pre-tsunami deposits have relatively high Paq (0.5-0.6), the several post-tsunami deposits (upper sand layer3, 4 and 5) show lower values (0.21-0.37). These tentative decrease of Paq value indicates change vegetation after tsunami.

CPI were at least 4.2, which clearly indicated predominance of odd carbon-number n-alkanes (Table.2). Fig.5b showing vertical profile of CPI tends to be higher in the upper peat sediments (5.70-11.29), while lower mud sediment shows relatively lower value (4.16-4.42). Fig.5d C30 ββ-hopane ratio (Farrimond et al., 1998) varied between lower mud sediments(ave.0.22) and peat sediments(ave.0.32). According to CPI and C30 ββ-hopane ratio, degree of early diagenesis is seemed different from offshore and peat sediment, maturity indexes might have potential as index whether allotopic biomarker contain in sediments. CPI of sand layer4, 5 were also relatively lower value (5.70-6.36) compared peat sediment. These n-alkane experienced early diagenesis could be attributed to carried other environment by tsunami during over 1000 years ago. But, upper sand layers (sand layer 1,2 and 3) have lower CPI value (6.19 – 9.88). This trend also seen in C30 ββ-hopane ratio, only sand layer 5 has lower value (0.28) compared from upper and lower peat sediment.

1.4.3. Biomarker analysis: polar fraction

In polar fraction(F4), Fatty acids, n-alkanol and steroids were dominantly detected in peat sediments and sand layers.

1.4.3.1 Steroids index marine/terrestrial ratio

In Akkeshi sediments, C27(cholesterol, cholestanol), C28 (campesterol. campestanol) and C29 steroid (stigmasterol, β-sitosterol, stigmastanol) were detected in both peat and sand layers(Summons et al., 1987). Fig.1.4.2. shows massfragmentograms of m/z 215(saturated steroids: stanol), m/z 129(unsaturated steroids: sterol) and m/z 66(internal standard: tetracosane) of tsunami layer, and pre- tsunami sediments. Dinosterol, biomarker of dinoflagellate a type of coastal algae reported from the 2011 Tohoku-oki tsunami (Shinozaki et al., 2015) was not detected in this sample. In pear sediments, Marine/terrestrial steroids ratio (C27 steroids/C27 steroids+C29 steroids) is very low(0.009-0.059), and even the lower mud layer, which has the highest marine/terrestrial ratio, tend to very terrestrial value (0.17). It indicates Akkeshi area is dominanted by terrestrial steroids, corresponded to the trend of n-alkanes composition. This trend also seen in all sand layers, it indicates the tsunami layer is more influenced by terrestrial plant eroded and redeposited than by C27 Steroids transported from marine organisms.

1.4.3.2 Steroid redox index

Stanol is known that it is formed under anoxic condition, thus the ratio of stanol/sterol can be used as a redox index(Wakeham, 1989; Wakeham and Beier, 1991; Nakakuni et al., 2017a). The change from sterol to stanol reacted quickly and has been detected in modern sediments, which is thought to accurately record the redox condition at the time of deposition(Nakakuni et al., 2017b). Redox index using C29 steroids(stanol/stanol+sterol) is constant in all sediments, ranged 0.5 to 1.1(Fig.1.4.5), indicates that the peatland sampled sediment core tend to anoxic conditions. Although terrestrial plant products stanols in plant body(Nishimura and Koyama, 1977), the amount of stanol generated in plant body is little and we interpreted the redox index of C29 steroids shows certain redox condition of sampling sites. Redox index of C28 steroids is similar to redox index of C29 steroids, although the index temporary show high value. Although C28 steroids is known that various organism product them, C28 steroids detected in Akkeshi core were originated by higher plants because of the trend of C28 steroid redox index is similar to C29 steroids redox index. On the other hands, Redox index for C27 steroids shows very anoxic value and tend to different trend from C28 and C29 steroids redox index (Fig.1.4.5). Especially sand layer1,2 3 and 5 have clearly anoxic peak compared to pre-and post-tsunami sediments. Compared to marine/terrestrial index (C27 steroids/C27 +C29) showing the same value in sand layer and peat sediments, redox index of C27 steroids indicates the source of C27 steroids is clearly different between the tsunami deposits and the peat layer. These results suggested that C27 steroid was transported from more anoxic environments (ex. seafloor, not peatland. The difference between Redox index of C27 steroids and C29 steroids may be an indicator to estimate the presence of allochthonous organic matter contained in sediments, thus we propose “allochthonous index” to quantify the difference in redox by C27 and C29 steroids (Fig.7c). In particular, the method to calculate the Redox Index by each Steroid may be important to pick up maritime pulses in tsunami sediments, especially when the influence of terrestrial materials is dominant, as in the tsunami sediments.

1.4.4 Degraded triterpenoids

We detected 6 aromatic degraded triterpenoids (diaromatic des-A oleanane, ursane, lupane, triaromatic des-A oleanane, ursane and lupane) in Akkeshi and Hamanaka cores. Degraded triterpenoids are known to be produced

under anoxic condition, they are related to specific terrestrial environments. Oleanane, ursane are the triterpenoids product by various angiosperm, lupane is specific triterpenoids product by some higher plants (Batulae, Cyperaceae, and Asteraceae). The percentage of each component of the des-A triterpenoids was shown in Fig.1.4.6. In the Akkeshi core, the composition of des-A triterpenoids shows complex behavior, which may reflect vegetation changes in the sample sites. The des-A triterpenoids in the sand layer may also reflect the vegetation in the surrounding area, the features seen in only tsunami deposits have not been found.

On the other hand, in the Hamanaka core, the uppermost sand layer and surrounding peat sediments has a very high percentage of diaromatic des-A lupane, while other des-A triterpenoids were rarely detected in these layers. Usually, huge tsunami eroded large areas of onshore and mixed and redoposited terrestrial OM, so we expected tsunami deposits contain various types of terrestrial OM. Thus, the sand layer other than the uppermost sand layer of Hamanaka core shows these characteristics indicating tsunami deposits. But, the uppermost sand layers is almost diaromatic des-A lupane, it indicates the source of the sand layer was limited for very small area where diaromatic des-A lupane is predominant. According to these results, we suggest the composition of degraded triterpenoids as proxy of event deposits.

1.5. Discussion

1.5.1. Preservation of organic matter -Possibility of disturbance and contamination

Biomarkers are generally insoluble in water, so there is no need to consider runoff or inflow due to rainwater, but it is possible disturbance or contamination by tsunami or post-tsunami sedimentation. Some sand layers (sand layer 2, 3) showed TOC values exceeding 3% even in the tsunami sediment layer, kerogen analysis of tsunami sediments showed a large amount of plant fragments in these sand layers, indicating that the erosion and redeposition of soil by huge tsunami2 The redox index (Stanol/Sterol) and Paq also shows a clear difference between the sand layers and the upper peat layer, suggesting that the free-form components in the tsunami sediments retain the characteristics of organic matter transported and redeposited by the tsunami. On the other hand, in the uppermost sand layer, redox index of C27 steroid shows anoxic tendency even in the lower peat layer. This may be due to the erosion of the lower peat layer and the inflow of the sand transported by tsunami.

1.5.2. Tsunami pulse recorded in sand layers

C27 Steroids (Cholesterol, Cholestanol) are mainly produced by algae, but not only coastal algae but also algae living on land produce them, so it cannot be assumed that they are of marine origin. However, by calculating the redox index from C27 steroids, it is possible to estimate the source where C27 steroids were deposited. In the peat sediments, the redox index of C27 steroids mainly fluctuates between 0.5 and 1.1, and its variation is corresponded to the redox index of C29 Steroids. This suggests that C27 steroids in the peat sediments are of terrestrial origin, as are C29 steroids from terrestrial higher plants. On the other hand, some tsunami layers (tsunami layers 1, 2, and 3), the redox index of C27 steroids is ranged 1.24-1.69, which is clearly higher than that of the surrounding peat sediments. The redox index of C29 steroids in sand layers, show values similar to those of the peat layer, unlike redox index of C27 steroids. This suggests the C27 steroids in the sand layers are allochthonous organic matter, not terrestrial origin. The anoxic environment around the sampling site is

considered to be seafloor or small pond (lake tokotan), we conclude that the C27 steroids in the tsunami sediments are derived from algae deposited on these anoxic environments. The difference in the redox index of C27 steroids may reflect the difference in the source. Therefore, we propose an index (Δstanol/sterol27-29) to measure the difference between the redox index of C27 steroids and that of C29 steroids; if Δstanol/sterol27-29 is small, C27 steroids is as likely as C29 steroids to come from terrestrial sources. The origin of the substance can be inferred.

On the other hand, the higher Δstanol/Sterol27-29 is, the source of C27 steroids and C29 steroids are different, and it can be inferred that allochthonous biomarker was mixed by the event flow such as tsunami. But, some sand layer deposited over 1000 years ago (sand layer 4, 5) don't show these trend, the results indicates tsunami deposits contain allochthonous biomarker transported by tsunamis, the type of organic matter varies with age, and we believe that various type of biomarker needs to be analyzed in identifying the long-term tsunami sediment record.

1.5.3 Investigation of transport processes of organic matter preserved in tsunami deposits

The sand layer exhibits a TOC of 1-3% and contains relatively little organic matter, this is probably due to the fact that the hinterland where the tsunami deposits were deposited is peat soil, and the tsunami heavily eroded and redeposited the peat soil, which is also reflected in the sea/land origin ratio by C27 and C29 Steroids. On the other hand, marine remains (foraminiferal linings and dinocyst), reducing steroids from marine algae(cholestanol), and even n-alkanes experienced early diagenesis and changed were transported from marine areas and deposited in the tsunami deposits. Therefore, the source of organic microfossils and organic components preserved in the tsunami sediments is more likely to be the bottom sediments or anoxic water column. The tsunami eroded the seafloor, causing roll-up of seafloor sediments and their incorporation into the tsunami water column, which reached the land area (Fig. 1.5). On the other hand, the results of this study suggest the biomarker index of the tsunami pulse changed from the even n-alkane to C27 Stanol around 1000 years ago. The possibility of a change in the seafloor environment off the coast of Akkeshi is considered as a possible factor, but there are no studies suggesting a change in the sedimentary environment off the coast of Akkeshi, and a major change in the barrier system between Akkeshi Bay and Lake Akkeshi has been pointed out as occurring as recently as 3000 years ago(Shigeno et al., 2013), this doesn't coincide with the timing of the tsunami pulse shift in this study. Therefore, it is possible that the tsunami's travel path and the oceanic area that is its main source changed after the past 1000 years, but no conclusion can be drawn at this time. However, the "chemical" characterization of past tsunami sediments by using organic matter may provide a new dataset that can be compared with tsunami sediments from other regions and used to examine tsunami generation factors and tsunami propagation pathways. The following is a brief summary of the results of the study.

1.6. Conclusion

In this study, we analyzed organic matter in multiple event deposits and attempted to estimate the depositional processes, especially the transport, deposition, and sorting processes of organic matter in each event deposit, and examined methods for identifying event deposits from an organic geochemical analysis. Organic analysis of tsunami sediments from the eastern coast of Hokkaido, Japan.

We analyzed peat cores containing narrow tsunami sediments obtained at two sites in Akkeshi-town and Hamanaka-town Kiritappu area, and obtained the following findings: The palynomorph composition of the tsunami sediments is consistent with the palynomorph composition of the peat cores. The kerogen analysis of the tsunami sediments also showed a predominance of terrestrial higher plant-derived particles, but a few foraminifera linings and dinoflagellate cysts were observed, strongly suggesting that the sand layers were formed by huge tsunamis. The redox (stanol/sterol ratio) using stanol, which is formed by microbial degradation of steroids in anoxic sedimentary environments, shows that the redox level in the sand layer tends to be higher for C27 steroids derived from coastal algae, and the difference with C29 steroids from terrestrial higher plants is also very large. This indicates that the tsunami transported marine and reducing organic matter from the seafloor. Stanols/sterols from marine C27 steroids may provide an indicator of the effect of the tsunami on the formation of the sand layer. Triterpenoids, which are reduced components, show a characteristic tendency to increase in abundance in some sand layers, suggesting that they were transported by flood currents, but the trend is different in the Akkeshi core.

The results of this study suggest that the triterpenoids were transported by the flood currents, but the results of the Akkeshi and Kiritappu cores show a different trend, which needs to be further investigated.

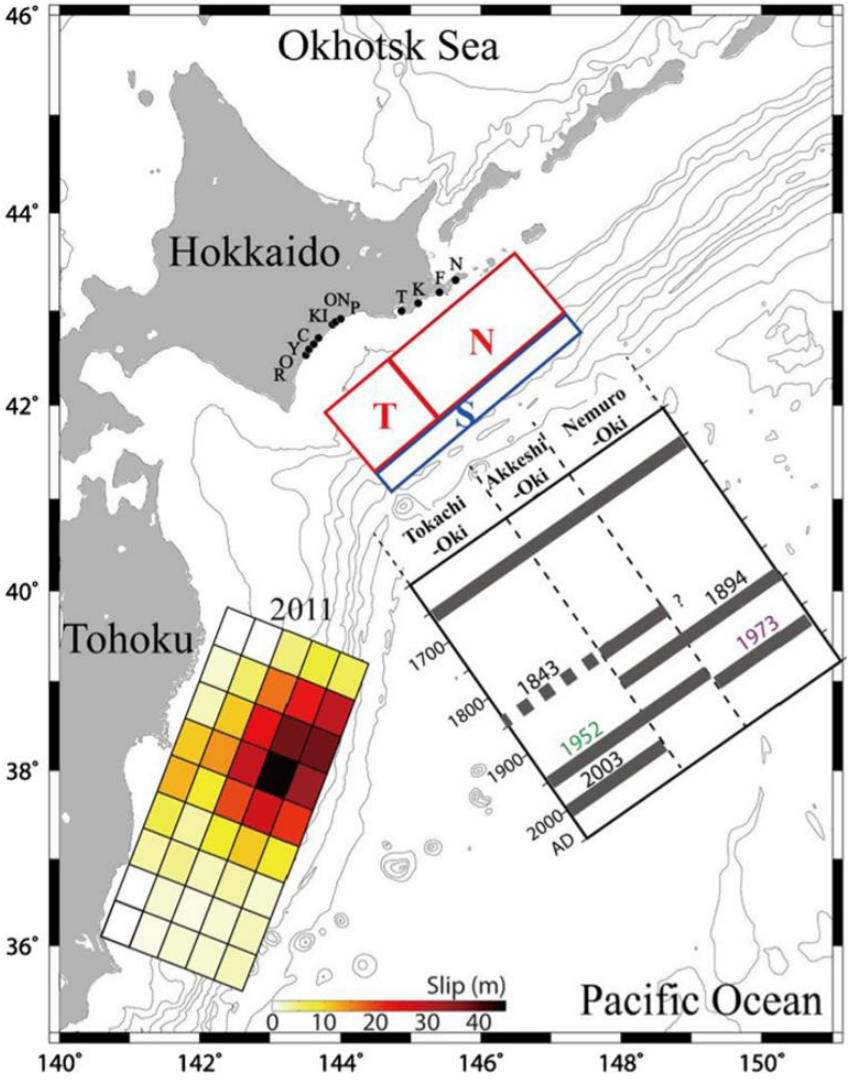

Fig.1.1. The fault model of the 17th century great earthquake is shown [T: Tokachi-Oki segment, N: Nemuro-Oki segment, and S: Shallow part of the plate interface] (Ioki et al.,2016)

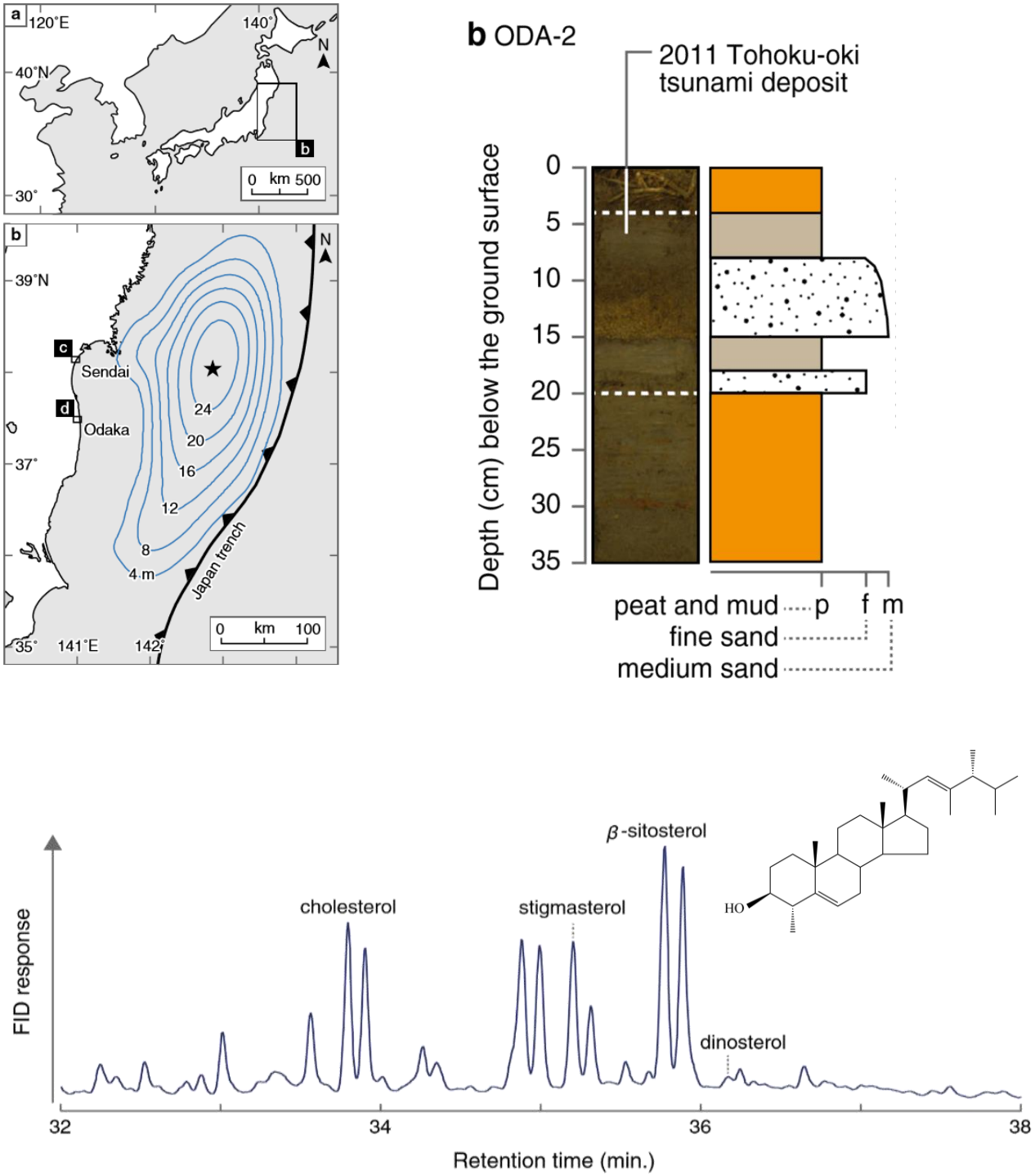

Fig1.1.2. Shinozaki et al. (2015); Detection of marine biomarker dinosterol from tsunami sediments of the earthquake 2011 in the northeastern Japan

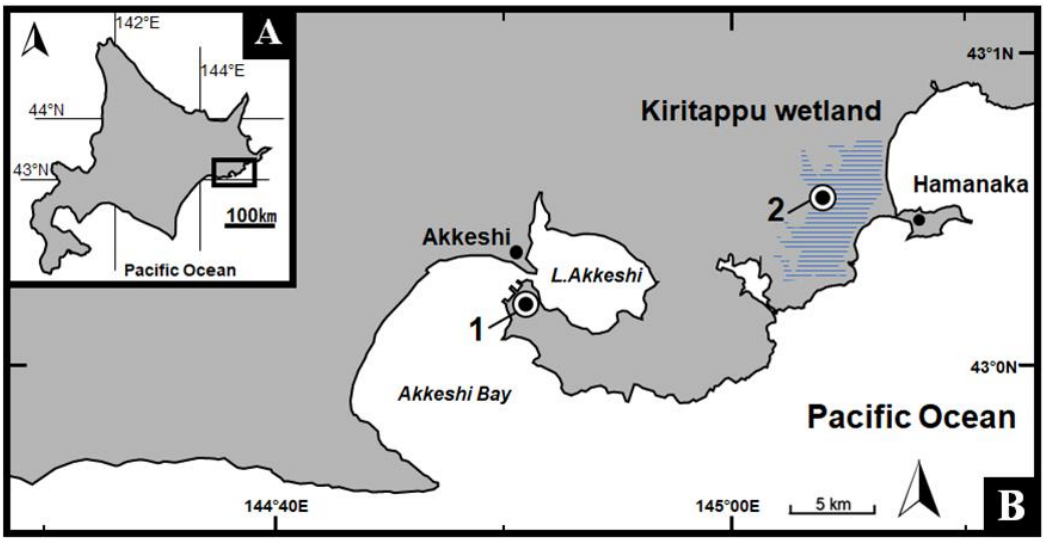

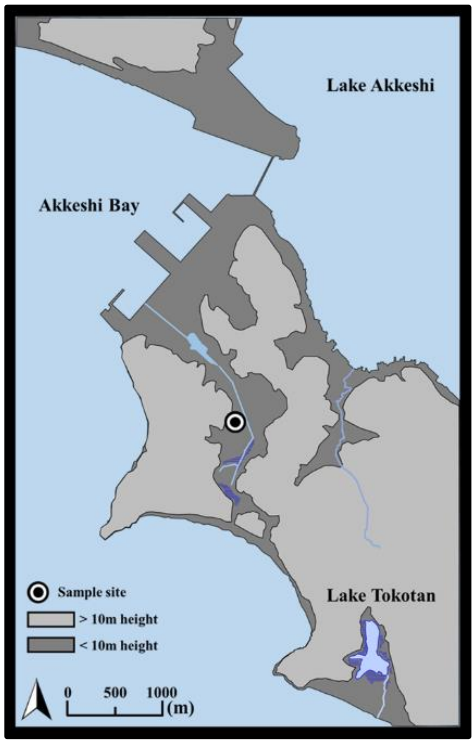

Fig.1.2.1. (A)and (B) Location of Akkeshi area on Hokkaido island. (C)detail and sampling location of Akkeshi area.

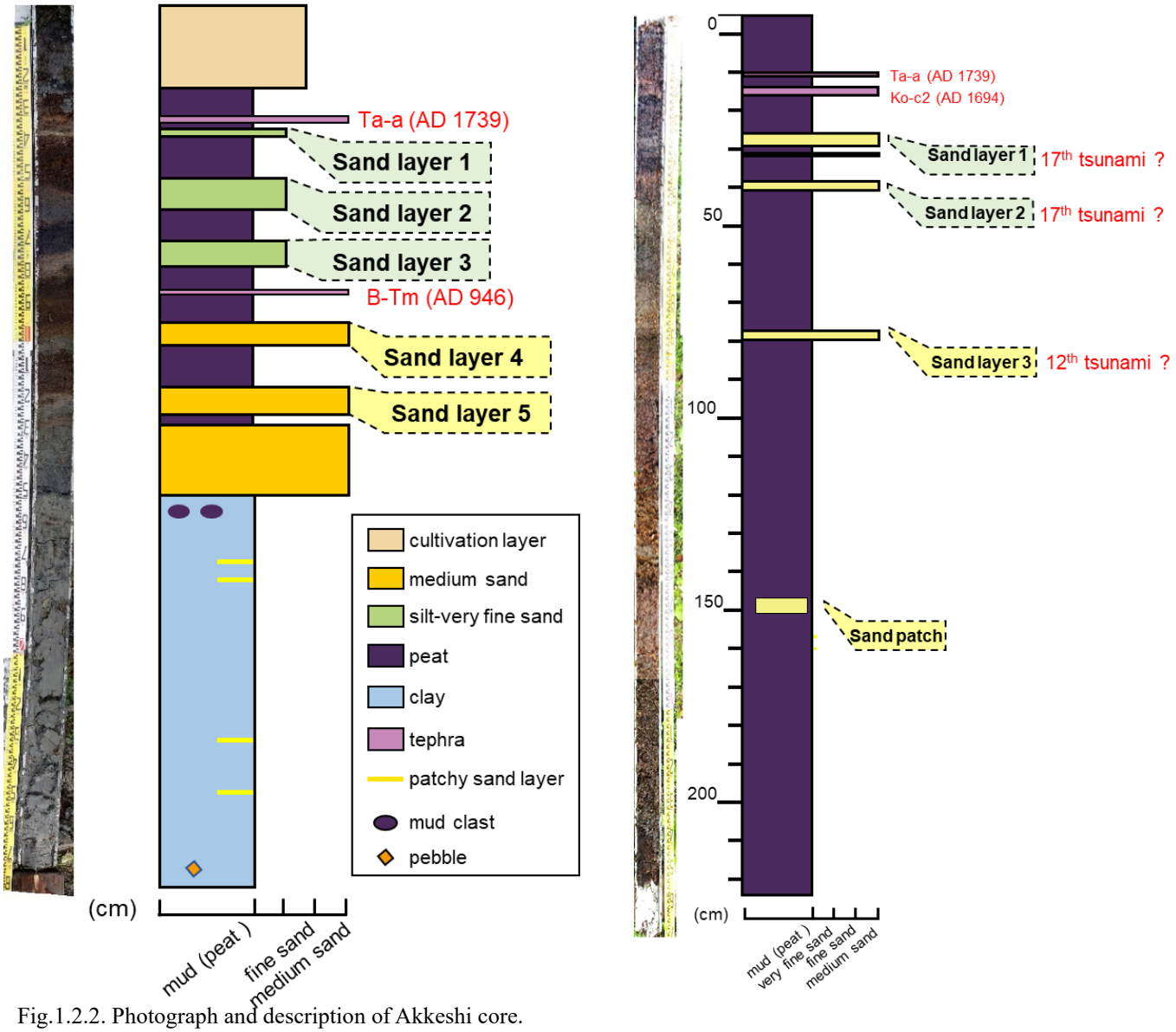

Fig.1.2.2. Photograph and description of Akkeshi core.

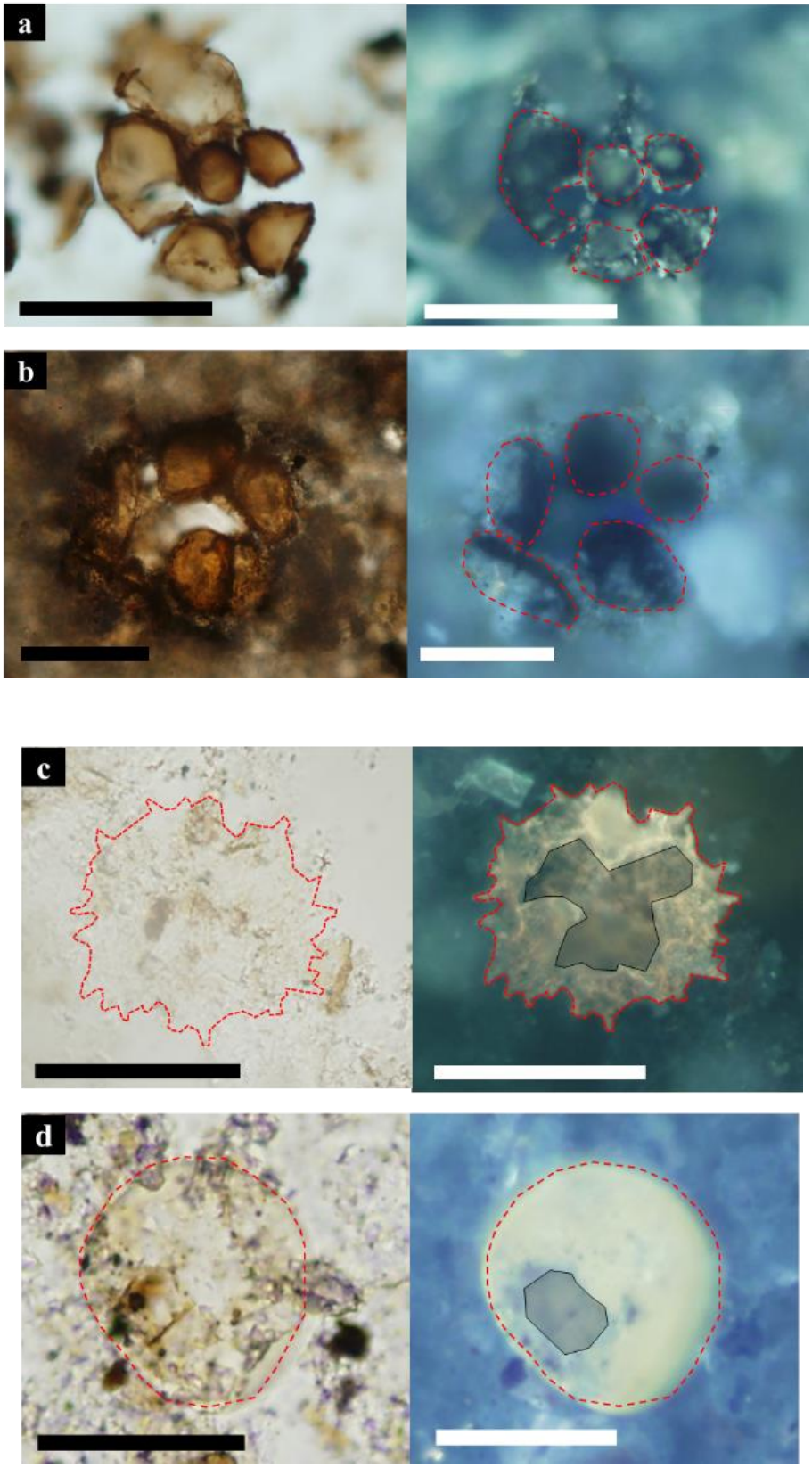

Fig.1.4.1 Photomicrographs of marine paticulars contained in sand layers. left side is under transmitted and right side is fluorescent. (a) is foraminifera lining of sand layer 3. (b) is foraminifera lining contained in sand layer 2. (c) and (d) is dinocyst formed by dinoflagellate of sand layer 4.

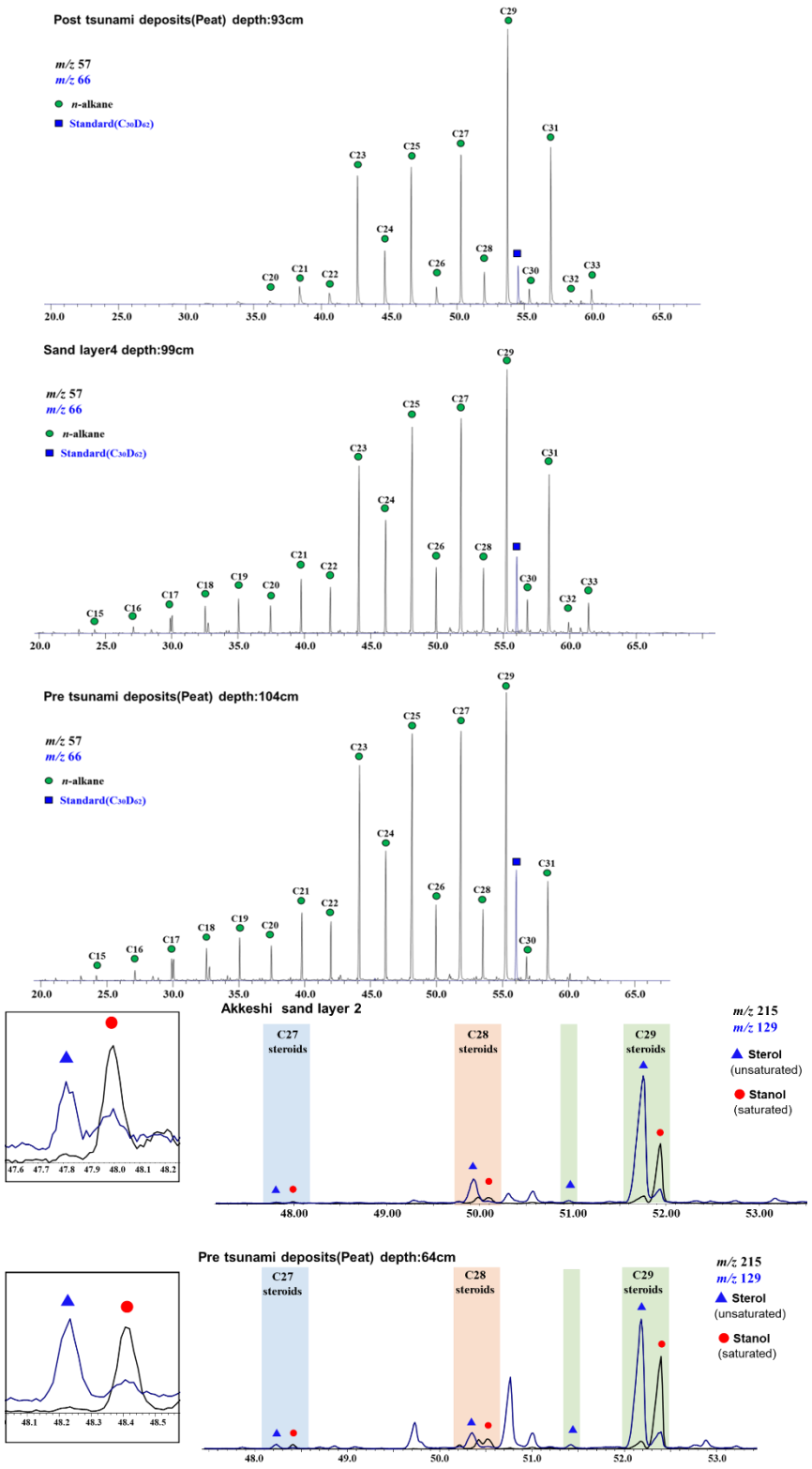

Fig.1.4.2. Mass fragmentgrams at m/z 57 (n-alkanes), m/z 66(internal standard; C24D50) of sand layer 4 and upper/lower peat sediment and mass fragmentgrams at m/z 215(stanols), m/z 129(sterols) of sand layer2 and lowerpeat

Table.1 Data of elemental analysis(TOC, TN and C/N ratio)

Sample Name	Depth (cm)	Lithology	*n*-alkane index			hopanoid index	steroid index				
			CPI	ACL	Paq	C_{30} ββ-hopane ratio	$C_{27}/C_{27}+C_{29}$	C_{27} steroid stanol/sterol	C_{28} steroid stanol/sterol	C_{29} steroid stanol/sterol	Δstanol/sterol 27-29
Sand layer 1	38	silt-very fine sand	7.22	28.32	0.32	0.31	0.033	1.69	0.84	0.45	1.24
Peat	42	Peat	7.06	27.61	0.57	0.27	0.039	2.24	1.16	0.66	1.58
Peat	47	Peat	9.84	27.75	0.40	0.31	0.038	1.05	0.72	0.60	0.45
Peat	52	Peat	7.18	27.64	0.61	0.32	0.020	1.13	0.62	0.50	0.63
Sand layer 2	57	silt-very fine sand	9.88	27.42	0.60	0.34	0.013	1.52	0.20	0.39	1.13
Peat	64	Peat	6.24	27.47	0.57	0.36	0.033	0.86	0.67	0.70	0.16
Peat	67	Peat	8.41	28.77	0.26	0.37	0.025	0.82	0.77	0.73	0.09
Sand layer 3	73	silt-very fine sand	6.19	27.09	0.61	0.31	0.018	1.24	0.76	0.67	0.58
Sand layer 3	75	silt-very fine sand	6.36	27.71	0.48	0.37	0.019	0.59	0.77	0.73	-0.14
Peat	83	Peat	9.37	27.40	0.57	0.21	0.016	0.90	0.79	0.67	0.23
Peat	87	Peat	11.29	27.87	0.30	0.32	0.013	1.00	0.59	0.69	0.31
Peat	93	Peat	7.35	28.41	0.37	0.25	0.020	1.06	0.80	0.81	0.26
Sand layer 4	99	medium sand	5.70	27.97	0.45	0.32	0.012	0.60	0.78	0.80	-0.20
Peat	104	Peat	6.21	27.48	0.54	0.28	0.013	0.53	1.04	0.90	-0.37
Peat	108	Peat	10.43	27.94	0.39	0.34	0.009	0.91	1.33	0.66	0.25
Peat	113	Peat	6.64	29.43	0.21	0.37	0.021	1.83	2.11	0.88	0.96
Sand layer5	118	medium sand	5.70	27.90	0.53	0.28	0.040	0.72	1.07	0.80	-0.08
Peat	124	Peat	6.43	27.76	0.49	0.36	0.059	1.81	1.04	0.85	0.96
Peat	126	Peat	--	--	--	--	0.045	0.74	0.93	0.87	-0.12
Sand putchy layer	167	silt-very fine sand	4.16	26.88	0.71	0.22	0.070	0.67	1.08	0.90	-0.23
Mud	170	Mud	--	26.01	--	0.16	0.084	0.76	1.25	1.09	-0.33
Mud	186	Mud	4.42	26.87	0.71	0.25	0.169	0.63	1.30	0.95	-0.33
Mud	196	Mud	4.20	26.93	0.71	0.22	0.161	1.08	2.15	1.33	-0.25

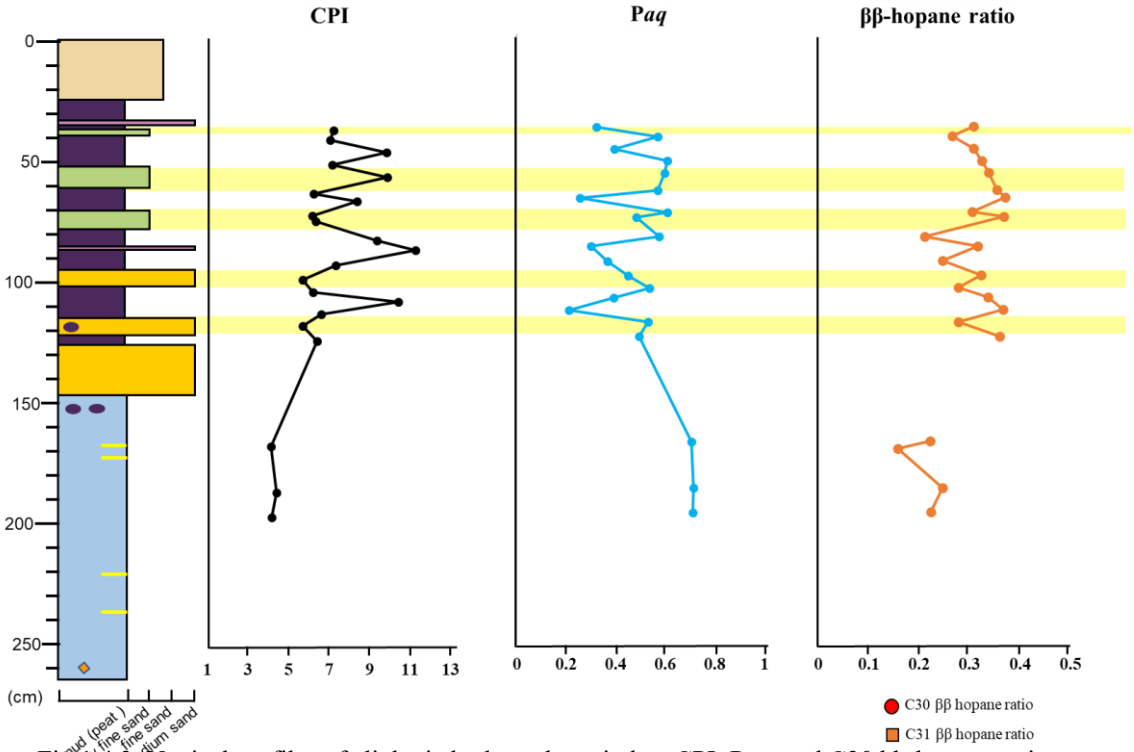

Fig.1.4.3. Vertical profiles of aliphatic hydrocarbons index, CPI, Paq, and C30 bb-hopane ratio.

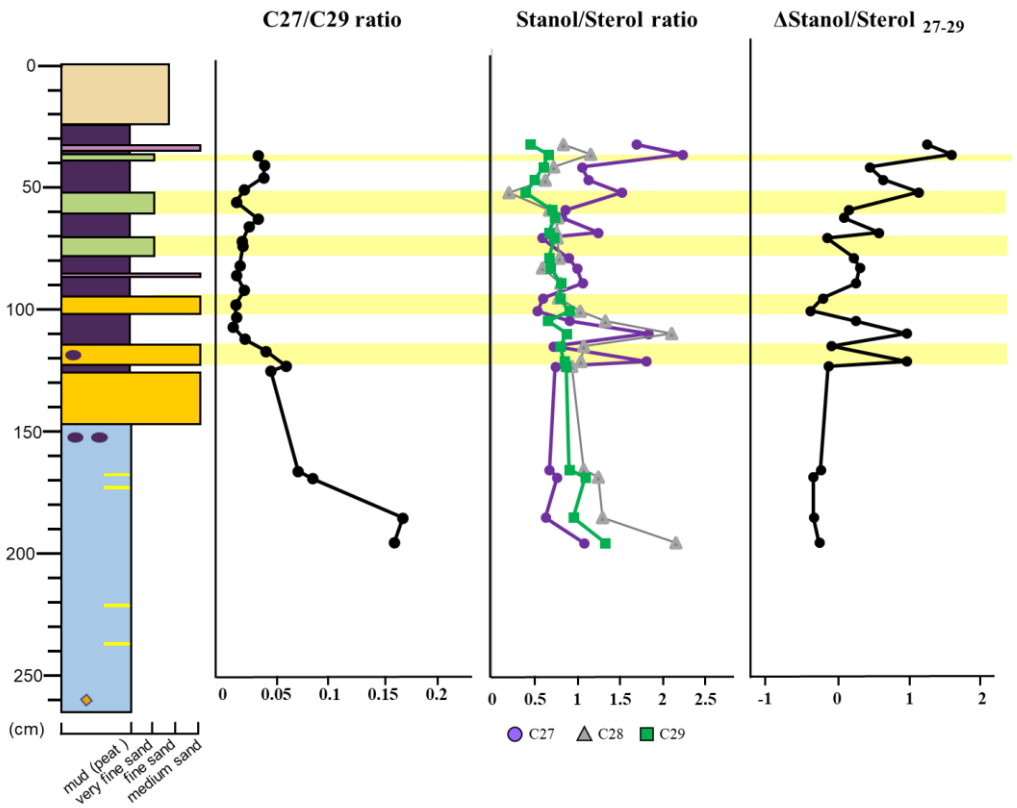

Fig.1.4.4. Vertical profiles of steroids index, (a)marine/terrestrial ratio(C27 steroids/C27+C29). (b) redox index(stanol/sterol) of C27, C28 and C29 steroids. (c) Δstanol/sterol27-29.

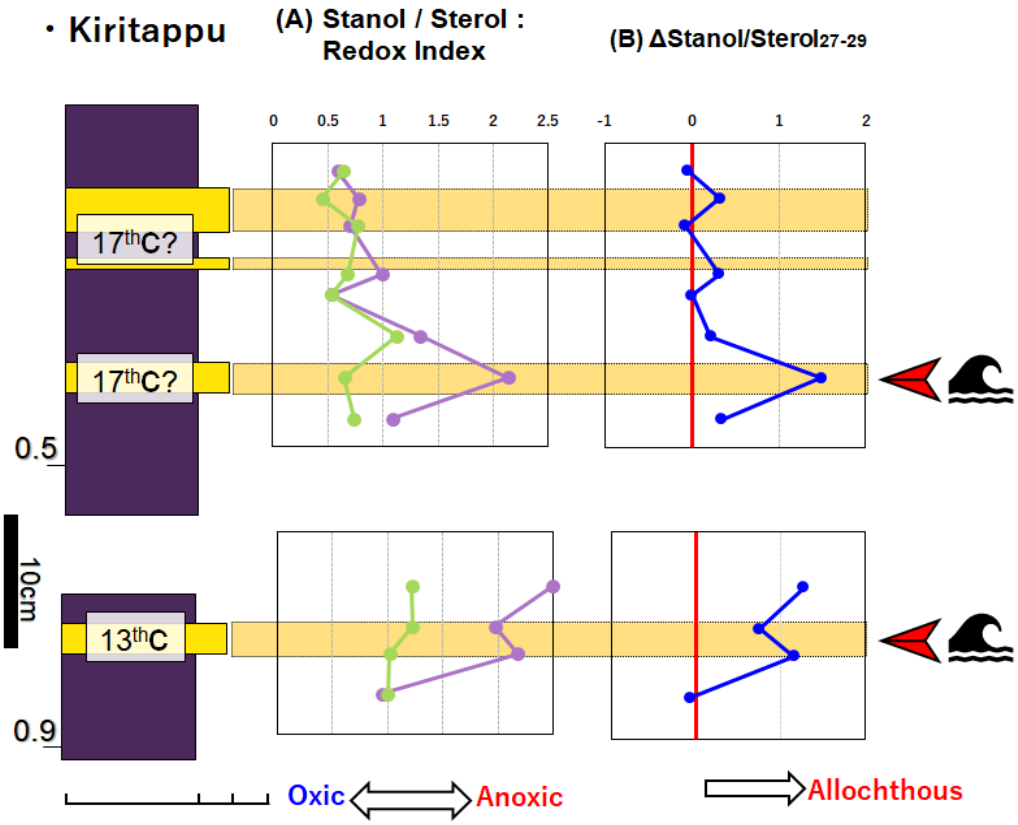

Fig.1.4.5. Vertical profiles of steroids index, redox index(stanol/sterol) of C27 and C29 steroids, Δstanol/sterol27-29 in Hamanaka core.

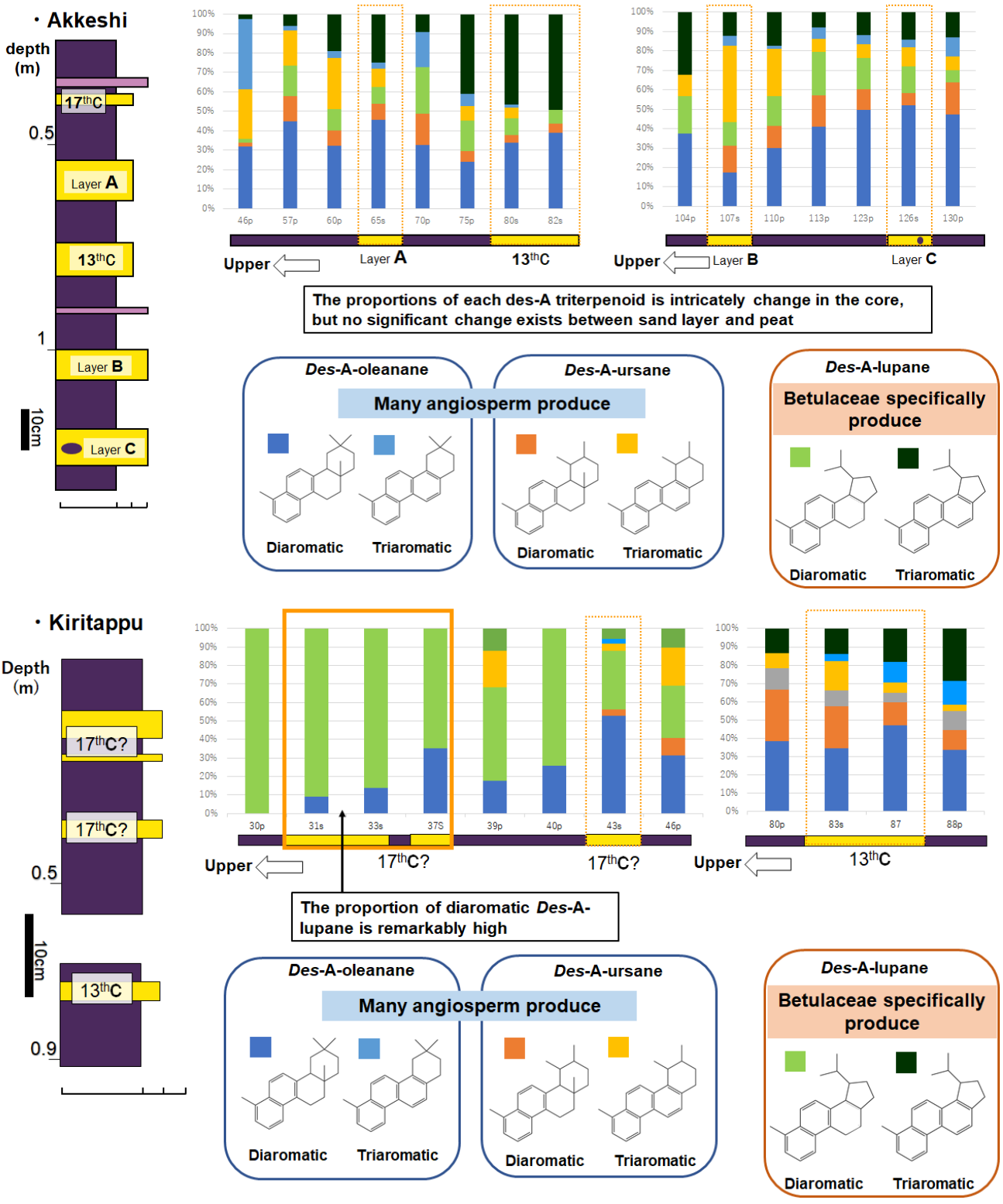

Figure.1.4.6. The composition of degraded triterpenoids detected in Akkeshi and Hamanaka cores

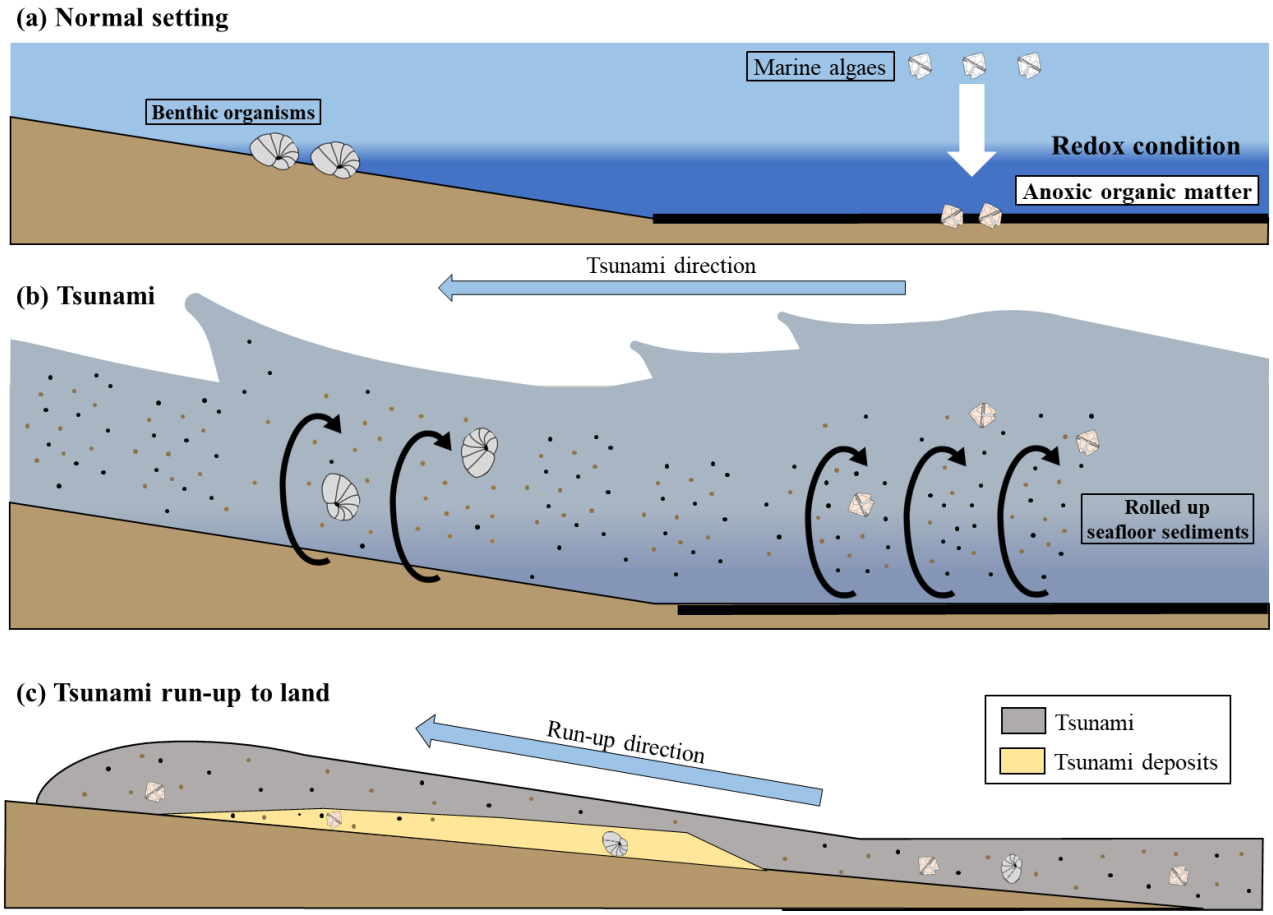

Fig.1.5.1 Scheme for transportation of marine organic particles. (a)normal condition (b)occurrence of huge tsunami (c)formation tsunami deposits on land.

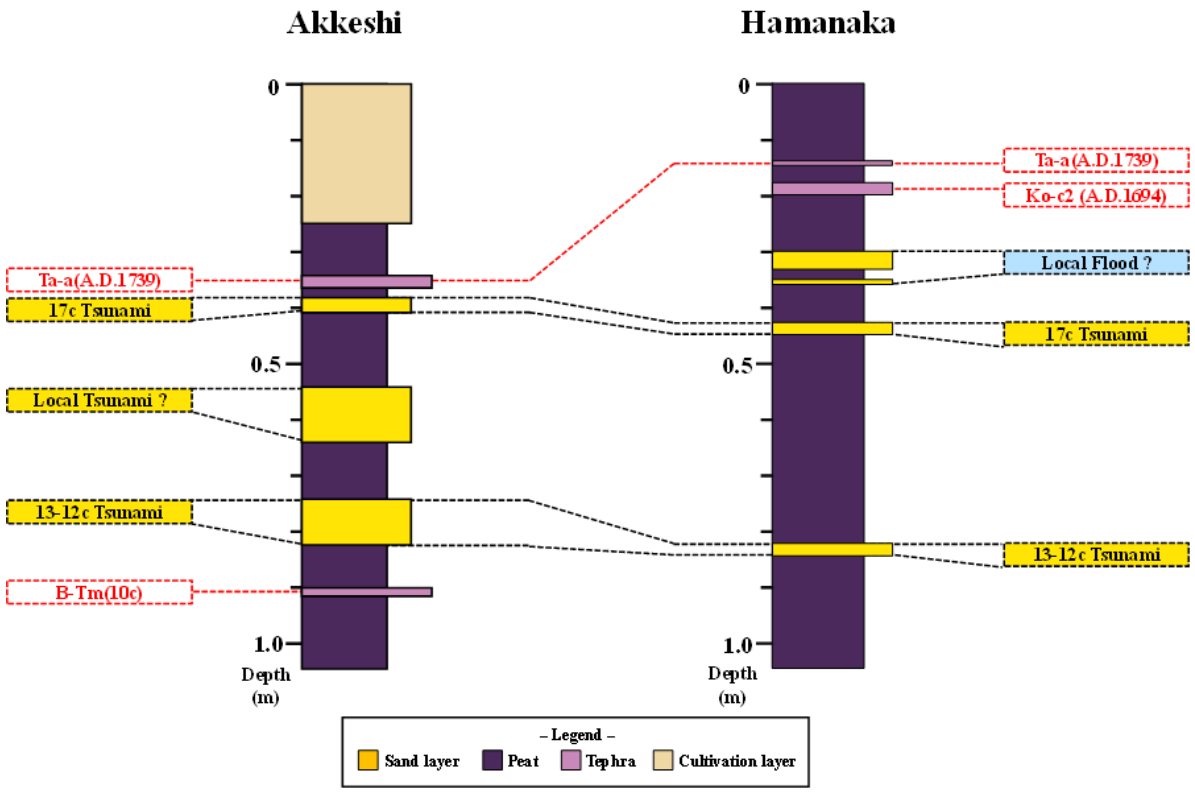

Fig.1.5.2 Contrast of event deposits between the Akkeshi and the Hamanaka core.

Chapter.2. Sedimentological and organic geochemical studies of Middle Miocene organic-rich turbidites deposited in Hokkaido, Japan.

2.1. Introduction

In recent years, it has become clear that flood sediments are preserved on the deep-sea floor. In particular, hyperpycnal flows, which have been discussed since 2000s, are density flows formed by flood and recognized as an important mechanism that keeps turbidity current to the deep-sea floor (Mulder et al.,2001; Saitoh et al.,2005). Zavala et al. (2016) recognized these sediments as event sediments, which are different from turbidites formed by submarine landslides, and referred to turbidites formed by submarine landslides as "intra-basinal turbidite. The intra-basinal turbidites are mainly gravity-flow turbidites which have high velocity, but once it reaches a plane submarine fan, it loses energy and stops flowing, so the area where turbidite deposited is limited to the area around the submarine fan. On the other hand, "extra-basinal turbidite" is thought to density flow, such as hyperpycnal flows. Turbidity current which formed extra-basinal turbidites has lower velocity and long duration time, up to several day. Hyperpycnal flows have recently been observed offshore of Taiwan, and it has been reported that deposited over a wider area and contain a large amount of terrestrial organic matter (J.D. Millim et al.,2005; Lina Jin et al.,2021). Flood related sediments are also known to be rich in organic matter, much of which is of terrestrial phytoclasts (Mulder et al.,2009; Zavala et al.,2011). Thus these sediments have recently been considered an important system for fixing terrestrial organic matter.

The Miocene Kawabata Formation exposed in the Yubari area of Hokkaido is characterized by large-scale sandstone-mudstone alternation. The Kawabata Formation is composed of turbidite deposited in the Ishikari Basin during Middle Miocene. The Ishikari Basin is a narrow, deep foreland sedimentary basin that existed between the Northwest Hokkaido formed by the rising Hidaka Mountains (Kawakami et al. 2003). The turbidites of the Kawabata Formation are characterized by their high organic matter content, and some of the organic matter-enriched sandstones have black bands within the turbidite sequence that strongly suggest that they were formed by flood flow, indicating that this was a depositional site where terrestrial organic matter was directly transported to the submarine basin (Furota et al.,2014; 2021).There are also many turbidites contrasting with the ordinary Bouma sequence, which also contain organic-rich units.

Although the organic-rich sandstones analyzed by Furota et al. (2014) and turbidites showing the Bouma sequence may share similar formation factors, the depositional processes that ultimately lead to the formation of turbidites may be different due to differences in depositional structures. In particular, Furota et al. (2014) found that in organic-rich sandstones, the lower part of the sandstone is enriched in terpenoids, which are abundant in wood chips, and the upper part is enriched in n-alkanes, which are components of leaf wax, suggesting that the turbidite is formed by the fractionation process of turbidite. The separation of these units is inferred to have been caused by the fractionation of turbidite during the formation of turbidite. Furota et al. (2014) suggested that these features may be due to the slow and longer duration of the turbidite flow, which is typical of hyperpycnal flows. Furota et al. (2014) speculate that these features were formed by slower and longer duration turbidite flows, such as hyperpycnal flows. However, no comparison of organic geochemical features with ordinary turbidite sequences such as the Bouma sequence was made, and it is not clear whether the features shown by Furota et al. It is not clear whether these features are common to turbidites or only

found in slower and longer duration turbidite flows, such as hyperpycnal flows. Therefore, it is important to compare the organic geochemical analysis of turbidite sequences with that of ordinary turbidite sequences in order to elucidate the transport and deposition of organic matter in turbidite flows.

The Hidaka Basin in the Hidaka region of Hokkaido, Japan, is located in the southern part of a narrow, long foreland sedimentary basin in central Hokkaido, Japan, and is rapidly filled with sediments and progresses from trough-filling turbidites to fan-delta sediments in the northwest Pacific margin that extends through the middle to late Miocene (Sagayama et al. 1992; Kase et al. 2018). The foreland sedimentary basins suggest a significant contribution of material transport from terrestrial sources, including flood flows, and evidence for this is provided by turbidites with concentrations of terrestrial organic fragments in the adjacent Ishikari Basin to the northwest (Furota et al., 2021). In the terrestrial hinterland, vegetation and transport systems are thought to change depending on the environment, and organic matter analysis is expected to be a tracer for estimating material transport from the land to the sea in sedimentary formations with high terrestrial organic matter content. In particular, changes in the composition of conifers, bbroadleaf trees, and the component of angiosperms that have experienced microkbial decomposition are considered to be useful indicators for examining the factors that cause turbidity currents. The Hidaka area has a wide distribution of sedimentary layers up to the Middle to Late Miocene, and it has recently become clear from age estimates based on radiolarian and diatom analyses that the area is a suitable field for considering temporal and spatial changes in sedimentary systems in sedimentary basins (Motoyama et al., 2009; Maruyama et al., 2018).
In this study, field surveys and organic geochemical analyses were conducted on sedimentary layers buried in the Hidaka Basin during the Middle to Late Miocene to examine the evolution of the sedimentary system in the basin and its relationship to the paleoenvironment of the terrestrial hinterland.

Furthermore, the authors discovered carbonate concretions intercalated with siliceous mudstone near the lowermost part of the Middle Miocene Nibutani Formation in the Hobetsu area, Mukawa-town, Hokkaido, Japan. Carbonate concretions include those formed by sedimentary and diagenetic processes and methane-derived authigenic carbonate rocks. Several examples of authigenic carbonate rocks formed during the Miocene in Japan have been reported (Maeyama et al., 2020; Ishimura et al., 2005; Miyajima et al.,2020), and all of them show methanogenic biomarkers and very low carbon isotope ratios, suggesting that they were formed by anaerobic This is interpreted as being formed by anaerobic oxidation of methane (AOM) by microorganisms during the ascent of methane-rich fluids from the subsurface. In this study, biomarker analyses of carbonate concretions and mudstone samples obtained from the Nibutani Formation will be conducted to investigate the relationship between the origin of the carbonate concretions and the depositional environment at that time.

During the Miocene in Hokkaido, narrow foreland sedimentary basins were formed in an area extending about 400 km from north to south and several 10 km wide due to island-arc collision. Muddy-sandy sedimentary rocks filling the Hidaka Basin, located in the southern part of the foreland sedimentary basin, are widely distributed in the Hidaka area (Kawakami et al., 2013). The sedimentary rocks of the Hidaka Basin are known to be particularly low-maturity. Haptophyte-derived alkenone, which is mainly used to quantify

Quaternary marine surface water temperatures, has been detected in the Nina formarion of the Haegawa outcrop in the field of this study and is considered to have great potential in paleoclimatic and paleoenvironmental reconstructions. Studies using oceanographic drilling cores in the East China Sea, the Japan Sea, and the North Pacific Outer Ocean are beginning to show that multiple cold events occurred in East Asia and the Northwest Pacific during the middle to late Miocene when the Hidaka Basin was filled, due to weakening of the 8-7 Ma EASM and expansion of the East Antarctic Ice Sheet (Matsuzaki et al.,2020). On the other hand, paleoceanographic information in the Pacific coastal and northern regions of the Japanese Archipelago is lacking, and we believe that paleoenvironmental data obtained from the Hidaka Basin sedimentary rocks, the field of this study, can supplement paleoceanographic information in these missing areas. In this study, we examine examples of alkenones detected in muddy sedimentary rocks of the Nina formation exposed in Haegawa, where sedimentary rocks from the Middle to Late Miocene are continuously exposed, and the marine surface temperature and basic marine production at that time inferred from the alkenones.

2.2. Samples

2.2.1. Soumokumaisawagawa River (Kawabata Formation)

In this study, we analyzed the Miocene Kawabata Formation turbidites exposed in the Yubari area of central Hokkaido, Japan. Two turbidite sequences were sampled (B sequence and L sequence) that represent the Bouma sequence (Bouma 1962). The two sequences differ in their thickness and lower sandstone unit (Ta section), with the B sequence being about 20 cm thick overall and the Ta section about 10 cm thick. The L sequence, on the other hand, has an overall thickness of about 80 cm and a Ta section of 50 cm, and is closer to the channel than the B sequence, suggesting that the velocity and energy at the time of flow were greater.

In order to reconstruct the organic matter transport and deposition process for each of these turbidite sedimentary structures, we divided them into units by sedimentary structure and sampled each unit.

The Bouma sequence is a sedimentary model of turbidite sediments proposed by Bouma et al. (1962), in which the complete Bouma sequence is classified from the bottom as Ta (massive sandstone), Tb (parallel foliation), Tc (oblique foliation), Td (weak parallel foliation), and Te (muddy). The Te section is classified as Et (turbidite mudstone) and Ep (pelagic mudstone).

Four units, Ta, Tb, Tc, and Te, are observed in the B sequence, and in the L sequence Ta, Tc, Td, and Et were observed. Since the upper part of Ta in the L sequence also shows a classified structure, Ta was divided into the lower, middle, and upper parts for analysis. In the upper part of the Et sequence, mudstones with weak parallel foliation are present, and these were analyzed separately from the Et sequence. In these two sequences, the Tc unit shows a black band of organic material concentrations, indicating that very large amounts of terrestrial organic material have been transported. Thin sections of the surrounding turbidite sequences were also observed, although not in the same sequence. Thin section observations were made of the lower sandstone layer (Ta) and the upper fine-grained layer (Td~E) of turbidite. Because the units of the turbidite sequence are different, the grain sizes are very different on both sides. Muddy particles and sea greenstone were also observed as characteristic materials. Muddy particles in the turbidite are considered to be mud and sea greenstone that were deposited on the seafloor at that time, while large quartz particles are the main materials in the Ta, but muddy particles larger than 0.2 mm and sea greenstone were also observed. On the other hand, the upper fine-grained layer contains more fine-grained mud particles and sea greenstone, which may provide a clue to how the turbidite-forming turbidite flow scraped and deposited the seafloor sediments at that time.

2.2.2 Horokanbesawa River (Abetsu and Nibutani formations)

Horokanbesawa river where located in Mukawa town is exposed upper Abstsu and Nibutani formation (about 2km). The Abetsu Formation (coarse-grained sand and mud alternation), the Nibutani Formation (fine-grained sand and mud alternation), and the Nina formarion (fine-grained sand and mud alternation and gravel) are exposed as Middle to Late Miocene sedimentary layers in the Hidaka Basin. These sedimentary layers have been dated by radiolarian and diatom assemblages, and the Abetsu Formation is estimated to be 15.3-12.5 Ma, the Nibutani Formation 12.5-9.7 Ma. Abetsu formation is consisted of turbiditic sandstone and mudstone and several turbidites has organic laminations and organic partucles, indicated these turbidites might

be formed by flood or flood-related turbiditic current. Nibutani formation is consisted of sandy mudstone and hardshale mudstone, and several nodules (siliceous and calcareous). Turbidites which deposited as Abetsu formation tend to about 10cm thickness, contain organic particles sometimes formed parallel lamination. These turbidites are similar to the turbidites in Kawabata formation in the presence of organic particles and lamination. However, the depositional setting is different between the Ishikari and Hidaka basins where the Kawabata and Abetsu formation was deposited, and these turbidites are important samples for studying the depositional process of turbidites containing organic matter. In this study, I sampled several types of sedimentary rocks. Turbidites containing organic particles were collected from Abetsu formation for comparing organic-rich turbidites sampled in Kawabata formation. Mudstone samples were collected from Abetsu and Nibutani formations to investigate paleoenvironment change in Hidaka basin during Middle-Late Miocene. Furthermore, calcareous nodule and surrounding sedimentary layers were sampled to investigate calcareous concretion forming. And, to compare other nodules, I analyzed other nodules exposed Horokanbesawa river.

2.2.3. Haegawa River (Nina formation)

The Haegawa River where this sample was collected is located in Hidaka Town. The Nina formation deposited during Late Miocene is exposed for about 4 km in the Haegawa River, and the upper part of the Nibutani Formation is distributed in the upper reaches of the river due to unconformity. The lithology consists mainly of mudstone to sandy mudstone, occasionally interbedded with turbidite beds with parallel lamination. Diatom assemblage analysis indicates that the age of the Haegawa Nina formation is 9.7-3.5 Ma (Maruyama et al. 2018), suggesting that sedimentary rocks from the late Miocene to early Pliocene are continuously exposed. I collected 77 mudstone sample for paleoenvironment research. Furthermore, the upper Nina formation tend to be coarse-grained, and the uppermost strata are dominated by conglomerates, which are considered to be channel-filling sediments. And several turbidites containing organic matter were also identified in the upper part of the Kana Formation. In this study, these turbidites were also sampled in order to compare them with the organic-bearing turbidites of the Kawabata and Abetsu formations.

2.3. Method

2.3.1. Biomarker Analysis

Lipid analysis was performed according to Sawada et al. (2013). Sedimentary rock samples were surface scraped and crushed, and extracted with methanol, methanol/dichloromethane (1/1 v/v), and dichloromethane. They were separated by silica gel columns into an aliphatic hydrocarbon fraction (F1), an aromatic hydrocarbon fraction (F2), a ketone ester fraction (F3), and a polar fraction (F4). The GC column was Agilent technologies DB5-HT (30 m x 0.25 mm x 0.1 μm). The GC column was Agilent Technologies DB5-HT (30 m × 0.25 mm × 0.1 μm). The GC inlet temperature was 310°C, and injection was performed in the splitless mode. The oven temperature was raised from 50°C to 310°C at 4 °C/min and held for 20 minutes after reaching 310°C. The carrier gas was high-purity helium. The carrier gas was high-purity helium at a flow rate of 2 ml/min. Ionization in the mass spectrometer was performed by the electron impact (EI) method at an

ionization voltage of 70 eV. Ion detection was performed at m/z 50-650 with a scan interval of 1.9 (scans/second) from 5 to 40 minutes and 1.3 (scans/second) from 40 to 89 minutes. The retention index (Kovats Index) was determined by GC/MS measurement of a sample containing a mixture of n-alkanes and n-C24D50 as an internal standard.

$$I = 100\ \{\log(tsa / tA) / \log(tA+1 / tA) + A\}$$

Where tsa: retention time of the compound to be measured, tA: retention time of the n-alkane detected immediately before the compound of interest, tA+1: retention time of the n-alkane detected immediately after the compound of interest, A: the carbon number of the n-alkane detected immediately before the compound of interest. The retention times for the aromatic hydrocarbon fraction (F2) and the ketone/ester fraction (F3), which do not contain n-alkanes, were calculated based on the retention times of the n-alkanes in the aliphatic hydrocarbon fraction (F1). Tetracosane-d50 (n- C24D50) was added as an internal standard for quantification.

2.3.2 Alkenone-SST calculation

UK'37 was used because 4-unsaturated C37 alkenone was not detected in the Alkenone paleowater temperature reconstruction (Prahl and Wakeham.,1989), and We were used several calibration curve to check reliability of SST reconstruction.

$$UK`37 = [C37:2]/[C37:2][C37:3]$$

$$SST^{UK} = (U^{K'37} -0.039) / 0.034 \text{ (Prahl et al.,1988)}$$

$$SST^{UK} = (U^{K'37} +0.204) / 0.044 \text{ (Sawada et al.,1996)}$$

$$SST^{UK} = (U^{K'37} +0.52) / 0.049 \text{ (Volkman et al.,1995)}$$

2.3.3. Kerogen analysis

The sample residues after organic solvent extraction were dried, each placed in a 500 ml plastic tube, and then 100 ml of 6N HCl was added and the samples were de-ashed in a bath shaker with the water temperature set to 60°C for about 12 hours with stirring. The sample was left to settle to the bottom, the supernatant solution was discarded, distilled water was added and centrifuged (3000 rpm, 20 min), and the supernatant was discarded. After repeating the centrifugation procedure two or three times, 50 ml of a mixture of 25 ml of 46% HF and 25 ml of 12N HCl was added to each tube, and the tubes were stirred in a bath shaker with the water temperature set at 60°C for about 24 hours. To each plastic tube, 50 ml of a mixture of 30 ml of 46% HF and 20 ml of 12N HCl was added and stirred for about 12 hours. The sample was allowed to settle, the supernatant was discarded, distilled water was added and centrifuged (3000 rpm, 20 min), and the supernatant was discarded. After repeating the centrifugation operation two or three times, the sample in the plastic tube was transferred to a centrifuge tube, distilled water was added, and further centrifugation (2500 rpm, 15 min) was performed until the washing solution became neutral, while checking with pH test paper.

A cover glass was placed on a hot plate covered with aluminum foil with the temperature set at 115-140℃. The sample after kerogen separation was diluted with distilled water until light passed through it when it was aspirated with a Pasteur, dropped onto the cover glass, dried, and then entranulated with a drop of entranulose. The cover glass was then inverted and placed over a glass slide. After adhering, the perimeter of the cover

glass was reinforced with manicure. The kerogen preparation was observed using a transmission microscope and a fluorescence microscope. Microfossils that were found during kerogen observation, which were thought to be dinoflagellate microfossils, were photographed in transmission and fluorescence, and the photographs were examined by Keiichi Hayashi of the Geological Research Institute, Hokkaido General Research Organization.

Equipment used

Olympus fluorescence microscope image analyzer: DP70
Microscope: Olympus: B×41
Gradient fluorescence system: Olympus U-LH100HG
Mirror unit: U-MWU2
Dichroic mirror : DM400
Excitation filter : BP330-385
Absorption filter : BA42
2-1.4.3. Total organic carbon content Powdered sediment samples were acidified with 3 M HCl to remove carbonate. Subsequently, these
samples were dried on hotplate for over 6 hours. Dry samples were analyzed for TOC content by a J-Science Micro Corder JM10 at the Instrumental Analysis Division, Equipment Management Center, Creative Research Institution, Hokkaido University

2.4. Result

2.4.1. Turbidites in the Kawabata Formation

n-Alkane derived mainly from plant wax components, mostly from plant leaves. Plants have only odd-numbered carbon n-alkanes under biosynthesis. n-Alkanes are largely contributed by leafy angiosperms and are sometimes considered as markers of angiosperms. n-Alkanes are the most basic constituents in organic geochemistry and have been the subject of a great deal of research. The concentration of n-alkane in the Kawabata Formation turbidites shows a maximum in the organic matter concentrated layer (Tc). In particular, the sharp peak in the L sequence indicates that n-alkane is concentrated. n-Alkanes were deposited in large amounts in the B sequence, although not as pronounced as in the L sequence.

Sterane is a serially modified component of sterol, a component of biological membrane lipids, and has a structure in which the hydroxyl group is removed from the sterol. It has a structure in which the hydroxyl group has been removed from the sterol, and the double bond has basically been lost. Like sterols, steranes are derived from different organisms depending on their carbon numbers. C27 steranes are mainly derived from marine algae, while C29 steranes are derived from higher plants. Characteristically, C29 sterane tends to be dominant at Tc in both B and L sequences, while other units do not show as high a value as Tc, indicating that terrestrial plant components are also concentrated at Tc in steranes. The C27 sterane, a marine algae component, showed little change in the B sequence, which is significantly different from the C29 sterane, and the L sequence was similar, but the concentration tended to increase in the upper fine-grained layer, indicating that the marine algae component was deposited after the terrestrial plant component was concentrated, indicating that the terrestrial component and the marine algae component were separated. The diterpenoids are also found in the upper fine-grained layer.

Terpenes are organic components composed of isoprene (C5). Diterpenoids are gymnosperm markers, with gymnosperms being the primary organism of origin. The components produced differ to some extent among plant species and can be used to restore coniferous vegetation (Aoyagi 2017). The diterpenoid concentrations are shown in the figure, and it can be seen that the trend is similar to that of n-alkanes, with higher values at Tc. However, the trend in diterpenoid concentrations is weaker than that of n-alkanes, and as mentioned above, the contribution of angiosperms to n-alkane concentrations is significant, and the trend observed for n-alkanes is weaker for diterpenoids, which may indicate that the fractionation effect that worked strongly for angiosperms is not so strong for gymnosperm components This result may indicate that the strong segregation effect in angiosperms is not so strong in gymnosperm components.

Triterpenoids (C30), composed of six isoprene, are produced by angiosperms and include oleanoid, ursanoid, and lupenoid synthesized by angiosperms and gammacerane-type bones synthesized by ciliates and some anaerobic protists. Tetrahymanol, which has a gammacerane-type skeleton, is synthesized by ciliates and some anaerobic protists. Unlike diterpenoids synthesized by gymnosperms, triterpenoids show little difference in composition depending on the species of origin, and triterpenoids are rarely used to restore angiosperm vegetation. However, it has been pointed out that only for lupenoids, there is a bias toward plants synthesized to some extent, and as described in the introduction, birch, alder, and katydid families are considered to be the main origins of lupenoids.

Tetracyclic triterpenoids with the A ring missing are called des-A triterpenoids (A-ring cleaved triterpenoids). des-A triterpenoids include oleanane-type, ursane-type, and lupine-type triterpenoids, which are distinguished by GC-MS Retention The oleanane, ursane, and lupine forms of Des-A triterpenoids can be distinguished by GC-MS retention time and cleavage pattern. In the aliphatic degenerate fraction, saturated des-A triterpenoids have a molecular ion peak (M^+) of 330, monounsaturated 328, and diunsaturated 326, which distinguishes components with different degrees of saturation. des-A triterpenoids were also detected in the aromatic hydrocarbon fraction, with monoaromatic (M^+: 310), diaromatic (M^+: 292) and triaromatic (M^+: 274) rings.

C-ring cleaved triterpenoids are components in which the C ring (carbon position 8-14) of a normal pentacyclic triterpenoid is opened. Although several examples have been reported (Nakamura et al. 2011; ten Haven et al. 1994), the mechanism of their formation is largely unknown. This component was also detected in Kawabata turbidite, and it is speculated that it may be related to des-A triterpenoids, but this study will not discuss this component.

The figure shows the concentrations of diterpenoids and triterpenoids from angiosperms, which show a similar trend to that of diterpenoids, but with more pronounced variations than diterpenoids. The trend is very similar to that of n-alkanes, suggesting that n-alkanes and triterpenoids have the same deposition and fractionation effects. The concentration of triterpenoids is also significantly higher than that of n-alkanes, indicating that the contribution of angiosperms to the organic matter contained in the turbidites of the Kawabata Formation is very high.

The number of carbons of n-alkanes differs roughly depending on the origin of the organisms, allowing for the reconstruction of past vegetation information. In particular, carbon numbers 23 (C23) and 25 (C25) are mainly synthesized by aquatic plants that grow in the aquatic environment, and an indicator including carbon numbers 29 (C29) and 31 (C31), which are mainly synthesized by terrestrial higher plants, has been proposed (Ficken et al.,2002). This index is expressed by the following equation and evaluates the contribution of aquatic vegetation to the total vegetation.

The Paq value at Ta overestimates the proportion of C23 and C25 n-alkanes. above Tc also showed a decreasing trend toward the top of the sequence, but this trend was not pronounced. The same is true for the B sequence. Furota et al. (2019), who analyzed organic matter-enriched sandstones, found a large increase in Paq in the sandstone section, suggesting a contribution from the aquatic environment, but no significant contribution from aquatic vegetation in the aquatic environment was found in the turbidites analyzed in this study.

The land/sea ratio in the sediments can be calculated from the ratio of C27 sterane to C29 sterane; C27/(C27+C29) showed a large variation in the L sequence. The contribution of the marine component is particularly large in the lower sandstone layer (Ta) and the upper fine-grained layer (Et/Ep), while in the organic-rich layer (Tc), the contribution of the marine component almost disappears and the terrestrial component becomes very large. A similar trend was observed in the B sequence, but it was not as pronounced as in the L sequence. This may be due to the fact that the B sequence is farther from the main body of the

turbidite flow due to the thickness of the sequence and the lower sandstone layers, and the scale of the turbidite flow and the velocity of the flow did not change as rapidly as in the L sequence.

The Carbon Preference Index (CPI) is an index of n-alkane concentration. This index evaluates the degree of sedimentary succession based on the odd dominance of n-alkane. In the L sequence, there is a gap in CPI values between the lower sandstone (Ta) and its upper layers, with a CPI as low as 1.5 to 2 in Ta and as high as 3 from Tc to the top, indicating that the degree of diagenesis differs between the lower and upper sandstone layers. Since this sequence was formed by a single turbidite flow, this difference in continuity may indicate that the n-alkanes were fractionated according to their degree of maturity. In the case of highly aged organic material, this phenomenon is expected to occur because the density of the material is expected to increase due to the carbonization process. It is also possible that this difference in maturity simply indicates that maturation was more advanced in the sandstone section. Although further discussion is needed, it is quite possible that n-alkanes are fractionated according to their degree of diagenesis, since no such trend is observed in the other diagenetic indices discussed below.

Sterane and diasterane, which are formed from sterols, have a chiral center at the 18th carbon position of the sterane skeleton and are classified into S- and R-bodies. In vivo, only R-body sterols are synthesized, but post-embedding diagenetic changes result in the formation of S-body steranes and diasteranes. The ratio of the two can be used to evaluate the degree of synthesis. The S/S+R ratios of both sterane and diasterane show little change within the sequence, indicating that there is no change in the degree of sterane-diasterane sequential formation within the sequence. This is different from the results of the CPI with n-alkanes, and the difference in the results between these derived indices may indicate the fractionation effect of n-alkanes by their derived degrees, as described above.

This index indicates the percentage of Des-A triterpenoids (All angiosperm) in all triterpenoids from angiosperms in the aliphatic hydrocarbon (F1) and aromatic hydrocarbon (F2) fractions. The percentage of des-A triterpenoids in both B and L sequences is more than 50%, indicating that the organic matter transported by the turbidity current contains a large amounts of des-A triterpenoids.

Diterpenoids are a component of conifers, of which Pinaceae is the major source, and the amount of diterpenoids is considered to be constrained by the Pinaceae vegetation in the hinterland. On the other hand, phyllocladane is not synthesized by Pinaceae conifers, and is mainly derived from conifers other than Pinaceae, such as Cypress. Therefore, the phyllocladane/diterpenoid ratio can be used to evaluate the proportion of non-pine coniferous components in coniferous components. The phyllocladane/diterpenoid ratios exceed 10% in both the B and L sequences, which is higher than the organic matter enriched sandstones reported in Furota et al. (2019). Only in the L sequence, values exceed 30% in the organic matter-enriched layer (Tc), suggesting that phyllocladane was enriched and deposited at Tc.

2.4.2. Turbidites in Hidaka basin (Abetsu and Nina Formation)

Turbidites in the Hidaka Basin contain gymnosperm (diterpenoids), angiosperm (triterpenoids), and microbially degraded angiosperm (hypocotyl triterpenoids) components. Diterpenoids and triterpenoids are thought to be formed in the vegetation at that time, while degraded triterpenoids undergoing microbial

degradation are thought to be formed in terrestrial aquatic environments such as wetlands and peatland. Diterpenoids and reduced triterpenoids remained almost unchanged in concentration throughout the sequence, while triterpenoids were present at high concentrations throughout the sequence. In particular, the maximum value was observed in the unit where organophytic foliage develops, suggesting that the turbidite flow that formed the Abetsu layer contained high concentrations of angiosperm components. The high concentration of triterpenoids only may be due to the direct transport of angiosperm components from the mountain areas.

The Nibutani Formation is composed of fine-grained sandy mud alternation and siliceous mudstone, and the frequency of turbidite layers decreases and becomes thinner than that of the Abetsu Formation. In a previous study, it was suggested that a change in the tectonic field may have reduced the sedimentation rate of sedimentary basins and weakened their burial effects (Kawakami, 2013). Siliceous mudstones may also indicate an increase in diatom production, suggesting that the sedimentary basin has changed to a pelagic environment. Among the terrestrial higher plant components, the capsid component is significantly reduced, and the organic matter composition suggests that the direct terrestrial mass transport observed in the Abetsu Formation has been weakened.

On the other hand, in the lower and middle part of the Nina Formation, fine-grained sand and mud alternation continues, and typical thick turbidite is not evident, but in the upper part of the Nina Formation, the sedimentary facies changes to one dominated by conglomerate, and coarse-grained turbidite is intercalated between the conglomerate layers. This lithological change is thought to have caused a shift from a relatively pelagic environment to one in which active burial occurred in the Nina formarion. In the coarse-grained turbidite beds, organic matter concentrations including branches and bark were observed, indicating that terrestrial higher plants were transported directly from the land, similar to the Abetsu Formation, and that active terrestrial material transport was driven intermittently in the Hidaka Basin from the middle to late Miocene. Changes in the organic matter composition of the Nina formarion will also be discussed.
[Paleoenvironment] Several species of cedaritic plant components were detected in all turbidite units as characteristic organic components. Since cedar plants grow in temperate regions with high winter precipitation, it is possible that a similar environment prevailed in the Hidaka area at that time. Since high winter precipitation is a factor that increases river water volume and snowmelt floods during the snowmelt season, a temperate climate with high winter precipitation may be a condition for a sedimentary system that transports organic matter to the ocean floor.

2.4.3. Calcareous concretion of Nibutani formation

The calcareous concretion is very hard, while the surrounding sedimentary layers are soft, suggesting that it was clearly formed by post-depositional processes. Observation of thin sections indicates that the concretion contains mudstone clast, which may have been incorporated during the formation of the calcareous concretion. Biomarker analysis shows anomalous concentration of phytane in the concretion, with a predominant peak in the F1 fraction. Peaks of methanogenic biomarkers such as PMI and squalane were also detected. On the other hand, n-alkane was present in low concentrations, especially in the long-chain n-alkane, suggesting a lack of biomarkers derived from terrestrial plants. This trend is also true for

other fractions (F2, F3), such as terpenoid, which is also at very low concentrations. In the mudstone layers surrounding the calcareous concretion, phytane, PMI, and squalane are detected, but not in as high concentrations as in the concretion. This suggests that the concentrations of Phytane and methanogenic biomarkers are unique to carbonate concretions. On the other hand, no such trend is observed in other nodules, suggesting that the concentrations of Phytane and methanogenic biomarkers are specific to the calcareous concretion of the lowermost Nibutani Formation.

2.4.4. Profiles of paleoenvironmental proxies in Hidaka basin deposited during Middle-Late Miocene

The mudstones exposed in the Haegawa River show low degree of maturity (CPI=ave.5.9) and preserved various biomarkers very well. In particular, alkenone which derived from haptophytes, was detected in almost mudstone samples of the Nina formation exposed in Haegawa river.

Alkenone is a proxy that could reconstruct past SSTs, but it is known that the SST calibrations is different depending on the producing species. The alkenone composition, which is important to determine alkenone-producing species, is mainly C37:2 and C37:3 alkenone, with little or no C37:4 alkenone which is produced by haptophytes living in coastal areas and lakes. This result indicates that alkenones detected in mudstone of Haegawa river were produced by Group III haptophytes. Three SST calibrations were examined for Group III haptophytes(Prahl et al.,1988; Volkman et al.,1995; Sawada et al.,1996). Among the three calibration, the calibration of *G.oceanica* in Mutsu Bay (Sawada et al.,1996) is the coldest and most realistic water temperature. According to this result, I used this calibration for reconstruction of SST. The SSTs temperature which reconstructs in Haegawa river tended to be generally hotter than modern Hokkaido, and the SST trend in Hidaka basin is gradually decreased during 10-6Ma. To evaluate ocean primary productivity, I calculated the concentration of C37 alkenone (C37:3 + C37:2 alkenone). The C37 alkenone concentration tended to increase gradually during 10-6M. On the other hand, there are some stratigraphic units with significantly low concentrations even in the upper part of the Nina formation. This may be due to the distribution of turbidite mudstones in the upper part of the Nina formation. The average chain length (ACL), which is a vegetation index, was calculated from n-alkane, which is derived from the wax component of terrestrial higher plants. The ACL varied widely throughout the Kana layer, suggesting that vegetation variation was recorded from 10-6 Ma.

2.5. Discussion

2.5.1. Organic Matter Transport and Separation in Mixed Flow

The concentrations of n-alkane (leaf component) and terpene (lumber component) are concentrated in the organic matter concentrated layer (Tc) in both the B and L sequences, indicating that no segregation of leaf and lumber components occurred in a typical turbidite sequence and that organic matter was concentrated at a certain velocity during turbidite flow. This is in sharp contrast to the results of Furota et al (2014), who reported the presence of fractionation of leaves and timber components in organic matter-enriched sandstones.

The organic matter-enriched sandstones reported by Furota et al (2014) do not have the upward-graded structures seen in typical turbidite sequences, and the ubiquitous presence of organic matter-enriched layers in

the sandstone section suggests that they were formed by flood flows that had a long duration of flow and constantly transported fresh organic matter from the land during flow It is believed to have been formed by flood currents that constantly transported fresh organic matter from the land during the downstream flow. When flood waters form sediments on the seafloor, they are generally known to flow at relatively slow velocities along the seafloor surface, like density currents, and their flow processes are different from those of turbidity currents in the form of gravity currents, which increase their velocity with each passing flow. Therefore, the organic matter-enriched sandstone reported by Furota et al (2014) is considered to have undergone fractionation reflecting the fine density difference between leaves and wood components under turbidity flow with relatively slow flow velocity and long duration.

On the other hand, the B-L sequence analyzed in this study was formed by turbidite flow with high velocity, such as gravity flow, and organic matter was deposited all at once instead of segregation reflecting the fine density difference between leaves and wood components. Therefore, it is considered possible to estimate the morphology of turbidite-forming turbidite flows from the concentration distribution of leaf and lumber components in turbidite.

An indicator supporting this characterization is Sterane's C27/C29 ratio. The C27/C29 ratio of the B-L sequence shows that the marine component is high in the lower sand layer (Ta) and the upper fine-grained layer (Td, Et, Ep), while the terrestrial component is dominant at Tc, where the organic matter is concentrated, and the leaf and wood components are concentrated at Tc. This result is in harmony with the results of Abundance. In the case of turbidity currents that form Bouma sequences, the high energy of the turbidity currents scours the seafloor, taking in high-density material and expelling low-density material, thereby maintaining gravity flow. The gravity flow is maintained. Therefore, in turbidites formed by such turbidity currents, it is considered that the Ta layer contains marine constituents abraded from the seafloor surface, while the upper fine-grained layer contains marine constituents of lighter density than those transported from the land. In fact, thin sections of the Ta and upper fine-grained layers both contain marine greenstone, which is formed on the seafloor. This suggests that the C27/C29 ratio reflects the physical and sedimentary processes of turbidite-forming turbidites, and is an important indicator for studying the formation process of turbidites and their organic depositional processes.

2.5.2. Variation of terpenoids transported by flood flow

Des-A triterpenoids are very abundant in the B-L sequence and are the major component of organic matter in turbidites. The percentage of Des-A triterpenoids accounts for 60% of the total terpenoids, indicating that many of the transported terrestrial components underwent special microbial degradation. This infers that the main hinterland of the B-L sequence was subjected to special microbial action. As indicated in the introduction, the conditions for des-A conversion to occur require a sedimentary environment in which anoxic water masses develop, such as peat bogs and closed lakes, etc. The organic matter-enriched sandstones in Furota et al (2019) show a relatively low percentage of Des-A triterpenoids compared to pelagic mudstones. This is different from the present results. This may be due to the transport of fresh components from mountain soils in the case of direct terrestrial plant components in the case of organic matter-enriched sandstones. In the

B-L sequence, on the other hand, peat bogs or closed lakes such as glacial lakes, which are subject to microbial decomposition, are thought to be the main depositional sites.

The Phyllocladane/Diterpene ratio, which indicates the contribution of phyllocladane (Phyllocladane) among all conifer components, exceeded 10% and was relatively high in the B and L sequences compared to Furota et al (2019). In addition, only in the L sequence, the value exceeded 30% in the Tc of the organic matter enriched layer, and phyllocladane was enriched, suggesting a contribution of conifers such as cypress. The relatively high contribution of phyllocladane may reflect the vegetation of the hinterland at that time. On the other hand, the reason for this phenomenon of phyllocladane enrichment at Tc is currently unknown. However, it is possible that a resin-like substance specifically formed by coniferous trees that produce phyllocladane, such as cypress, may concentrate at Tc. To elucidate this phenomenon, it is necessary to observe rock thin sections of the phyllocladane-enriched facies and compare them with other turbidite sequences in the riverbed.

The following figure summarizes the results of the biomarker analysis and the depositional effects of the L-sequence: both the organic-rich sandstone of Furota et al (2014) and the B and L sequences analyzed here contain large amounts of organic matter, suggesting that they were affected by flood flow, but the biomarker analysis showed significant differences between them. analysis showed significant differences between the two. The study of turbidites off the coast of Italy by Mulder et al. (2011) indicated that flood currents transform into gravity flow turbidity currents after flowing down to the ocean floor as flood currents, which is typical of turbidite sequences even in flood currents. It is possible that even flood flows exhibit a typical turbidite sequence structure. Therefore, the B-L sequence may have been formed by turbidity flow with a changed flow pattern as pointed out by Mulder et al. (2011), and the depositional effect is considered to be different from that of turbidites formed by turbidity flow of flood origin flowing along the seafloor. The difference in paleo-vegetation information from the terpenoids was described as reflecting the difference in hinterland, but we could not infer at this time what the relationship is between the difference in hinterland and the discharge pattern of the flood flow. Further analysis and comparison of various samples will be necessary in the future.

2.5.3. Process of calcareous concretion forming

Several methanogenic components such as PMI, squalane, and isoprenoid ketones are mainly detected in the carbonate concretion, and the PMI/C27 sterane values are very high, suggesting a high contribution of methanogens. However, PMI and squalane are also detected at significantly higher concentrations in all samples of the Nibutani Formation. This suggests that methanogens were active throughout the middle Miocene in the Hidaka sedimentary basin and were deeply involved in the formation of carbonate concretions. The Pr/Ph ratio, which indicates the redox state, was almost constant at around 0.6 throughout the Nibutani Formation, suggesting a hypoxic environment. Furthermore, the Pr/Ph ratio in the carbonate concretion was extremely low at 0.05. This may be due to the phytane produced by the decomposition of C40 biphytane from methanogens, and may reflect the redox conditions in the sedimentary layer after burial rather than the bottom sedimentary environment at the time of deposition. The relatively high proportion of C27 sterane in the Nibutani Formation indicates a semi-pelagic environment. On the other hand, terrestrial plant-derived

biomarkers such as diterpenoids and des-A triterpenoids were also detected as major components, suggesting that terrestrial source organic matter was actively transported to the deep-sea floor of the ocean basin. The active supply of organic matter from both terrestrial/oceanic sources may have promoted the consumption of dissolved oxygen by microbial decomposition, creating an anoxic environment where anaerobic methane oxidation could have occurred. Therefore, the Hidaka Basin is considered to have provided conditions for the formation of authigenic carbonate rocks throughout the middle Miocene. Therefore, the presence of carbonate concretions is associated with methane-rich fluids, which may have been produced in terrestrial organic-rich turbidite formations.

2.5.4. Paleoenvironmental change of central-southern Hokkaido during Middle-Late Miocene

SST^{UK} shows a consistent decrease from 9.3-8.7 Ma to the end of the Miocene, with minor increase and decrease in SST^{UK} from the end of the Miocene. Ma, 22.3°C from 7.7 Ma to 6.5 Ma, and 18.9°C after 6.5 Ma. These results indicate that the relatively high SST in the Hidaka sedimentary basin has been accompanied by a sudden decrease in water temperature since 8.7 Ma, which is considered to be linked to the decrease in SST in the Japan Sea area due to the weakening of EASM from 7.7 Ma to 6.6 Ma that has been reported so far. The cooling after 6.5 Ma is also suggested to be due to the cooling caused by the weakening of the Kuroshio Current reported from the Pacific region (ODP site 1208) (Matsuzaki et al., 2020). The Hidaka Basin is considered to have been influenced by both the Japan Sea and the Pacific Ocean, but the degree of influence varies with time, suggesting a transition from a phase strongly influenced by the Japan Sea to a phase strongly influenced by the Pacific Ocean at the Miocene/Pliocene boundary.

The concentration of C37 alkenone tends to be relatively high in the stratigraphic levels that indicate cooling. In particular, a maximum of 0.45 μg/g-sedi was observed in the stratigraphic levels after 6.5 Ma. These results suggest an increase in basic production due to enhanced ocean circulation caused by cooling of the ocean surface layer.

The terrestrial vegetation composition calculated from the ACL shows a woody trend between 9.3 and 8.7 Ma, and a more herbaceous trend after that. However, this trend is weaker than the SST variability, which shows large changes. ACL and SST indicates weak negative correlation (R2 = 0.499), suggests an increase in herbaceous vegetation with colder temperatures. Especially after 6.5 Ma, when the SST average is 18.9℃, the correlation coefficient increases to R2=0.623. This suggests that the transition from woody to herbaceous vegetation may occur actively during the cold season, and that the decrease in SST due to the decrease in the Kuroshio inflow may have caused significant changes in the terrestrial vegetation, especially in the Hidaka Basin.

2.6. Conclusion

Samples of two typical turbidite sequences in the Kawabata Formation were analyzed by sedimentary unit and compared with the results of organic-rich sandstones reported by Furota et al.

In the analyzed turbidites, the terrestrial component is predominant in the organic-rich sedimentary unit corresponding to Tc, while the marine component tends to increase in the Ta (lower sandstone) and Td-E (upper fine-grained) sediments.

Sedimentological and organic geochemical analyses were conducted on turbidite sequences of the Abetsu Formation deposited in the Hidaka Basin. Two different types of turbidite were classified into Thin/Thick OM laminations. Differences in the biomarker results may reflect the differences in sedimentary processes and may allow us to identify the origins of flood generating turbidity currents. These differences indicate that the terrigenous matter in the turbidites of the Abetsu Formation was transported from different type land area and/or different source vegetation to the deep sea. Declining triterpenoids show a high contribution throughout the sequence, suggesting possible transport by flooding, as shown by Furota et al (2014).

Among the nodules in the Horokanbesawa nodule, the carbonate nodule contains a high percentage of ANME components, suggesting that it was formed by AOM. Among the polar fractions in the concretion (carbonate), the detection of polymeric components was lower than in the upper and lower layers, suggesting that selective fractionation may have occurred in the inflow of organic matter during concretion formation. In the Nibutani Formation, a reducing environment with ANME has existed throughout the middle Miocene, and the presence of methane-rich pore water may have been a factor in the formation of the carbonate concretion.

Alkenones were preserved until 10Ma, no clear evidence of selective degradation of alkenone.
Tectonic influence on the Haegawa outcrop is considered to be small, which may have contributed to the preservation of the alkenone-SST changing suggesting that the Hidaka sedimentary basin was influenced by both regions. Furthermore, ACL and SST showed a tendency to correlate after 6.5 Ma.

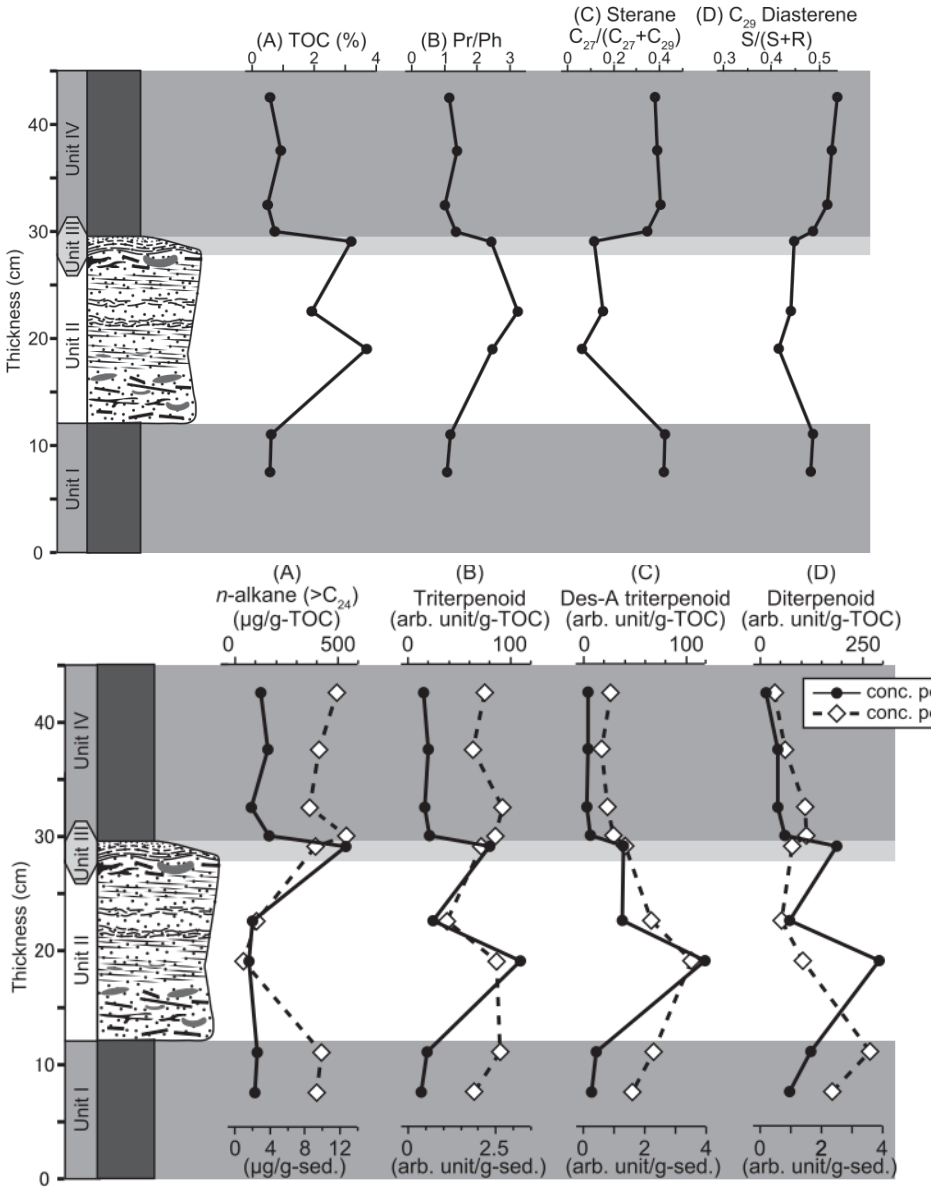

Figure 2.1.1 the profiles of TOC, biomarker index(Pr/Ph, sterane S/S+R, diasterane S/S+R), n-alkane and terpenoid concentrations(triterpenoids, diterpenoids and des-A triterpenoids) [Furota et al.,2014]

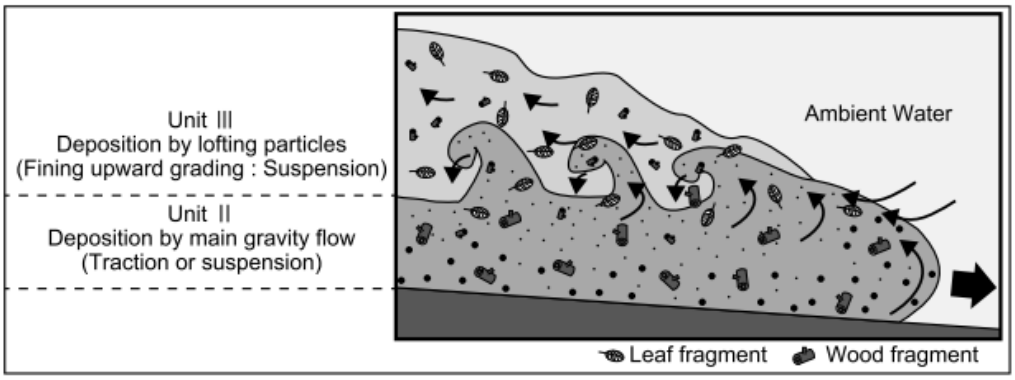

Figure 2.1.2 Scheme for hydrodynamical behavior of terrestrial plant leaf- and woody-derived particles in gravity flow depositional system. [Furota et al.,2014]

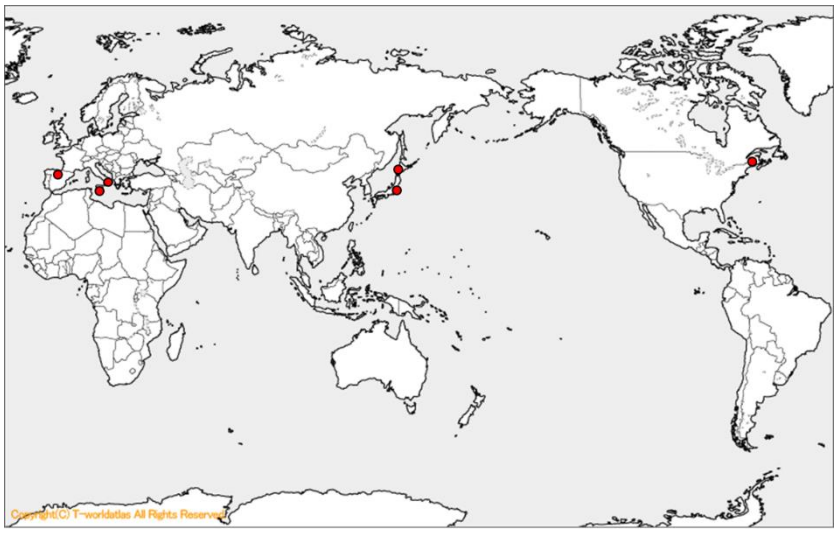

section	country	age	reference
Kiwada Formation	Japan	Pleistocene	Kajita et al.(2021)
Vrica section(southern Italy)	Italy	Pleistocene	Laura.C.Creaveland et al.(2009)
Sicilian Trubi Formation	Italy	Pliocene	C.Beltran et al.(2011)
Yorktown Formation (eastern Virginia)	America	Pliocene	Harry J. Dowsett et al.(2021)
Nina Formation (Hidaka basin)	Japan	Miocene	this study

Figure 2.1.3 the list of the alkenone record detected from land outcrop

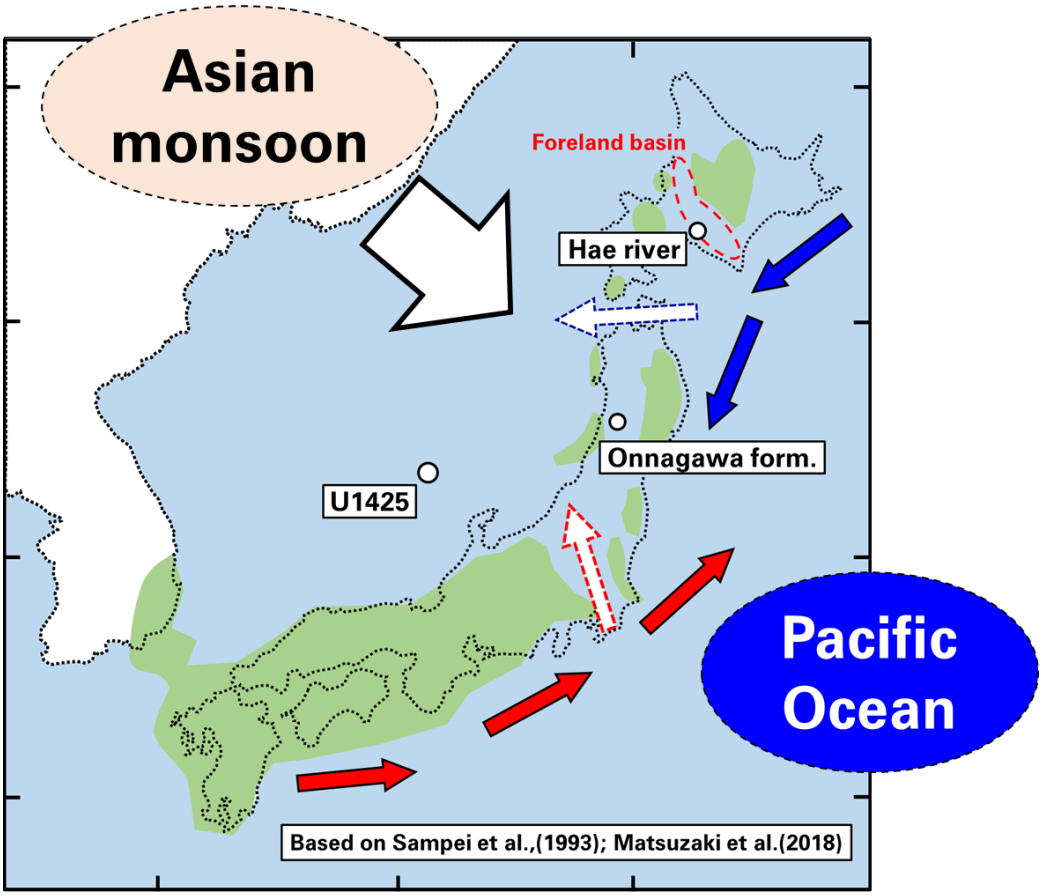

Figure 2.1.4 The geography of Japan during Middle – Late Miocene.

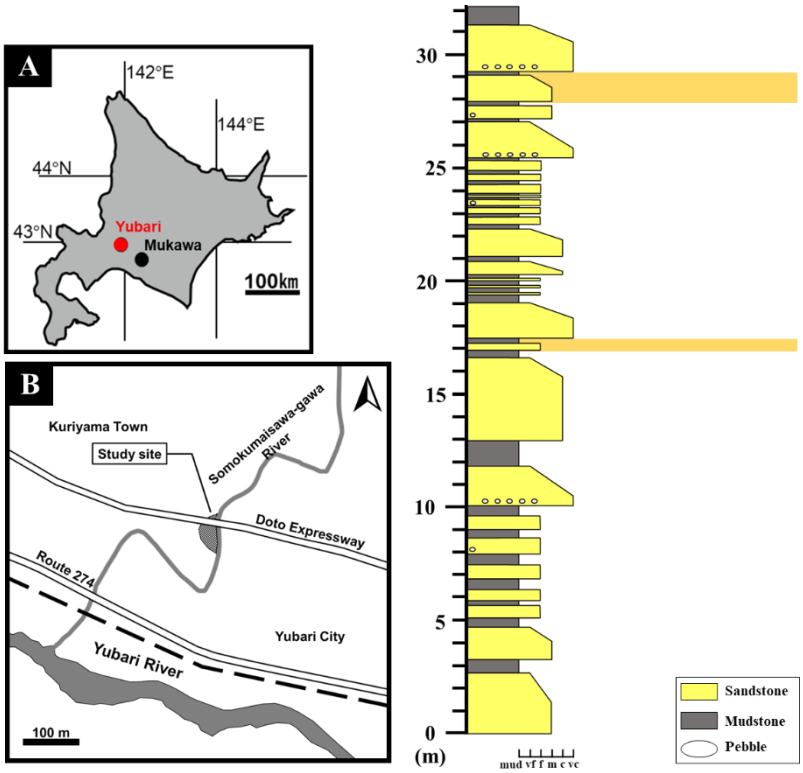

Figure 2.2.1 Index maps showing (A) location of study areas (Yubari and Mukawa, south-central Hokkaido, Japan), sampling locations in (B) the Somokumaisawa-gawa River, Kuriyama town, and lithologic sections of (a) the Kawabata Formation in the Somokumaisawa-gawa River

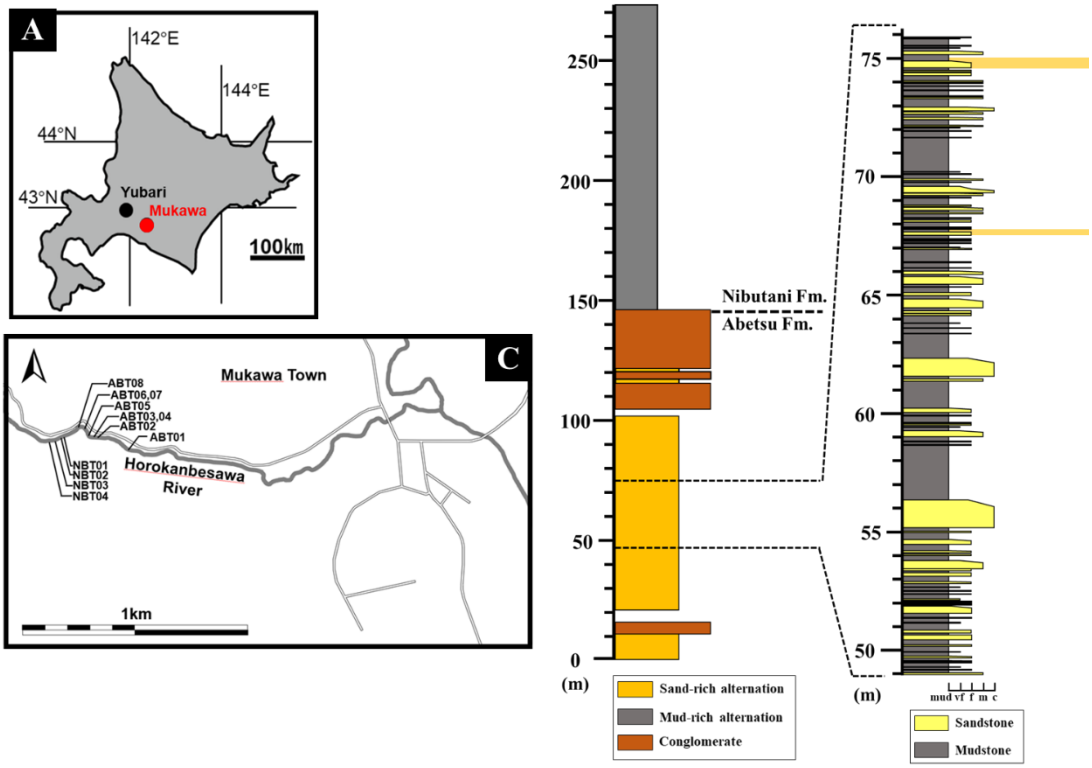

Figure 2.2.2 Index maps showing (A) location of study areas (Yubari and Mukawa, south-central Hokkaido, Japan), sampling locations in (C) the Horokanbesawa-gawa River, Mukawa town, and lithologic sections of the Abetsu and Nibutani formations in the Horokanbesawa River.

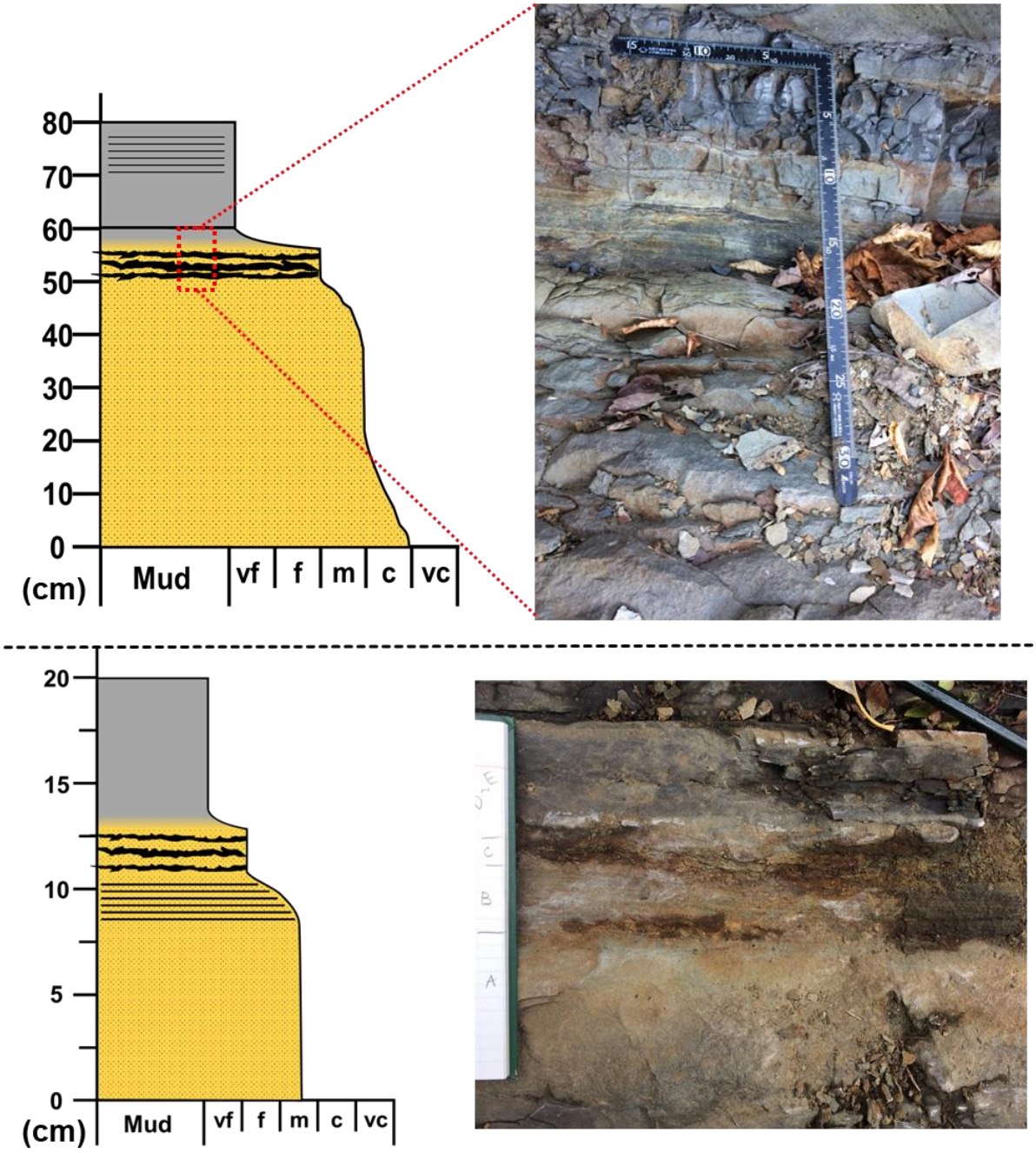

Figure 2.2.3 The geological column and sedimentary structures of turbidite sequence sampled from Soumokumaisawagawa-river (Kawabata Fm.)

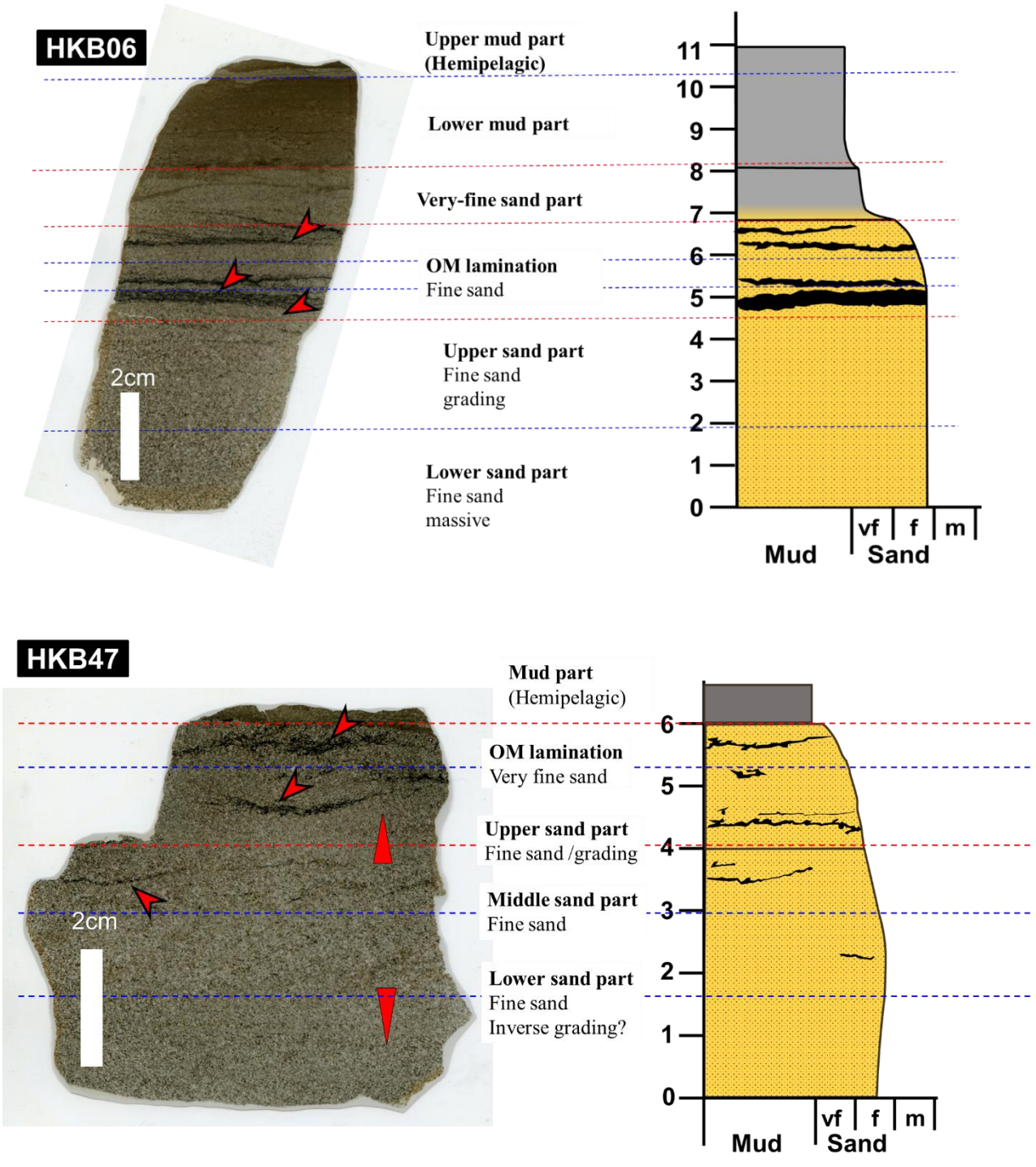

Figure 2.2.4 The geological column and sedimentary structures of turbidite sequence sampled from Hrokanbesawa-river (Abetsu Fm.)

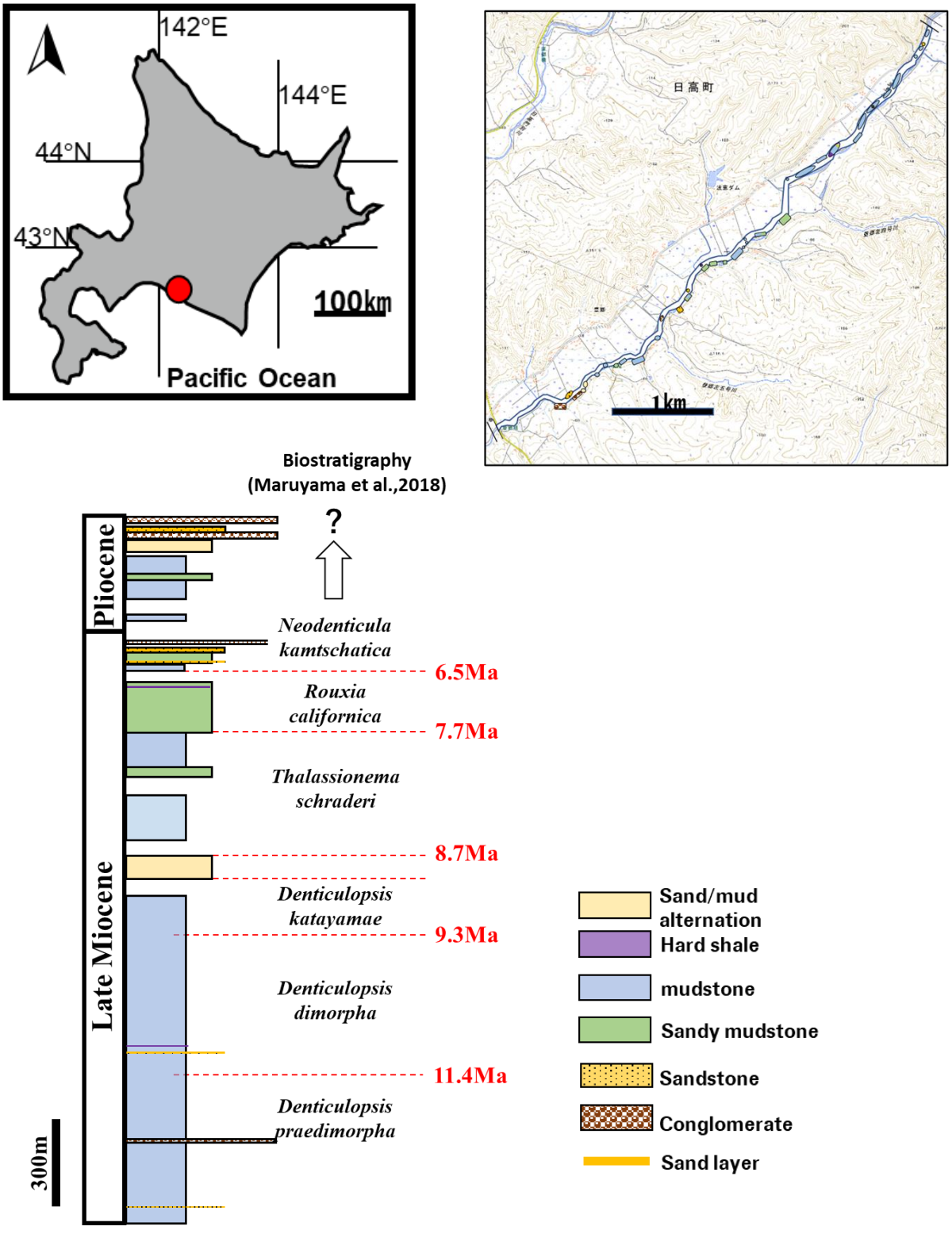

Figure 2.2.5 Index maps showing location of study areas in the Haegawa River, Hidaka town, and lithologic sections of the Nina formation.

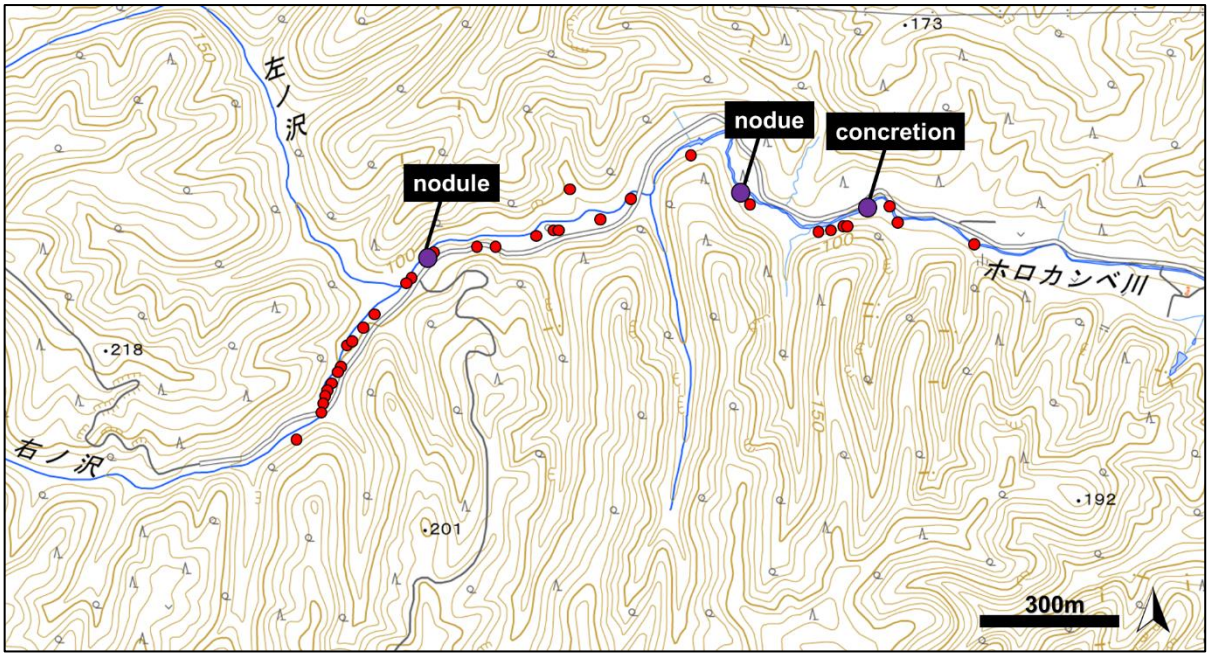

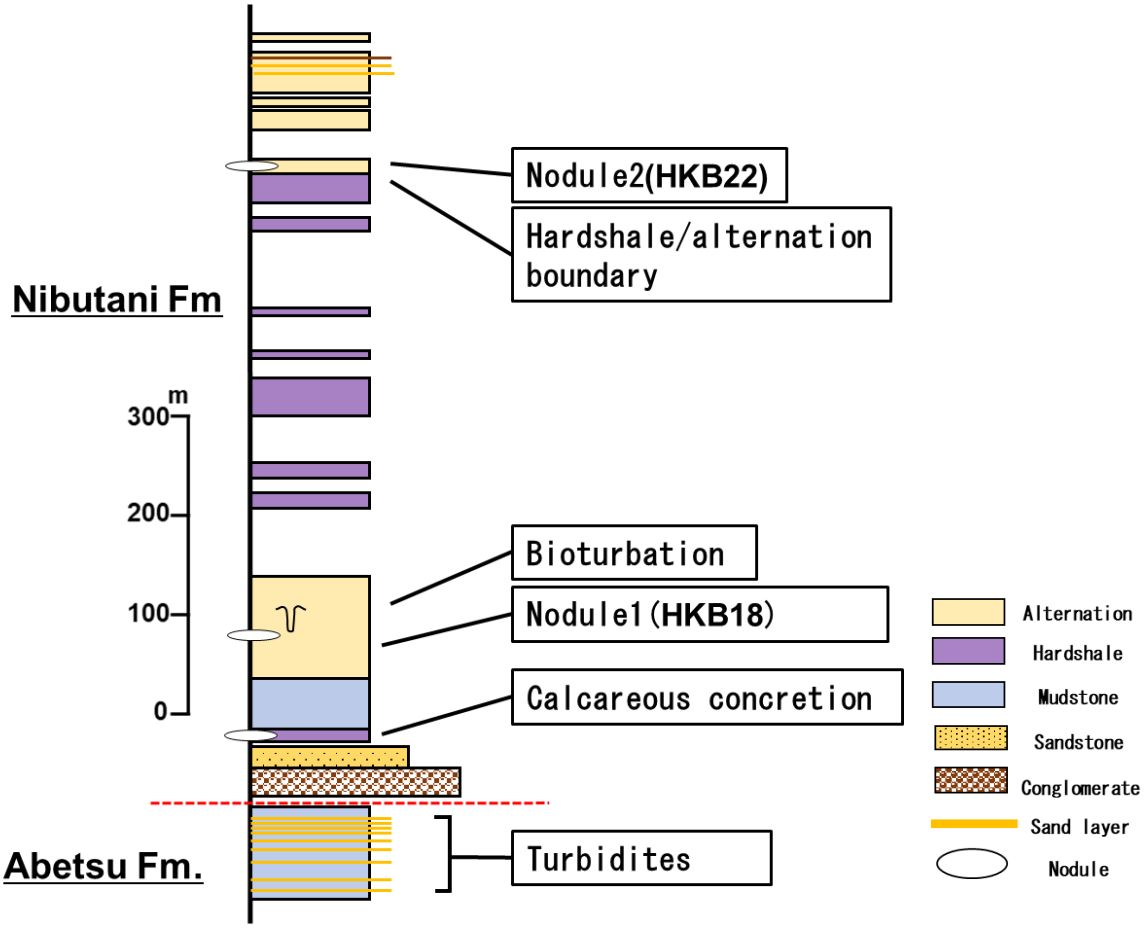

Figure 2.2.6 The maps showing location of study areas in the Horokanbesawa-river, Mukawa town, and lithologic sections of the Nina formation.

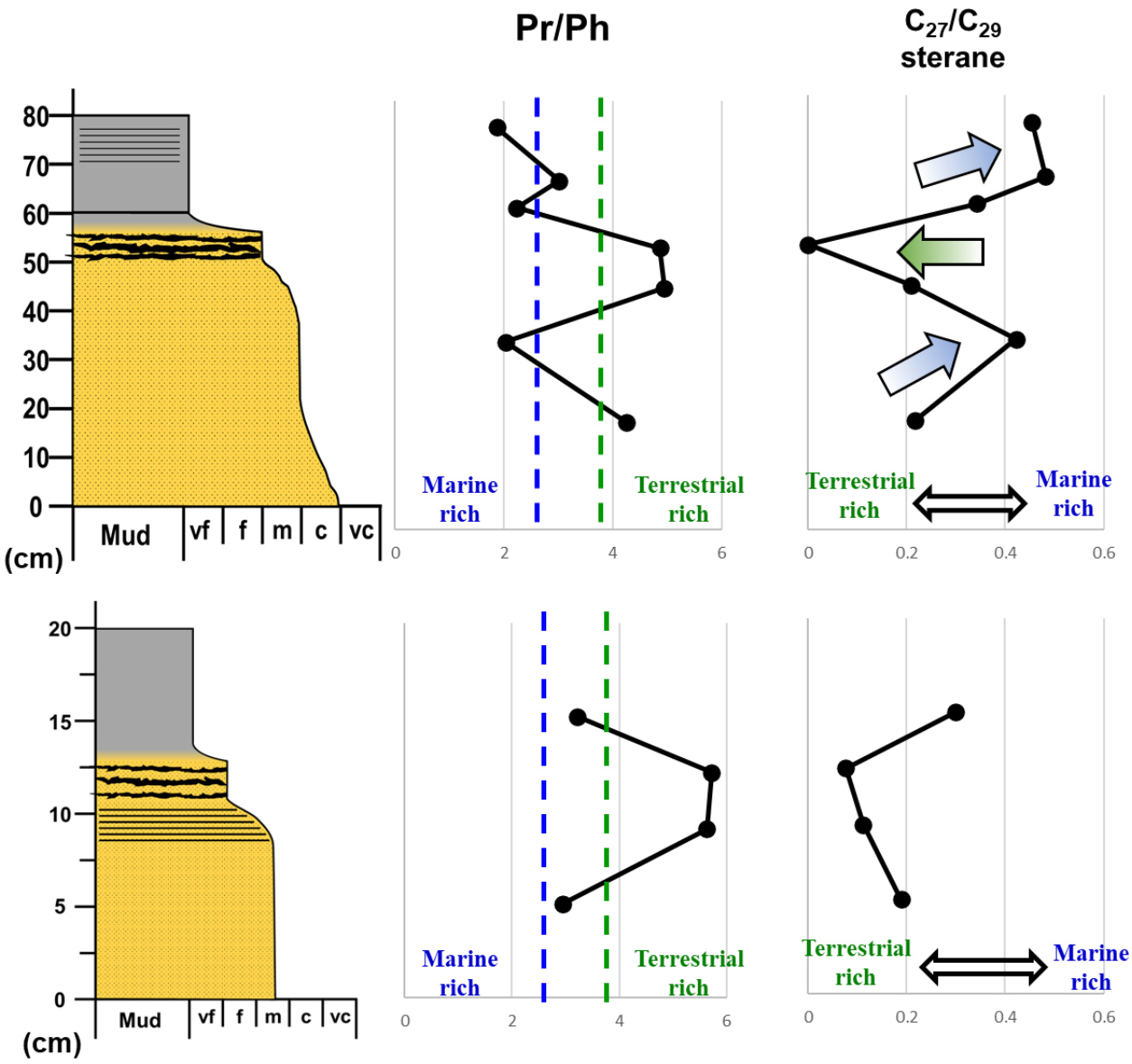

Figure 2.4.1 The vertical profiles of Pr/Ph (redox index) and C27/C29 sterane ratio (marine/terrestrial ratio) of turbidite sequences sampled from Soumokumaisawagawa-river (Kawabata Fm.)

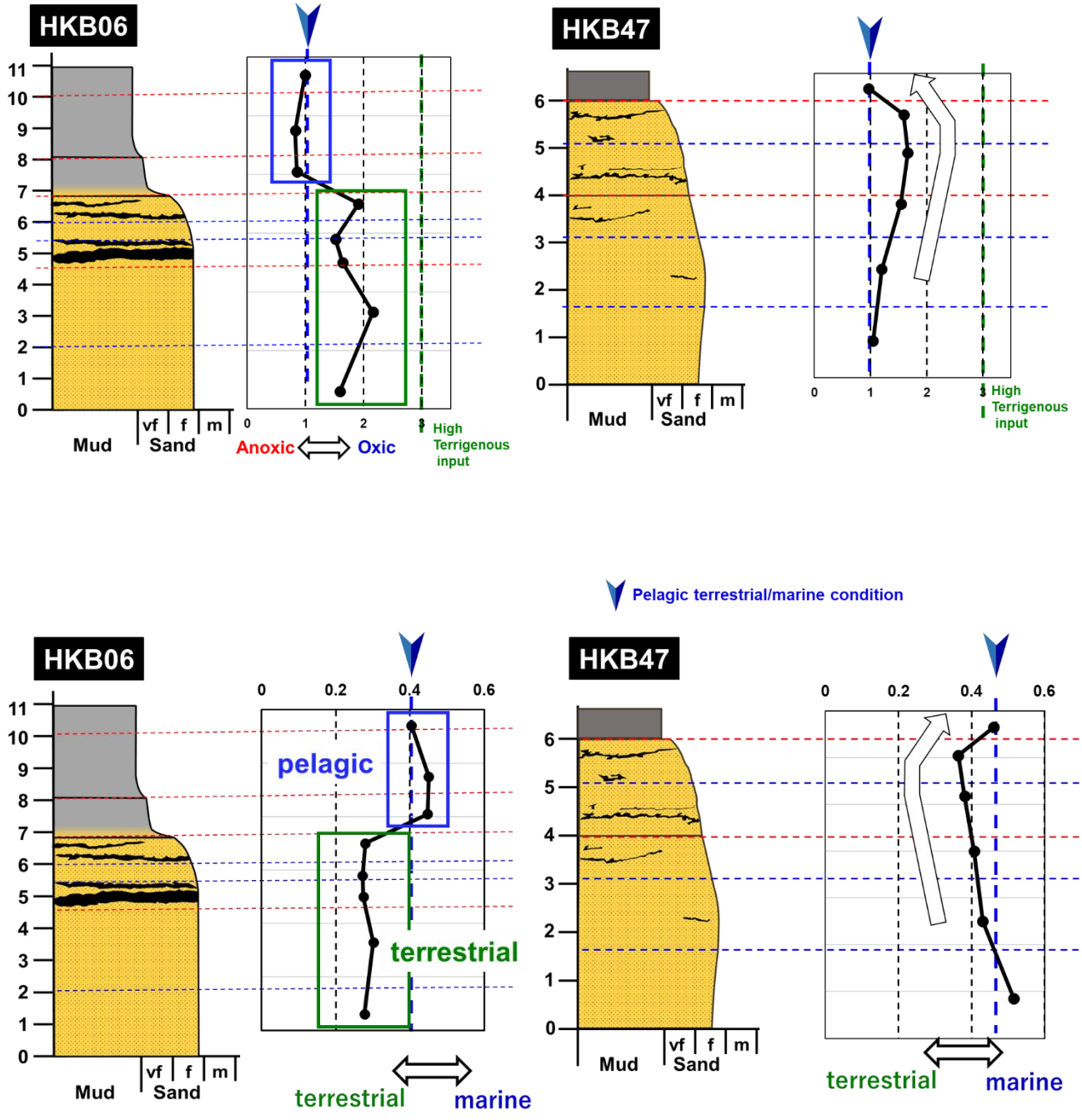

Figure 2.4.2 The vertical profiles of Pr/Ph (redox index) and C27/C29 sterane ratio (marine/terrestrial ratio) of turbidite sequences sampled from Horokanbesawa-river (Abetsu Fm.)

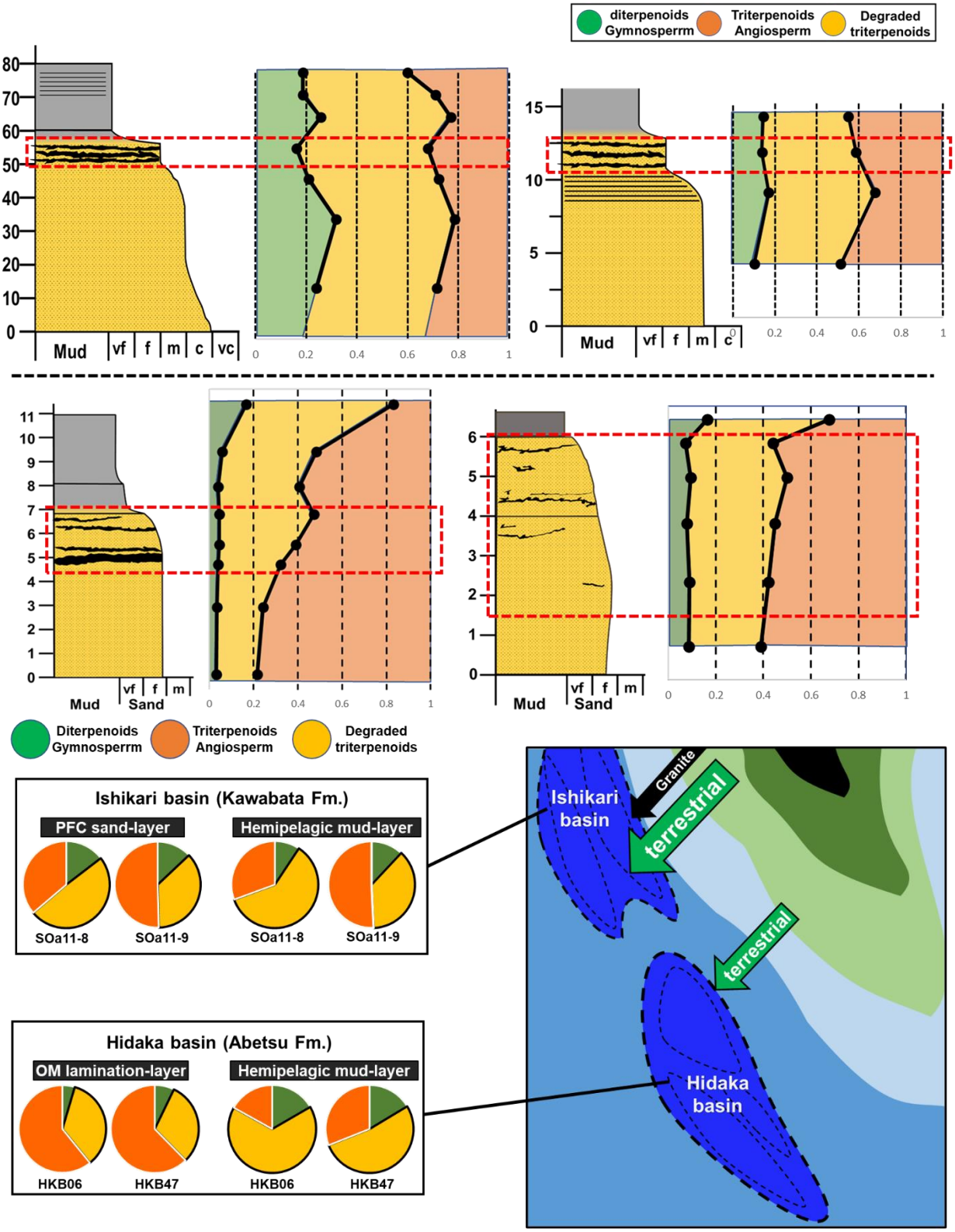

Figure 2.4.3 The vertical profiles of terpenoids composition (diterpenoids:gymnosperm, degraded triterpenoids:angiosperm&anoxic condition, triterpenoids:angiosperm) of turbidite sampled from Kawabata Fm. and Abetsu Fm. And the difference of the composition of terpenoids from Ishikari basin and Hidaka basin.

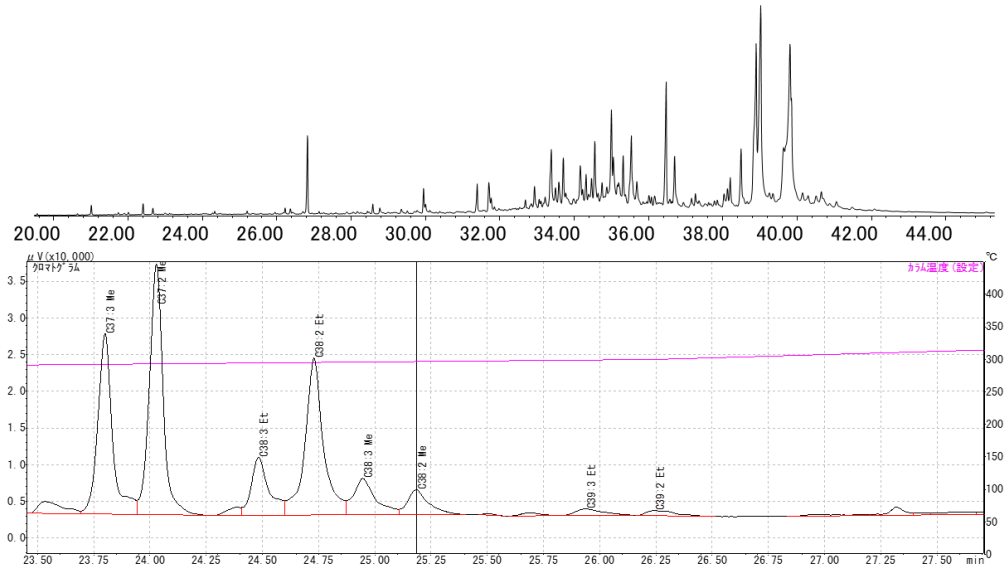

Figure 2.4.4 The TIC chromatograph of Nina formation detected on GC-MS and GC-FID.

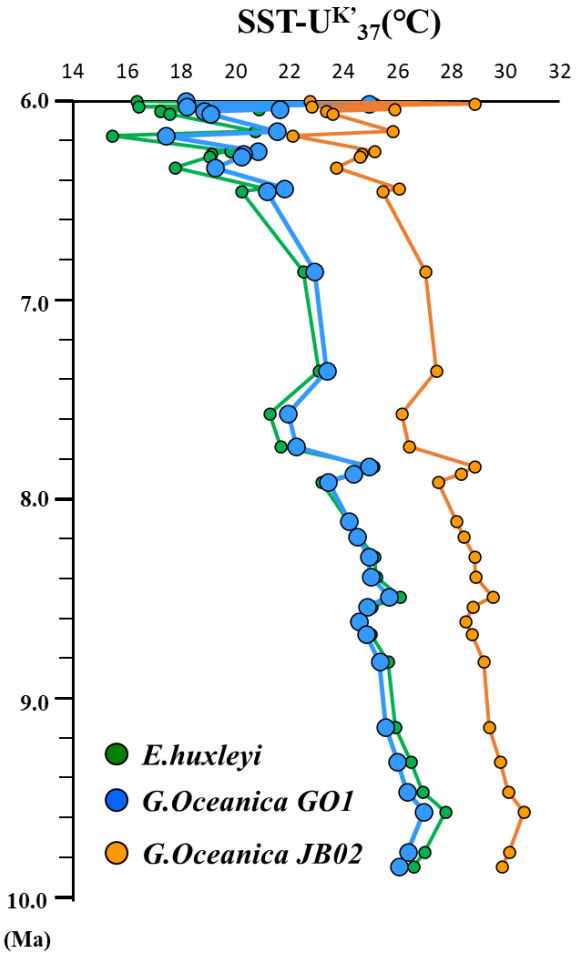

Figure 2.4.5 The vertical profiles of SST calculated by alkenone and alkenone concentration of Nina formation during Late Miocene and reconstruction of paleoceanography of Hidaka basin according to Prahl et al. (1988), Volkman et al. (1995), Sawada et al. (1996).

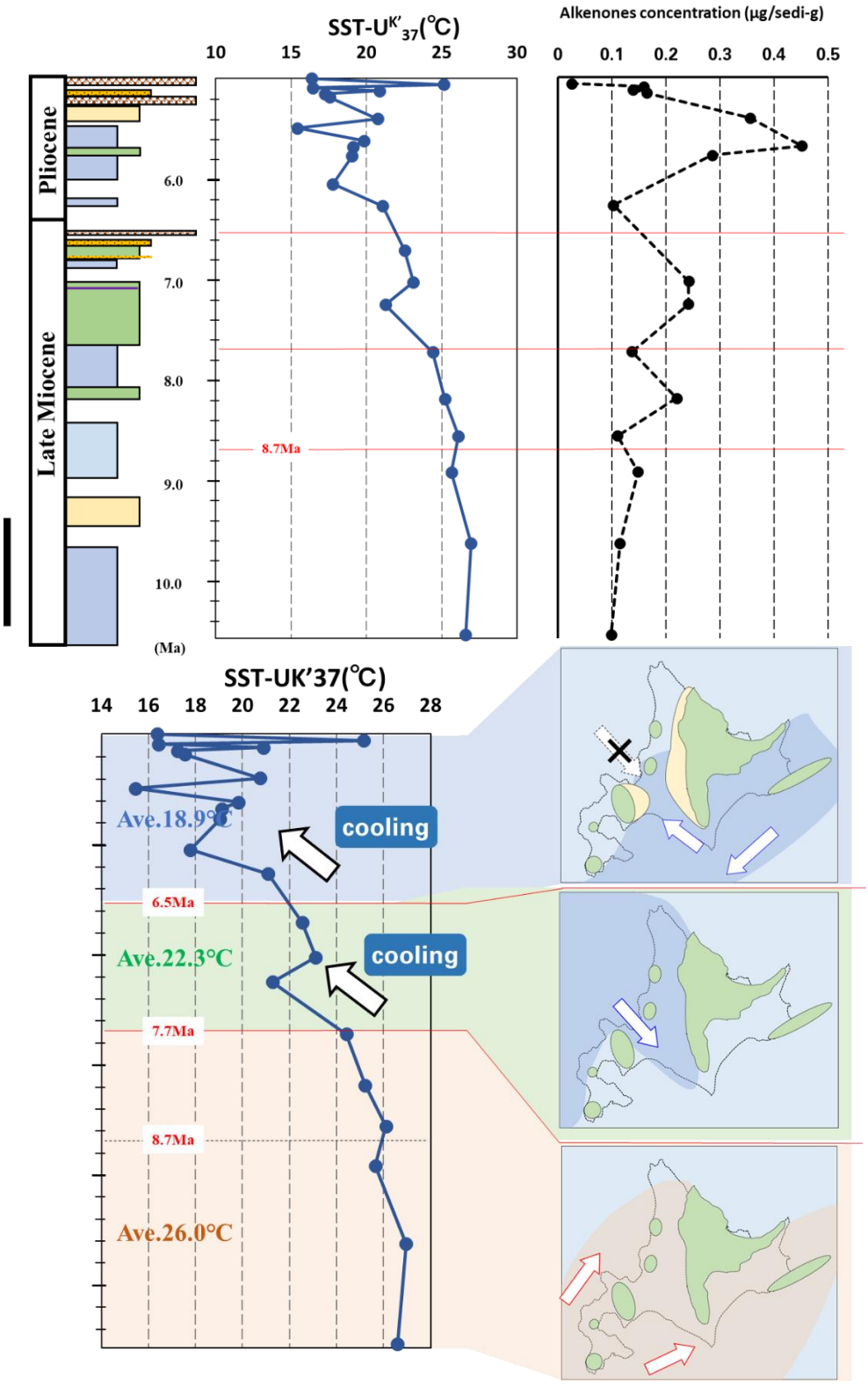

Figure 2.4.6 The vertical profiles of SST calculated by alkenone and alkenone concentration of Nina formation during Late Miocene and reconstruction of paleoceanography of Hidaka basin.

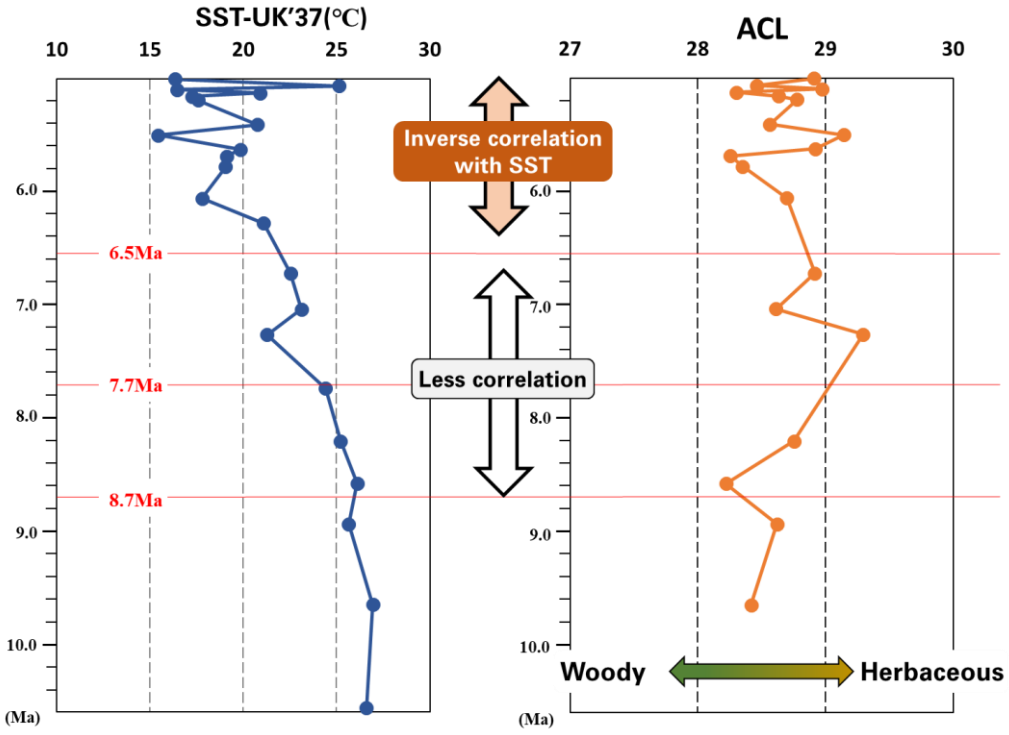

Figure 2.4.7 The vertical profiles of SST and ACL.

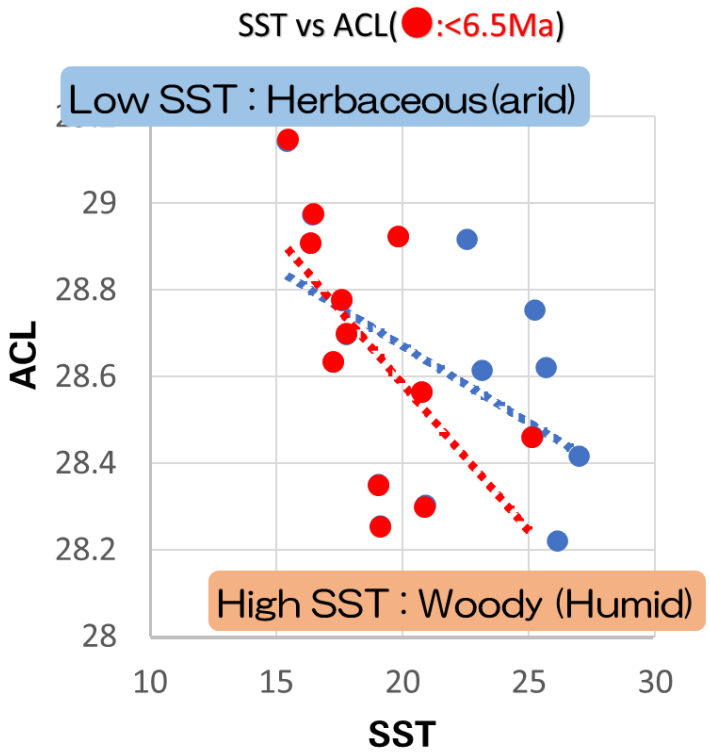

Figure 2.4.8 The relationship of SST and ACL

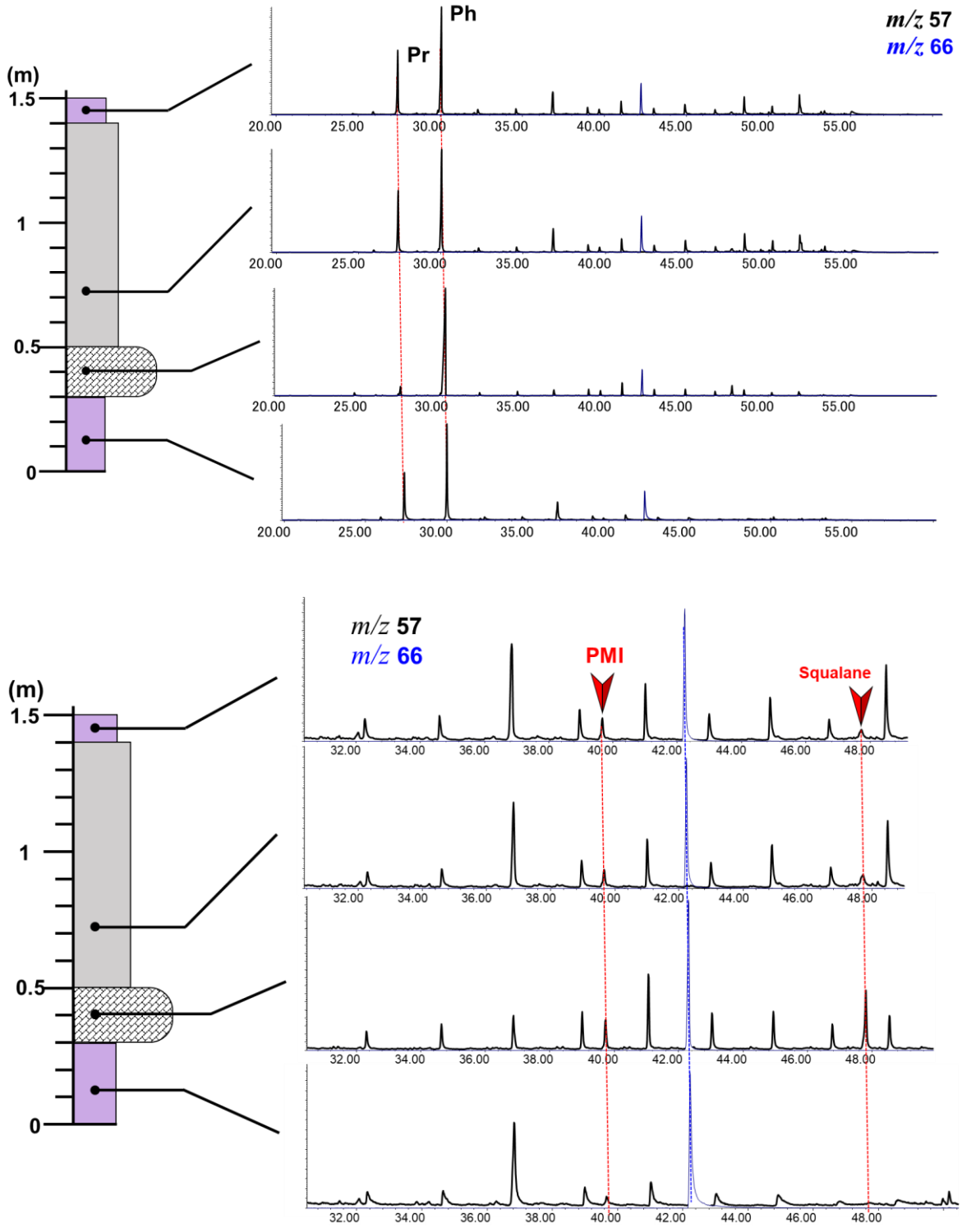

Figure 2.4.9 The TIC of nodules and calcareous concretion exposed in Horokanbesawa-river.

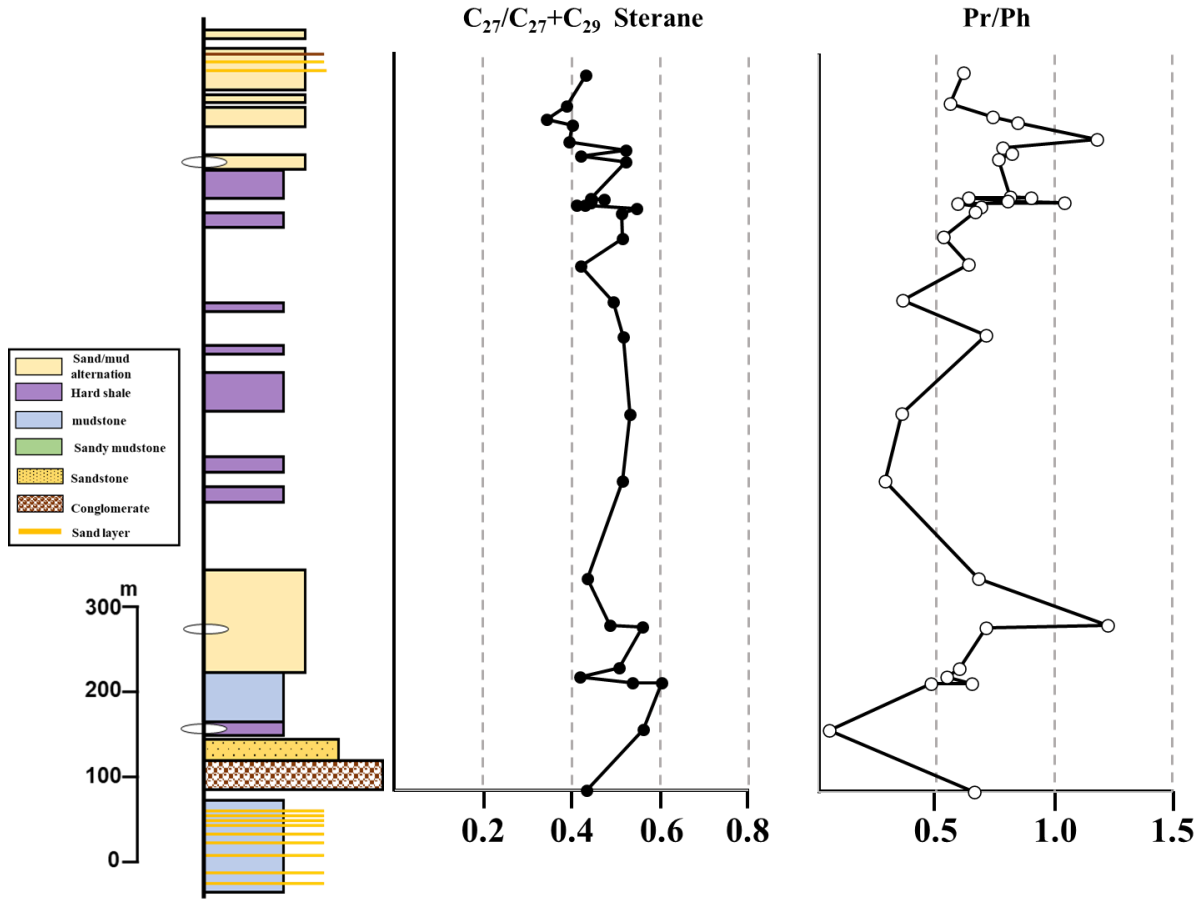

Figure 2.4.10 The profiles of $C_{27}/C_{27}+C_{29}$ ratio and Pr/Ph in Abetsu and Nibutani formations, sampled in Horokanbesawa river.

Chapter.3. Organic geochemical studies of degraded triterpenoids using Middle Miocene mudstone

3.1. Introduction

Marine turbidite sediment provides multiple information for both marine and terrestrial environments because it contains autochthonous matter produced by marine organisms and allochthonous terrigenous matter transported from land areas. Many organic geochemical studies of turbidity currents have been performed in the suspended particles of water column, modern surface sediments (e.g., Hedges and Keil, 1995; Thomsen et al., 2001; Laurier et al., 2003; Treignier et al., 2006; Selvaraj et al., 2015; Pruski et al., 2022), and turbiditic sedimentary sequences (e.g., Hoefs et al., 2002; Okano and Sawada, 2008; Yoshida et al., 2009; Hage et al., 2020; Furota et al., 2021). These studies demonstrated that geochemical characteristics were controlled by sources such as marine / terrestrial organisms as well as the types and phases of transport, redeposition, and post-depositional diagenesis of the turbidites.

Terrestrial plant-derived pentacyclic triterpenoids (TTs) commonly occur in marine sediments, and moreover, it has been found that some of marine turbidite sediments significantly contained the angiosperm-derived TTs in which the ring-A was degraded, des-A TT (Furota et al., 2014; Méjanelle et al., 2017). The reactions for the A-ring cleavage are accompanied by aromatization of B- to D- rings (Freeman et al., 1994; Simoneit et al., 2005). The aromatic des-TTs were generally detected in modern and immature samples, indicating that the aromatization was likely to occur at the earlier stages of diagenesis, probably via microbially mediated reactions. Thus, the des-A TTs were consider to be formed by microbial alteration of biological TTs such as β-amyrin at the earlier diagenesis under anoxic condition (Trendel et al., 1989; Wolff et al., 1989; Lohmann et al., 1990). In fact, the des-A TTs were frequently identified in sediments and particles in waters from wetland and lacustrine environments (e.g., del Rio et al., 1992; Logan and Eglinton, 1994; Jaffé et al., 1996; Jacob et al., 2007; Huang et al., 2008; Stefanova et al., 2008; van Bree et al., 2016, 2018; Lopes et al., 2021; He et al., 2022).

In the present study, we observed high abundances of the des-A TTs in the Miocene turbiditic sediments collected from south-central Hokkaido, Japan, and systematically investigated their concentrations and class distributions to discuss sources and transport processes of the degraded TT, and moreover, the applicability of the proxy for paleoenvironmental reconstruction.

3.2.Samples

Geological settingThe Yubari and Hobetsu areas (south-central Hokkaido, Japan; Fig. 1A) are located in Ishikari and Hidaka sedimentary basins, respectively, in the Ishikari–Teshio Belt, where is characterized by N-S trending foreland basins developed along the western side of the Hidaka Mountain during the middle to late Miocene (Hoyanagi, 1989; Kawakami et al., 2004; 2013). The Ishikari sedimentary basin was filled with thick coarse sediments, which is the middle Miocene Kawabata Formation. The Kawabata Formation consists of turbidites and related coarse clastics, and is interpreted as a channel-filled turbidite facies deposited in slope to deep-sea basin (Kawakami et al., 2004). Paleo-water depth of depositional environment of the Kawabata Formation was estimated to be deeper than 1000 m water depth by the presence of microfossil species

inhabiting lower middle bathyal marine zone (e.g. benthic foraminifera Uvigerina proboscidea: Tsubakihara et al., 1990). Some of turbiditic sand layers in lower member contain plant fragments at their upper part, which might be corresponding to Tb - Td units of the Bouma sequence (Bouma, 1962). In addition, a few sandstone layers contain a large amount of plant fragments, which presumed that the turbidites formed by huge flood flows (Furota et al., 2014; 2021).

Although few reports for geological and geochemical investigations in the Hidaka basin, the Hidaka sedimentary basin is occupied by thick Miocene sedimentary rocks, which are Sakae, Abetsu, Nibutani, and Nina formations. These Miocene rocks consist mainly of sandstone, mudstone, gravity flow deposits such as sandstone and conglomerate, siliceous hard mudstone, as well as diatomaceous mudstone (Shinzawa et al., 2009). Ages determined by radiolarian assemblage analysis reported that the Abetsu and Nibutani formations are 15.3 to 12.5 Ma (middle Miocene) and 12.5 to 9.7 Ma (middle to late Miocene), respectively. The Abetsu, Nibutani, and Nina formations are correlated to the Kawabata Formation in the Ishikari basin (Kawakami et al., 2002). The Abetsu Formation consists of turbidites and related coarse clastics, which is resemble to the Kawabata Formation, while the Nibutani and Nina formations are characterized by porcellanitic sandstone and mudstone as well as diatomaceous mudstone (Shinzawa et al., 2009).

Sedimentary rock samples were collected from a large outcrop (ca 50 m width) of the Kawabata Formation in the Somokumaisawa-gawa River of Yubari City (Fig. 1B) during 2017–2018, and river bed outcrops of the Abetsu and Nibutani formations in the Horokanbe River of Mukawa town (Fig. 1C) during 2020–2021 in south-central Hokkaido, Japan. All samples in the Kawabata and Abetsu formations were the mudstones within the Bouma sequence, but the samples of the Nibutani Formation were hemipelagic mudstones. We collected the upper and lower parts (ca 2–5 cm above and below the attached sandstone layers) of individual mudstone layers of some samples such as SO11-08, SO11a-08, and SO11a-09 of the Kawabata Formation and ABT01 of the Abetsu Formation (Table 1 and Fig. 2). These upper and lower parts of mudstones were evaluated to correspond to Ep (hemipelagic mud) and Et (turbidite mud) layers, respectively (Okano and Sawada, 2008). However, the upper layer of mudstone in SO11a-08 might be the Et because the parallel lamination was clearly developed in this layer. All samples were collected from 10–20 cm below surface of outcrop to minimize the effect of weathering. Before organic geochemical analyses, whole rock samples were cleaned, and any weathered surface was removed by a penknife. The samples were then crushed to a fine powder in an agate mortar.

3.3. Method

3.3.1.Biomarker analysis

Lipids were extracted from the powdered sediment samples with dichloromethane (DCM) and MeOH(Sawada, 2006). Separation of lipids was achieved by adding distilled water to the combined extracts and then DCM layer was siphoned out and passed through an anhydrous Na2SO4 column. The extract was dried in a rotary evaporator and then re-dissolved in hexane. The lipid-containing hexane extract was then passed through a silica gel column (95% activated), and the aliphatic hydrocarbon (F1), aromatic hydrocarbon (F2), ketone-ester (F3) and polar lipid (F4) fractions were eluted with hexane, hexane-toluene (3:1 v/v),

hexane-ethyl acetate (9:1 v/v) and ethyl acetate-MeOH (1:1 v/v), respectively. Tetracosane-d50 and n-hexadecanone were added prior to extraction as the internal standards for quantifying the F1 and F3 compounds, respectively. After these elutions, the triacontane-d62 was added to F2 and F4 fractions as external standards. The F4 fraction was silylated (60ºC, 1h) using N, O-bis(trimethylsilyl) trifluoroacetamide (BSTFA, Wako) at 60ºC. These fractions were analyzed by gas chromatography (GC) and gas chromatography / mass spectrometry (GC-MS).

Identification of the lipid was carried out by GC-MS with a Hewlett Packard 6890 attached to a DB-5HT column (30 m x 0.25 mm i.d. J&W Scientific) directly coupled to a Hewlett Packard XL-MSD quadrupole mass spectrometer (electron voltage, 70 eV; emission current, 350 μA; mass range, m/z 50-550 in 2.91 s) at Organic Biogeochemistry Laboratory, Hokkaido University. The GC temperatures were programmed as follows; F1 and F2: 50□C for 4 min, 50 - 310□C at 4□C /min and 310□C for 20 min, Identifications of the compounds were made from mass spectra and relative retention times in comparison with library data (NIST05 and NIST14) and the literature. The lipids were also quantified with a Hewlett Packard 6890 capillary GC equipped with a flame-ionization detector (FID) at Hokkaido University, and capillary column and temperature program used were the same as GC-MS conditions.

Quantifications of the degraded triterpenoids were made from the peak areas determined by the FID responses, and/or the responses of individual base peaks (e.g., m/z 123 for des-A lupane) using response factor. Response factors of degraded triterpenoids were calculated in this study, first identified and determine base peak of degraded triterpenoids using GC-MS, then analyzed GC-FID using same GC column and calculated response factor as following.

RF = [Compound area MS][Std area GC]/([Compound area GC]/[Std area MS])

The n-alkane indicators (CPI and Paq) were individually calculated by using conventional equations as following; CPI (Carbon preferential index): CPI = 2([C25] + [C27] + [C29] + [C31]) / [([C24] + [C26] + [C28] + [C30]) + ([C26] + [C28] + [C30] + [C32])], [Cx]: concentrations of n-Cx alkanes (Bray and Evans, 1961). Paq (aquatic macrophyte n-alkane proxy): Paq = ([C23] + [C25]) / ([C23] + [C25] + [C29] + [C31]) (Ficken et al., 2000)

3.3.2. Total organic carbon content (TOC)

A portion of the powdered sediment samples was acidified with 1 M HCl and allowed to stand for half a day to remove carbonates. Carbonate-free samples were then vacuum dried and analyzed for total organic carbon (TOC) content by a J-Science Micro Corder JM10 at the Center for Instrumental Analysis, Hokkaido University.

3.4. Results

3.4.1. Total organic carbon (TOC) content

TOC content (%) of mudstone samples in the turbidite sequences of the Kawabata and Abetsu formations range 0.52–1.77 and 0.40–0.83, respectively (Table 1). The remarkable highest TOC contents were observed in the turbidite mudstone layers (SO11-8L and SO11a-08U). The TOC values tend to be higher in the turbidite

mudstone layers in the Kawabata Formation, which might be caused by containing a significant amount of plant fragments transported by turbidity currents. Meanwhile, the TOC values are almost similar between the hemipelagic and turbidite mudstones in the Abetsu Formation. Indeed, the terrigenous matter such as plant fragments was hardly contained in the turbidite mudstone layers in the Abetsu Formation. The TOC content of hemipelagic mudstone samples from the Nibutani Formation are slightly higher values (0.73–0.97) than those of the Abetsu and Kawabata formations.

3.4.2. n-Alkane, pristane, phytane, and hopane isomer ratios

Figure 3 shows representative total ion chromatograms (TICs) of apolar fractions (F1) of the Kawabata and Abetsu formations. It can be seen that the peaks of n-alkanes are clearly appeared, especially odd carbon number homologues, in the TICs of the Kawabata Formation, which is common n-alkane distribution in sedimentary rock, while those are inconspicuous in the TICs of the Abetsu Formation. Table 1 shows concentrations of n-alkanes, n-alkanes / TOC ratios, n-alkane proxies such as carbon preference index (CPI) and aquatic plant index (Paq), and pristane / phytane (Pr/Ph) ratios. Concentrations of n-alkanes range 1.63–8.34 μg/g rock of the Kawabata Formation, and 0.71 – 3.08 μg/g rock of the Abetsu and Nibutani formations. The n-alkane concentrations are higher inn the Kawabata Formations than others. There is a quite higher value (8.34) in a turbidite mudstone sample (SO11a-08U) of the Kawabata Formation. However, the n-alkane / TOC ratios are almost similar (0.11–0.76) between the Abetsu, Kawabata, and Nibutani formations.

The CPI values of the Kawabata Formation (2.51–3.58) are significantly lower than those of the Abetsu and Nibutani formations (2.95–6.92). The CPI represents the odd/even carbon number ratio of n-alkanes and has been commonly used to estimate the maturity (diagenetic level) of the sediment and the input of terrestrial plant-derived material (e.g. Venkatesan and Kaplan, 1982; Venkatesan, 1988; Madureira et al., 1995). The typical n-alkane CPI values in vascular plant waxes are ca. 4–10 (Rieley et al., 1991). From these insights, the CPI values indicate that all sediment samples commonly originate from vascular plant waxes, and influenced diagenetic alteration, especially in lower CPI values of the Kawabata Formation. On the other hand, the Paq values of the Kawabata Formation (0.35–0.77) are slightly higher than those of the Abetsu and Nibutani formations (0.16–0.77). the main sources of the C23 and C25 n-alkanes are thought to be non-emergent and submerged/floating aquatic macrophytes in lacustrine environments (Ficken et al., 2000; Zhang et al., 2004). The Paq index was established as an indicator for the contribution of such aquatic macrophytes to n-alkane sources (Ficken et al., 2000). Our results indicate that contributions of aquatic macrophytes were slightly higher in the Kawabata Formation than the Abetsu and Nibutani formations.

The Pr/Ph ratios, which is usually used as depositional redox indicator, are quite lower (0.48–0.96) in the Abetsu and Nibutani formations, while the ratios are higher (1.52–3.21) in the Kawabata Formation. High Pr/Ph ratio (>1.0) indicates oxic condition in depositional environment, while the low value (<1.0) indicates anoxic condition (Didyk et al., 1978). Also, much higher Pr/Ph value (>3.0) is caused by high contribution of terrestrial organic matter (Powell, 1988). Therefore, high Pr/Ph ratios in the Kawabata Formation are resulting from high contribution of terrestrial organic matter. Okano and Sawada (2008) and Furota et al. (2014) have reported that the Pr/Ph values of the hemipelagic mudstones of the Kawabata Formation were lower (>2.0),

indicating the Miocene sediments were deposited under poorly oxygenated (dysoxic) condition in the bottom of the Ishikari basin. On the other hand, extremely lower Pr/Ph ratios in the Abetsu and Nibutani formations suggest smaller input of terrestrial organic matter and extremely reductive (anoxic) condition in the sedimentary environment of the Hidaka basin. However, the Pr/Ph ratios in the turbidite mudstones are significantly higher in the Abetsu Formation. From these results, it is presumed that extremely anoxic waters were widely distributed in the bottom of the Hidaka basin during the deposition of the Nibutani Formation (about 9 Ma).

We evaluated maturity of organic matter in the mudstone samples by the ratios of 22S to 22R isomers of C31 hopanes (22S/(22S + 22R)) (Table 1). The 17β(H), 21β(H)-hopanes, which are derived from bacterial membrane lipids, are predominant with one diastereomer 22R in recent and immature sediment. Meanwhile, in ancient sediment and oils, the more stable 17α(H), 21β(H)-hopane series usually predominates with the mixture of the diastereomers 22R and 22S resulting from transformation of (22R)-17β(H), 21β(H)-hopane during diagenesis. The C31 hopane 22S/(22S + 22R) ratios are consistently about 0.29–0.38 throughout the Kawabata Formation sample, which agreed with the results as reported by Okano and Sawada (2008). The 22S/(22S + 22R) ratios of the Abetsu and Nibutani formations range 0.21–0.36, and slightly lower than those of the Kawabata Formation. These results indicates that the organic matter is thermally immature in all samples.

The 20R C27 – C29 regular steranes are detected from all sediment samples, but 20S regular steranes are hardly detected (Fig. 3), and the distributions of the steranes are almost similar in all study samples (Table 1). The C27 steroids are generally derived from marine phytoplankton and zooplankton in the marine environments, and C28 steroids are derived from more specific phytoplankton such as diatom (Volkman, 1986). The C29 steroid is commonly originated from terrestrial higher plants (Huang and Meinschein, 1979). In our study, the ratios of regular steranes (C27 / (C27 + C29)), which are used for estimating the contribution of terrestrial and marine organic matter, are mid-range values and nearly constant. These results indicate that organic sources of the mudstones were likely to be mixtures of terrigenous and marine materials. The dinosteranes (C30 4, 23, 24-trimethylcholestanes), which are known as specific biomarkers for dinoflagellates (Summons et al., 1987), were also identified in the Kawabata Formation. However, there were no dinosteranes in the Abetsu and Nibutani formations. The dinosteranes/C30 hopane (Dino/Hop) ratios varied ranging from 0.14 to 0.47, without relation to hemipelagic or turbidite mudstones, in the Kawabata Formation (Table 1). These results suggest that the dinoflagellates were significantly contributed as marine algal source organisms, and their production might vary in the Kawabata Formation, but no (or poor) productions of dinoflagellates in the Abetsu and Nibutani formations.

3.5. Discussion

3.5.1. Identification of the des-A triterpenoids

Degraded TTs were identified in aliphatic (F1) and aromatic (F2) fractions. Figure 4 shows a TIC and mass fragmentograms (MFs) of m/z 109, m/z 123, m/z 313, m/z 177, and m/z 326 in F1. According to fragmentation pattern of major des-A TT, we tentatively identified 3 isomers of des-A TTs (Fig.5; 1: des-A

bisnorlupane, 8: des-A norursane:, 10: des-A norlupane). These des-A nor- series compounds may be formed via many intermediates by degradation processes in the Kawabata Formation. Also, des-E-D:C-friedhop-22(29)-ene were identified as major components in the mudstones of the Kawabata Formation. It was reported that this compound was found in the Triassic black shale and suggested to be formed by the degradation of bacterial hopanepolyols (Hauke et al., 1993). , We tentatively identified the compound 17 with des-A lupane isomer because mass spectra of this compound was resemble to that of the des-A lupane (Table 2: 15). Compound 18 has similar characters to fragmentation pattern of the des-A TT in the mass spectra, and was determined to be unknown des-A TT.

Figure 5 shows the TIC and MFs of m/z 145, m/z 187, m/z 213, m/z 231, m/z 274, m/z 292, and m/z 295 in F2. The compound b, which was detected as a major peak in the Kawabata Formation, was identified with monoaromatic des-A oleanane or ursane due to their fragment ions of m/z 145 and m/z 310 as well as the molecular weight as reported previously (Asahi and Sawada, 2019). In some cases, C-ring in the des-A TTs is degraded, through the cleavage of C14–C18 bonds and aromatization of B- and D-rings as identified from the Miocene Iberian coals (de las Heras et al., 1991). In our study, the C-ring cleaved diaromatic des-A oleanane was identified (Table 2 and Fig. 5; a). In addition, degraded hopanoids, des-E-D:C-friedo-25-norhopa-5-7-9-triene (Table 2 and Fig. 5; d and e), were identified. These might be formed by the degradation of bacterial hopanepolyols as aliphatic des-E hopenes as mentioned above (Hauke et al., 1993).

3.5.2. Concentrations and class distributions of des-A TTs

Concentrations of total degraded TTs (des-A oleananes, ursanes, and lupanes, and des-E hopanes) were found to be remarkably higher (1.56–8.68 μg/g rock) in the mudstones of the Kawabata Formation, and significantly contained (0.29–1.13 μg/g rock) in the Abetsu and Nibutani formations (Table 1). The total degraded TTs / TOC ratios were also higher (0.30–1.19 μg/mgC) in the Kawabata Formation, and were lower (0.04–0.12 μg/mgC) in the Abetsu and Nibutani formations (Table 1). These values tended to vary without relation to hemipelagic or turbidite mudstones. Mean values of the total degraded TTs / TOC ratios (ca 0.30–0.64) in the Kawabata Formation are about 100 to 10000 times of those of previous reports (Regnery et al., 2013; Lopes et al., 2021). The maximal concentration and relative abundances per TOC of the des-A TTs in the Kawabata Formation are likely to be greatest, champion data, over the previous studies. The huge amounts of the des-A TTs were possibly transported and deposited in the Ishikari basin during the deposition of the Kawabata Formation of the late Miocene.

The class distributions of the degraded TTs are individually shown in aliphatic and aromatic compounds in the study samples (Fig. 6). The distributions of aliphatic degraded TTs in the Kawabata Formation are characterized by high relative abundance of des-A lupenoid type compounds, which account for about 40–50 % in total aliphatic degraded TTs. On the other hand, the des-A oleanoid type compounds are the most major compounds among total aliphatic degraded TTs (ca 50–75 %) in the Abetsu and Nibutani formations. In aromatic degraded TTs, the relative abindances of des-A oleanoid type compounds are overwhelmingly higher in the all formations, although these values are slightly lower in the Abetsu Formation. The des-A ursane type compounds are clearly more abundant in the Abetsu Formation than others. Des-E hopanoids tend to 10% of

the whole degraded TTs in all samples, indicating that des-E hopanoids were constantly minor components in mudstone of all formation. On the whole, the relative abundances of des-A lupanes in aliphatic degraded TTs could be obviously distinguished between the samples from the Ishikari basin (Kawabata Formation) and Hidaka basin (Abetsu and Nibutani formations). In addition, the differences for the majority of des-A lupanes between aliphatic and aromatic compounds were presumably caused by the less occurrences of aromatization in the precursor lupenoids, which have no double bonds in the carbon skeleton.

3.5.3. Paleoenvironmental factors to changes of the degraded TTs abundances

To examine the factors of variability in the degraded TTs abundances in marine turbidite sediments, we compared the degraded TTs / TOC ratios with several biomarker proxies such as the Paq, CPI, Pr/Ph, and C27/C29 sterane ratios in the mudstones from the Ishikari (Kawabata Formation) and Hidaka (Abetsu and Nibutani formations) basins (Figs. 7 and 8). We found that the degraded TTs / TOC ratios are correlated with the Paq values in the Kawabata and Abetsu formations. Particularly, the correlation coefficient of the degraded TTs / TOC vs. Paq is high ($r^2 = 0.66$) in the Abetsu Formation (Fig. 8). The higher Paq values are interpreted to be high contribution of aquatic and submerge/floating macrophytes, and moreover, were commonly observed in lake and pond environments (Ficken et al., 2000; Zhang et al., 2004). The des-A TTs are formed from bio-TTs, which were derived from angiosperm leaf and bark (e.g. Barker, 1982; Nakamura and Sawada, 2010), via biodegradation in dysoxic or anoxic aquatic conditions such as pond and rain forest with wetter and high water table (Trendel et al., 1989; Jaffé et al., 1996; Stefanova et al., 2011; He et al., 2018), or photochemical reaction (Simoneit et al., 2009). It therefore, is reasonable that the degraded TT abundances were closely linked to the Paq. Lopes et al. (2021) reported that these relationships between the degraded TT abundances and Paq were similarly observed in the suspended particulate organic matter (SPOM) from waters in the Amazon floodplain lake. On the basis of the data described in their study, we obtained the regression line and high correlation coefficient of the degraded TTs / TOC vs. Paq ($r^2 = 0.67$) in the SPOM of the Amazon lake (Fig. 8), which supported that the places of the degraded TT formation were closely associated with the terrestrial areas flourishing the aquatic macrophytes.According to these insights, large amounts of the degraded TTs were possibly produced by biodegradation of the transported angiospermous TTs in the dysoxic or anoxic environments such as ponds and wetlands. Furthermore, it is presumed that the organic matter deposited in the Ishikari basin was transported from wetland or marsh areas of the paleo-Hokkaido (paleo-Hidaka Island; Fig. 9).

The degraded TTs / TOC ratios were not correlated with the CPI and Pr/Ph values in all study samples (Figs. 7 and S1). These results indicate that the degraded TT abundances were not related to the maturity (diagenetic level), abundances of vascular plants, and redox conditions of the bottom waters and sediment-water interfaces in depositional environments. Thus, it can be pointed out that the degradation of TTs occurred before deposition, i.e. during transport and/or accumulation in hinterland, not during and after the deposition of turbidite sediments. This interpretation is concordant with the inference that the degraded TTs were formed by biodegradation under dysoxic or anoxic condition in ponds, lakes, and wetlands.

The C27/C29 sterane ratios were found to be reversely correlated with the degraded TTs/TOC in the Kawabata Formation (Fig. 7). Lower C27/C29 sterane ratios, indicating high contribution of terrigenous organic matter, correspond to higher degraded TTs/TOC ratios. These trends indicate that the degraded TTs were efficiently transported under the depositional setting which larger terrestrial input.

According to the results of the degraded TTs, we comprehensively interpreted the paleoenvironments of the Ishikari and Hidaka basins (Fig. 9). These basins were thought to be formed by the arc-arc collision event (Kimura, 1996), and were explained as narrow and deep depressions. Therefore, many turbidites were deposited in the Abetsu and Kawabata formations with derect transport of large amounts of terrestrial plant materials by hyperpycnal flow and flood-related turbidity flow (Furota et al., 2021). The authors demonstrated that the floods might have accumulated terrigenous organic matter from wide areas, including marshes and wetlands, and transported these to the deep-sea floor in Ishikari and Hidaka basins during the middle Miocene. In the Ishikari basin, the remarkably large amounts of the degraded TTs imply that the lakes, ponds, marshes, and wetlands were widely distributed in hinterlands of the paleo-Hidaka Island, and the degraded TTs were efficiently formed in these areas. Moreover, higher relative abundances of the des-A lupanes in the only Ishikari basin (Kawabata Formation) suggest that the TTs had been supplied from mountain forest areas, where lupenoid-producing woody plant taxa might be spreaded. This assumption is supported by the results that the granites, which were distributed in the mountain areas, were contained as major sedimentary particles in the Kawabata Formation (Kawakami et al., 2004). Meanwhile, the less abundance of the des-A lupanes and no granite-derived sediments in the Abetsu and Nibutani formations are likely to be no or less supply of TTs from the mountain forest areas in the Hidaka basin.

3.6. Conclusion

Aliphatic and aromatic degraded TTs including des-A and des-E TTs were investigated in the turbidite and hemipelagic mudstones from the Miocene Kawabata Formation (Ishikari basin) and Abetsu and Nibutani formations (Hodaka basin), south-central Hokkaido, Japan. We found that the concentrations and relative abundances per TOC of total degraded TTs, especially des-A TTs, were remarkably higher in the Kawabata Formation, and significantly contained in the Abetsu and Nibutani formations. These results clearly indicate that the huge amounts of the des-A TTs were possibly transported and deposited in the Ishikari basin during the deposition of the Kawabata Formation of the late Miocene. The degraded TTs / TOC ratios are correlated with the Paq values in the Kawabata and Abetsu formations. The higher Paq values are interpreted to be high contribution of aquatic and submerge/floating macrophytes, and moreover, were commonly observed in lake and pond environments. The des-A TTs are formed from bio-TTs, which were derived from angiosperm leaf and bark, via biodegradation in dysoxic or anoxic aquatic conditions such as pond and rain forest with wetter and high water table or photochemical reaction. Thus, large amounts of the degraded TTs were possibly produced by biodegradation of the transported angiospermous TTs in the dysoxic or anoxic environments such as ponds and wetlands. Furthermore, it is presumed that the organic matter deposited in the Ishikari basin was transported from wetland or marsh areas of the paleo-Hidaka Island.

The class distributions of the aliphatic and aromatic degraded TTs varied in the samples from these formations. In the Kawabata Formation, the des-A lupanes are detected as major compounds, but the des-A oleananes are the most major compounds in aliphatic degraded TTs in the Abetsu and Nibutani formations. The higher relative abundances of the des-A lupanes in the only Ishikari basin (Kawabata Formation) suggest that the TTs had been supplied from mountain forest areas, where lupenoid-producing woody plant taxa might be spread. Meanwhile, the des-A lupanes are less abundant in the Abetsu and Nibutani formations, suggesting no or less supply of TTs from the mountain forest areas in the Hidaka basin.

Further research using other types of turbidite sediments is needed to strengthen the utility of the degraded TT records in paleoenvironmental and sedimentological studies and support the application of these biomarkers to a wider range of deep-sea environments.

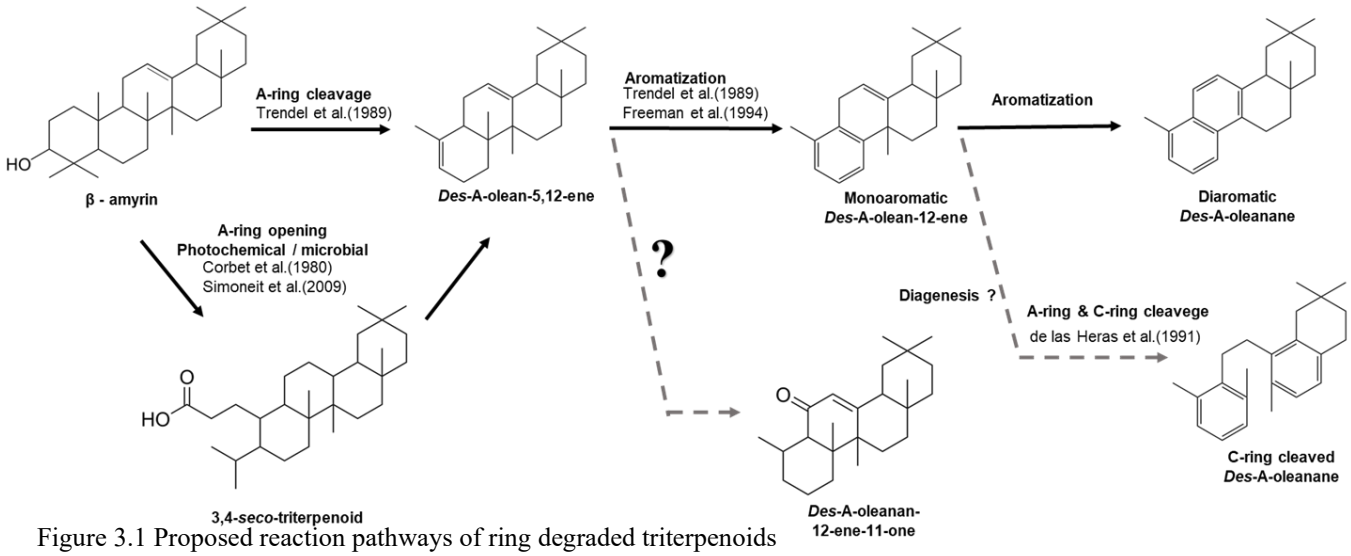

Figure 3.1 Proposed reaction pathways of ring degraded triterpenoids

Table 3.1 the list of the sites detected degraded triterpenoids

Setting	Country	Age	Aliphatic	Aromatic	Reference
River					
Amazon river	Brazil	modern	○	×	Lopes et al.(2021)
Shark river	Florida(US)	modern	○	×	He et al.(2018)
Lake					
Caco lake	Brazil	Holocene	○	×	Jacob et al.(2007)
Dethlingen paleolake	Germany	Pleistocene	○	○	Regnery et al (2013)
Challa lake	Kenya	Holocene	○	×	van Bree et al.(2016)
pond ner Hulternheim	France	modern	○	×	Trendel et al. (1989)
Clarkia paleolake	Idaho(US)	Miocene	○	○	Logan et al.(1994)
Peatland					
Dajihuhu peat	China	Holocene	○	×	Huang et al.(2008)
Hani peat bog	China	Holocene	○	×	Zheng et al.(2010)
Orinoco basin(soil)	Venezuela	modern	○	×	Jaffe et al.(1996)
Marine					
Baffin Bay	Greenland	Miocene	×	○	ten Haven et al.(1992)
Ishikari basin	Japan	Miocene	○	○	Furota et al.(2014)

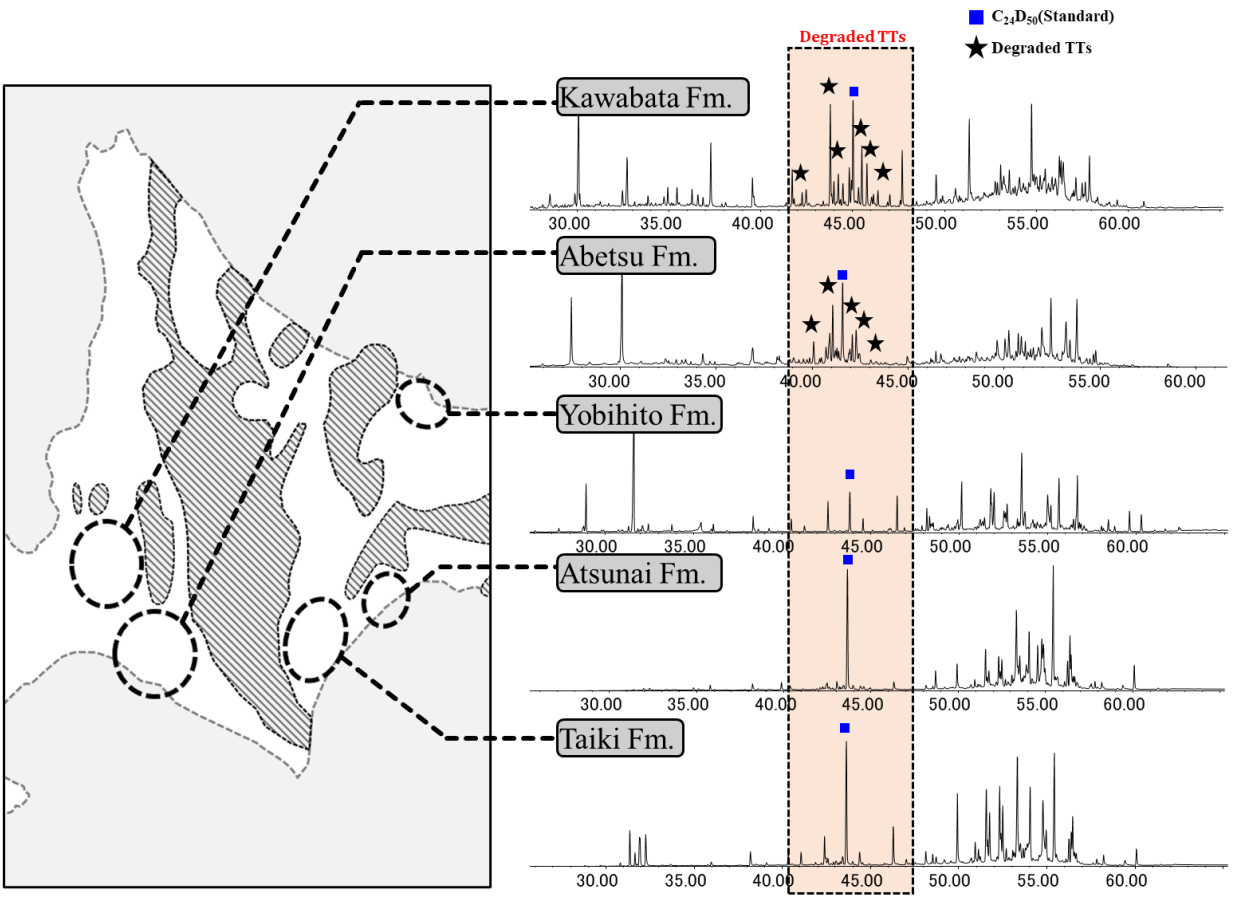

Figure 3.2 The detections of degraded Triterpenoids from middle-late Miocene mudstones sampled several Hokkaido areas.

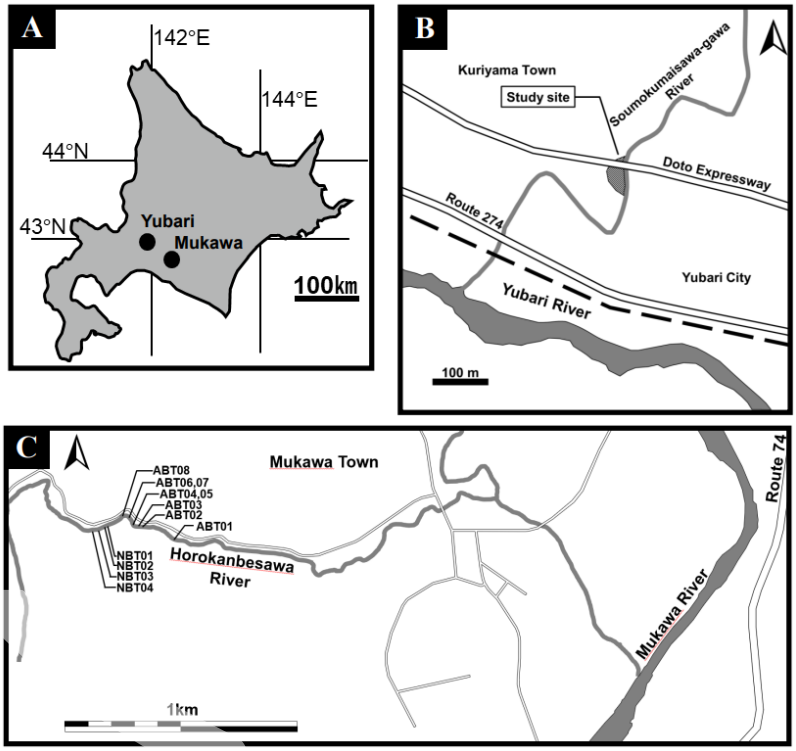

Figure 3.2.1 Index maps showing (A) location of study areas (Yubari and Mukawa, south-central Hokkaido, Japan), sampling locations in (B) the Somokumaisawa-gawa River, Kuriyama town, and (C) the Horokanbesawa River, Mukawa town (Hobetsu area).

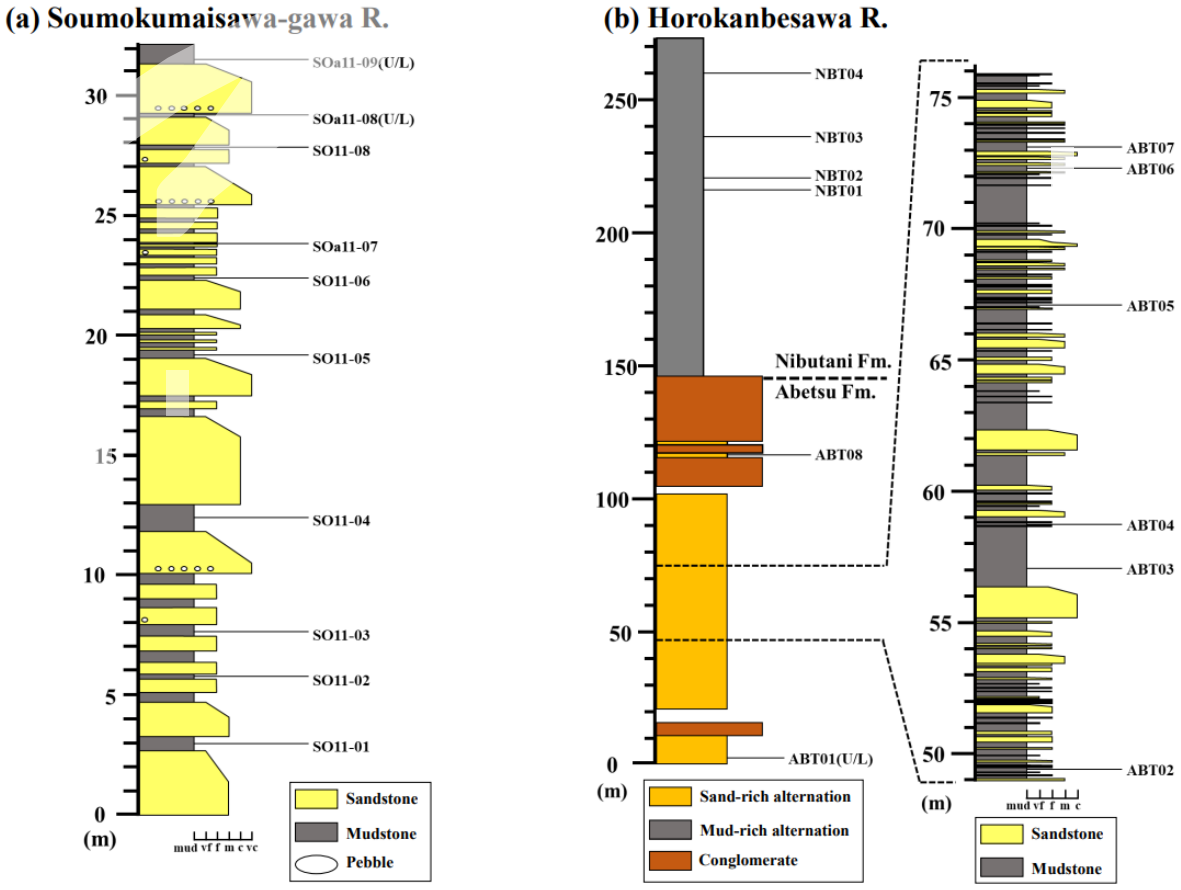

Figure 3.2.2 Lithologic sections of (a) the Kawabata Formation in the Somokumaisawa-gawa River, and (b) the Abetsu and Nibutani formations in the Horokanbesawa River.

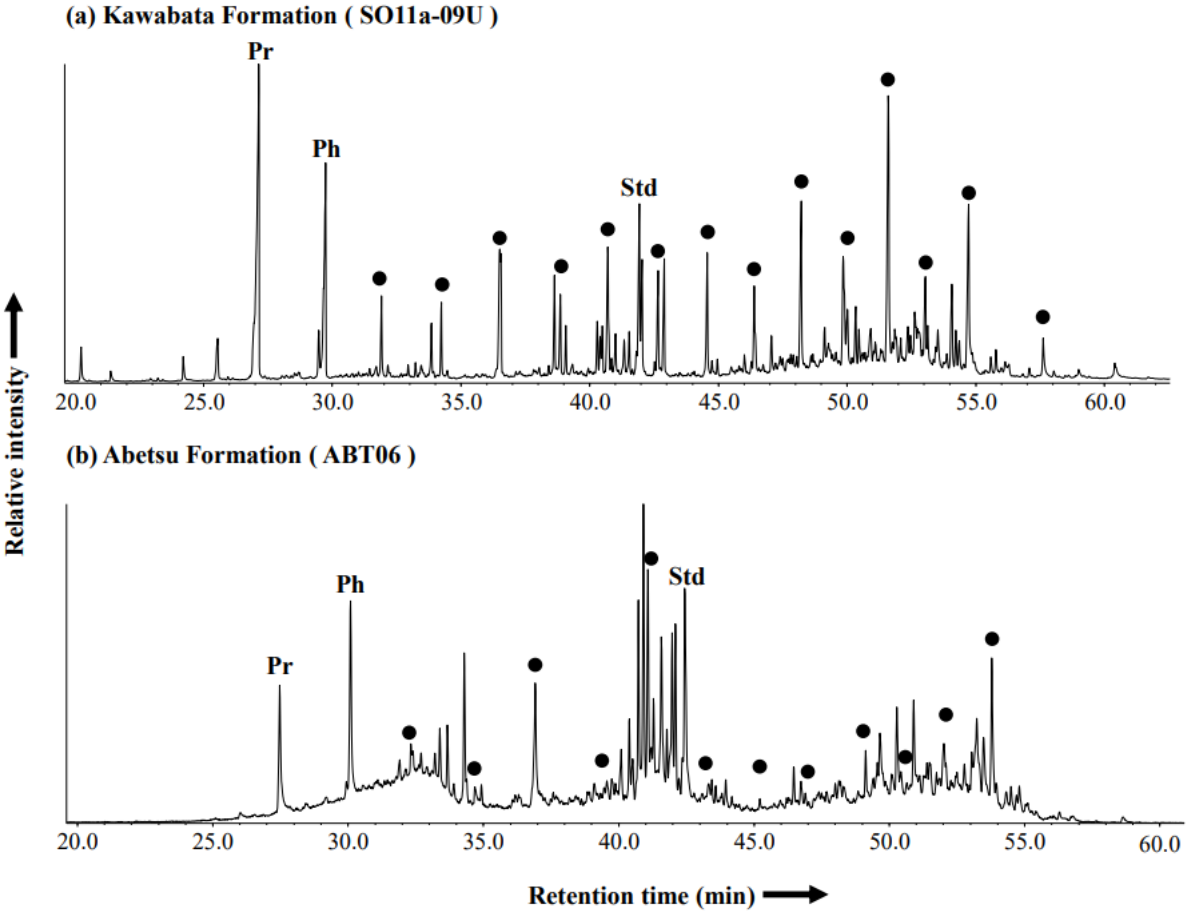

Figure 3.3.1 Total ion chromatograms (TICs) of aliphatic fractions of (a) the Kawabata Formation (sample No) and (b) the Abetsu Formation (sample No).

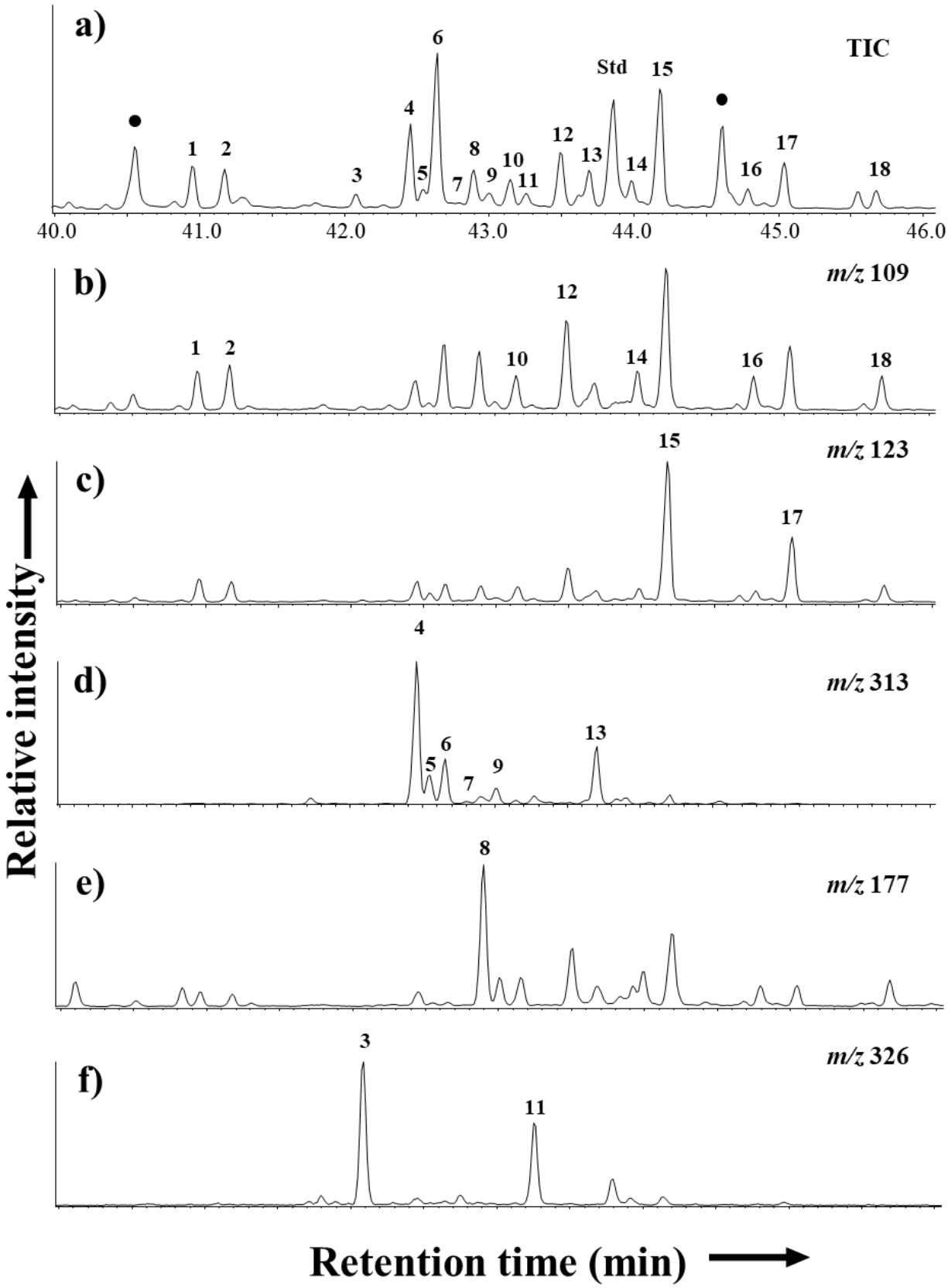

Figure 3.3.2 (a) TIC and mass fragmentograms of (b) m/z 109, (c) m/z 123, (d) m/z 313, (e) m/z 177, and (f) m/z 326 of aliphatic fraction of (sample No).

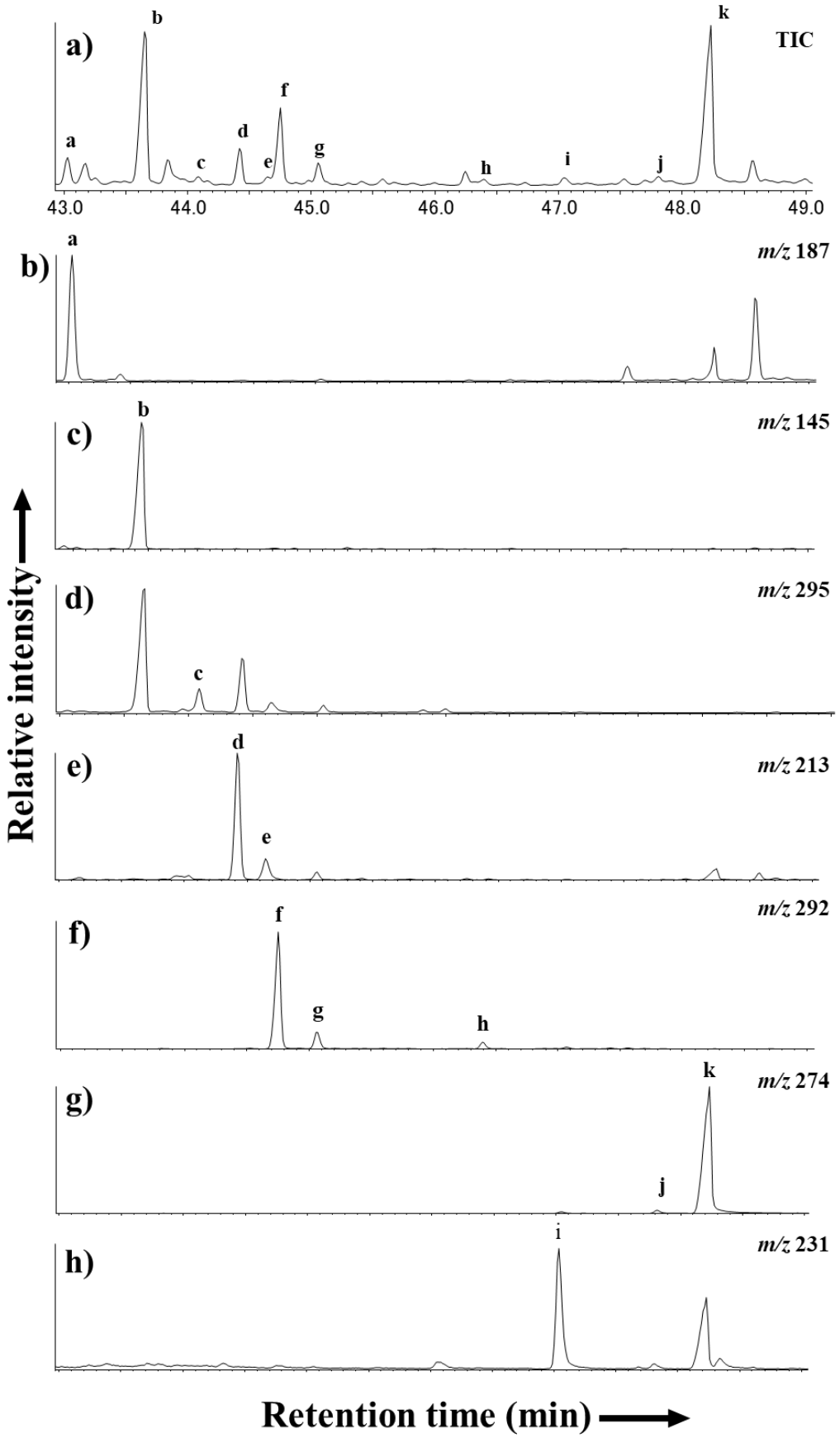

Figure 3.3.3 (a) TIC and mass fragmentgrams of (b) m/z 187, (c) m/z 145, (d) m/z 295, (e) m/z 213, (f) m/z 292, (g) m/z 274, and (h) m/z 231 of aromatic fraction of (sample No).

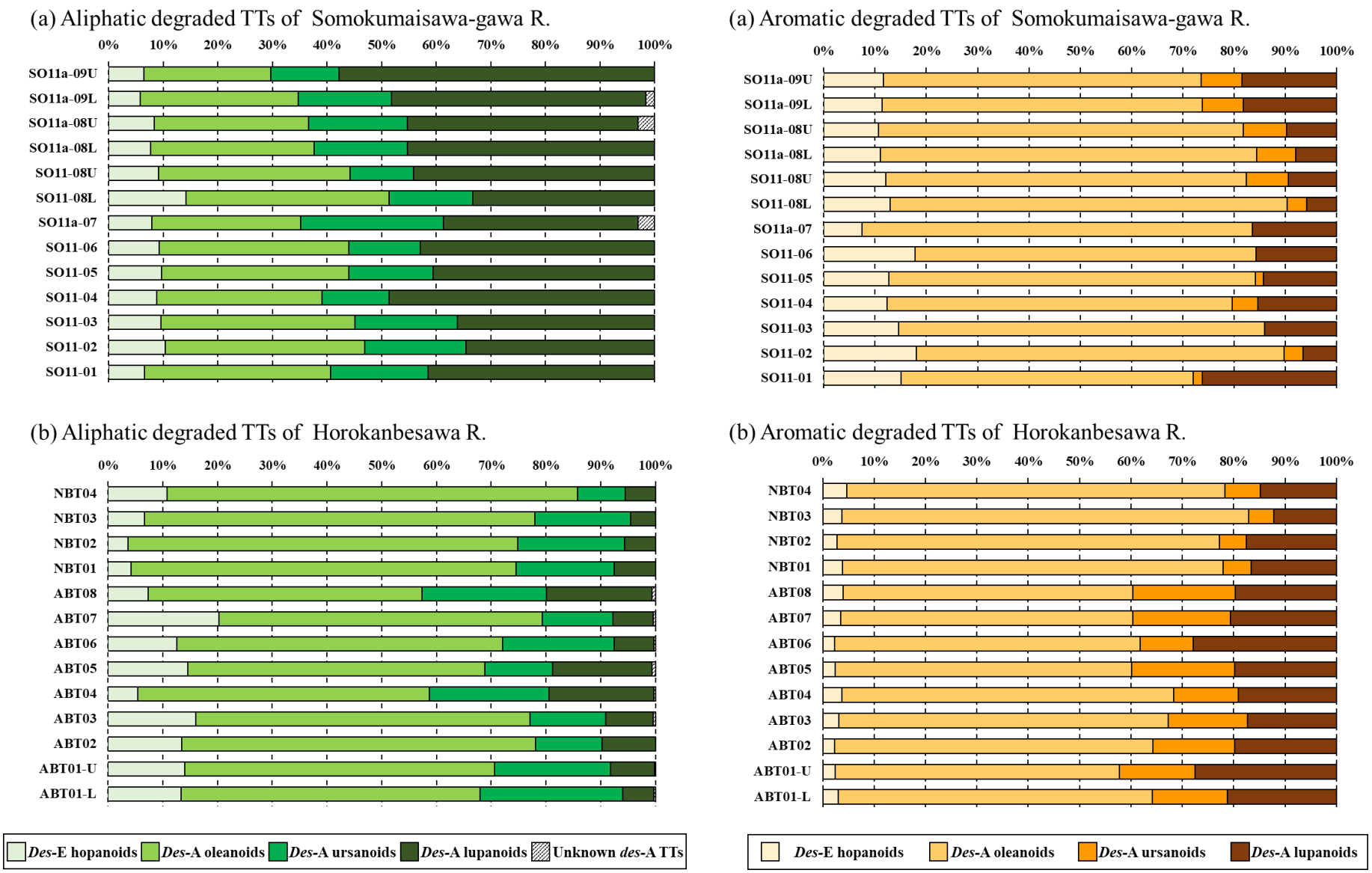

Figure 3.3.4 Class distributions of des-A TTs of (a) aliphatic and (b) aromatic fractions in the Abetsu, Kawabata, and Nibutani formations.

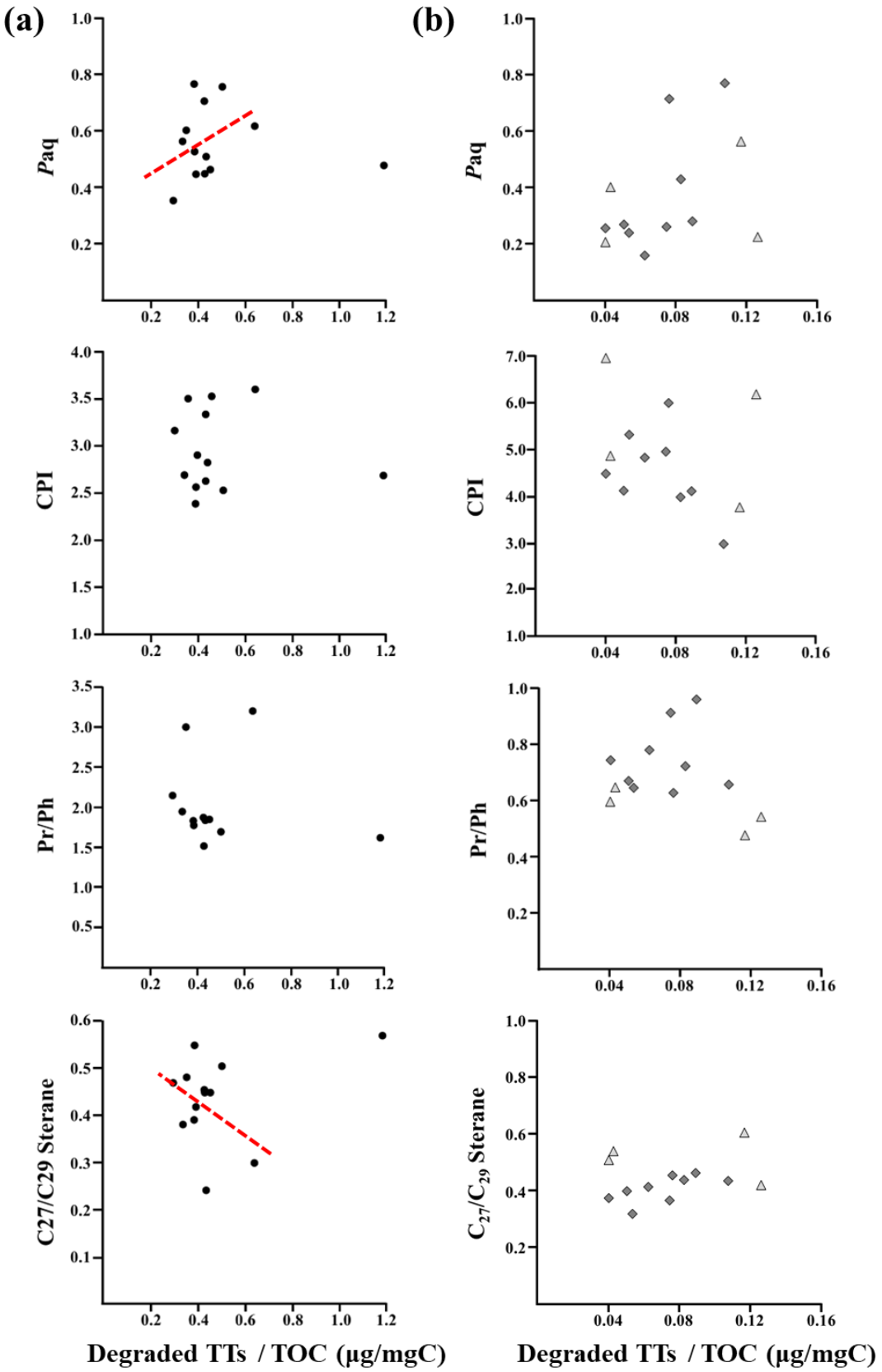

Figure 3.3.5 Relationships between the des-A TTs / TOC (μg/mgC) and n-alkane proxies (Paq and CPI), Pr/Ph ratios, as well as C27/C29 sterane ratios in (a) the Kawabata Formation and (b) Abetsu and Nibutani formations.

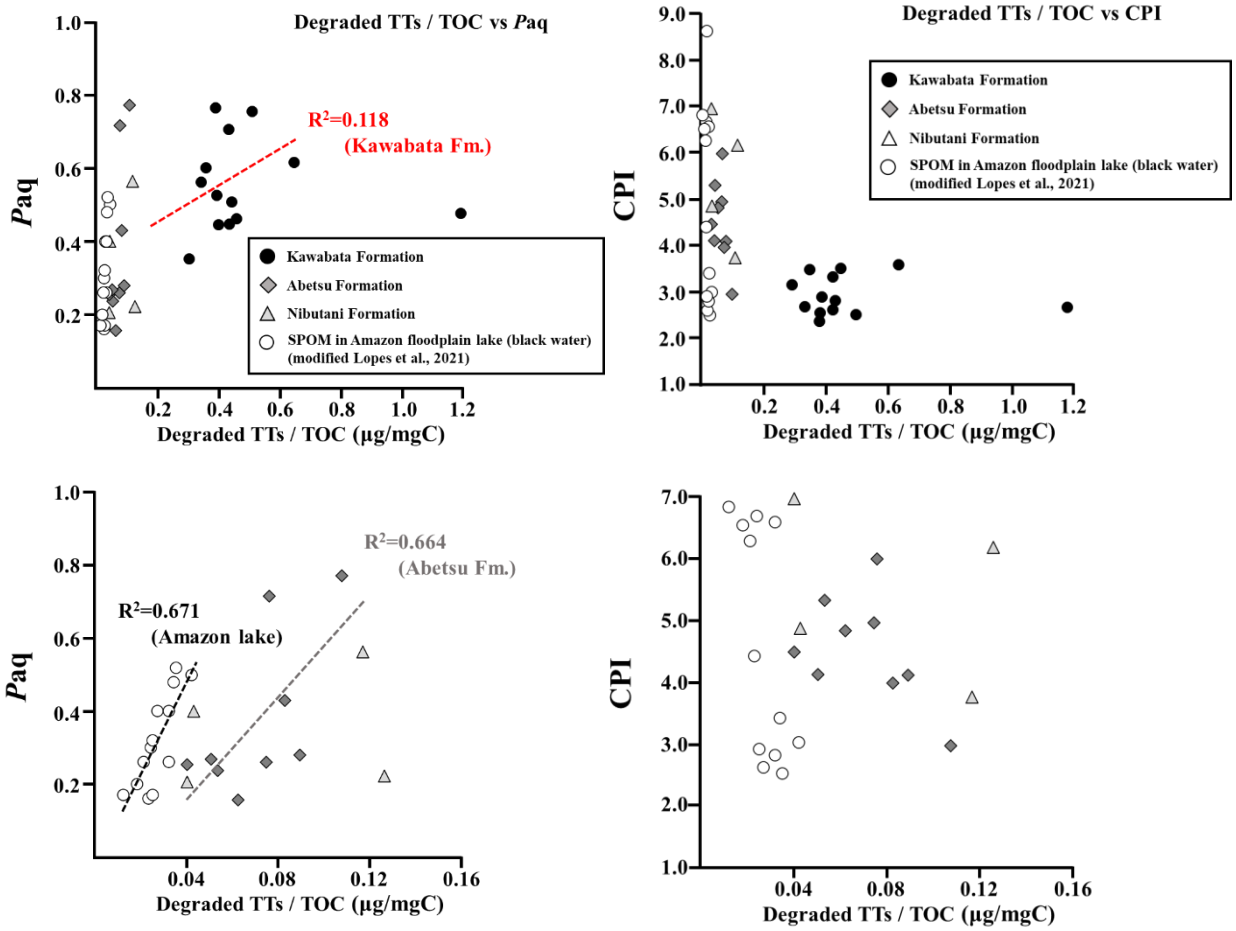

Figure 3.3.6 Integrated plots of relationships between the des-A TTs / TOC (µg/mgC) and Paq and CPI values in this study (the Abetsu, Kawabata, and Nibutani formations), as well as previous study (suspended paticulate organic matter (SPOM) in Amazon floodplain lake (black water) modified Lopes et al., 2021)..

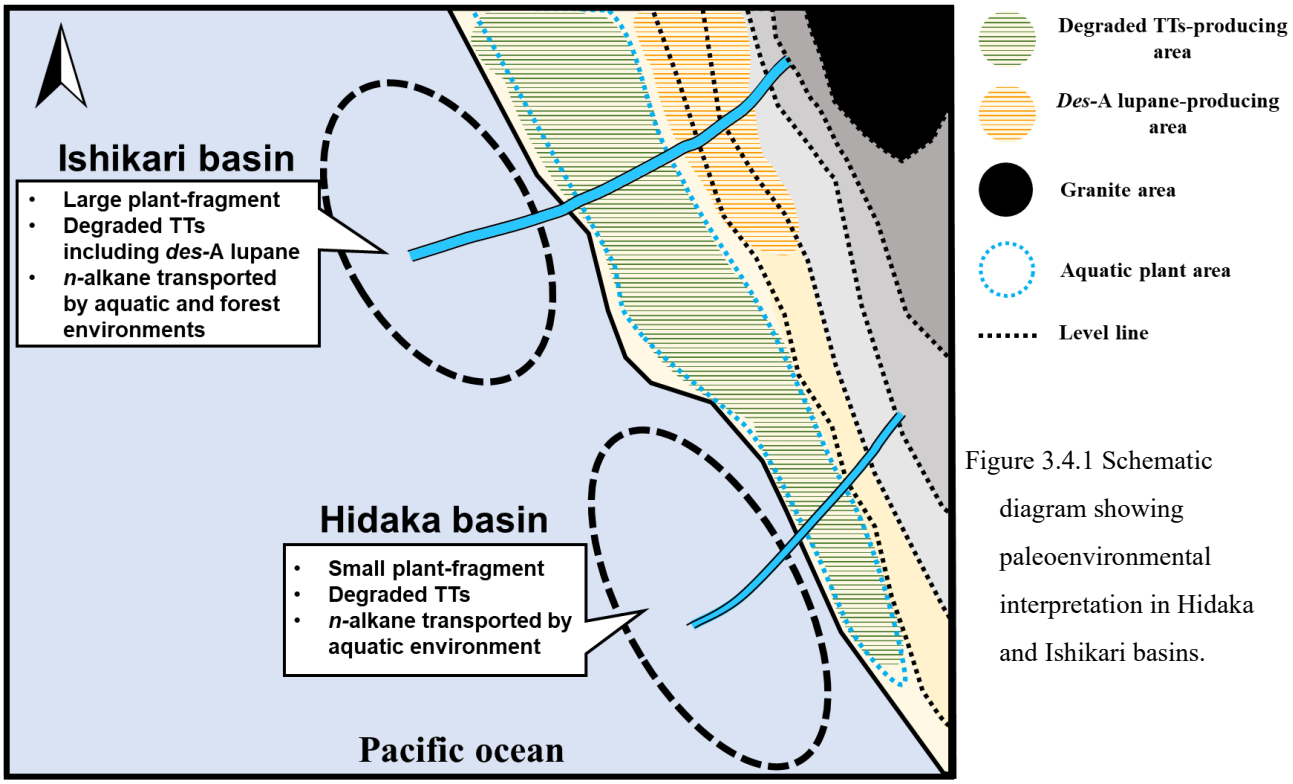

Figure 3.4.1 Schematic diagram showing paleoenvironmental interpretation in Hidaka and Ishikari basins.

Table 3.3.2 Data of total organic carbon content (TOC; %), concentrations of total n-alkanes (μg/g rock) and the ratios of total n-alkanes against TOC (μg/mgC), n-alkane indicators such as carbon preferential index (CPI) and aquatic plant n-alkane proxy (Paq), pristane/phytane (Pr/Ph) ratios, C31 hopane 22S/22R isomer ratios, C27/C29 sterane ratios, dinosterane / hopane (Dino/Hop) ratios, concentrations of all des-A TTs (μg/g rock) as well as the ratios of all des-A TTs against TOC (μg/mgC) in mudstones of the Abetsu, Kawabata, Nibutani Formations in south-central Hokkaido, Japan

Location/ Formation	Sample No.	Depth (m)	Lithology	TOC%	Alkane conc. (μg/g-rock)	Alkane/TOC (μg/mgC)	CPI	*Paq*	Pr/Ph	C31 hopane 22S/(22S+22R)	$C^{27}/(C^{27}+C^{29})$ Sterane	Dino/Hop	All degraded TTs conc. (μg/g-rock)	All degraded TTs /TOC (μg/mgC)
Somokumaisawa-gawa River														
Kawabata Fm.	SO11a-09U	32.00	Hemipelagic mud	0.52	3.96	0.76	3.15	0.35	2.15	0.34	0.47	0.41	1.56	0.30
	SO11a-09L	31.90	Turbidite mud	0.76	2.58	0.34	2.37	0.77	1.84	0.37	0.39	0.31	2.95	0.39
	SO11a-08U	29.00	Turbidite mud	1.77	8.34	0.47	3.32	0.71	1.87	0.32	0.45	0.21	7.64	0.43
	SO11a-08L	28.90	Turbidite mud	0.71	2.50	0.35	3.48	0.60	3.01	0.34	0.48	0.30	2.53	0.36
	SO11-08U	27.50	Hemipelagic mud	0.73	2.05	0.28	2.67	0.48	1.62	0.32	0.57	0.24	8.68	1.19
	SO11-08L	27.30	Turbidite mud	1.72	3.02	0.18	2.81	0.51	1.84	0.29	0.24	0.47	7.57	0.44
	SO11a-07	23.90	Turbidite mud	0.57	2.88	0.50	3.58	0.62	3.21	0.32	0.30	0.43	3.67	0.64
	SO11-06	22.30	Hemipelagic mud	0.69	1.63	0.24	2.68	0.56	1.95	0.34	0.38	0.24	2.35	0.34
	SO11-05	19.10	Hemipelagic mud	0.59	1.32	0.22	2.89	0.44	--	0.34	0.42	0.22	2.34	0.40
	SO11-04	12.40	Hemipelagic mud	0.66	1.69	0.26	2.51	0.76	1.70	0.35	0.50	0.22	3.35	0.51
	SO11-03	7.70	Hemipelagic mud	0.58	2.25	0.39	2.61	0.45	1.52	0.36	0.45	0.15	2.51	0.43
	SO11-02	5.70	Hemipelagic mud	0.58	1.97	0.34	3.51	0.46	1.85	0.36	0.45	0.14	2.65	0.46
	SO11-01	2.95	Hemipelagic mud	0.70	3.74	0.53	2.55	0.52	1.78	0.38	0.55	0.17	2.74	0.39
Horokanbesawa River														
Nibutani Fm.	NBT04	259.00	Hemipelagic mud	0.85	1.48	0.17	6.92	0.20	0.60	0.26	0.51	N.D.	0.34	0.04
	NBT03	236.00	Hemipelagic mud	0.73	1.05	0.14	6.14	0.22	0.54	0.25	0.42	N.D.	0.92	0.13
	NBT02	215.00	Hemipelagic mud	0.84	0.95	0.11	4.84	0.40	0.65	0.21	0.54	N.D.	0.36	0.04
	NBT01	213.00	Hemipelagic mud	0.97	1.58	0.16	3.73	0.56	0.48	0.24	0.60	N.D.	1.13	0.12
Abetsu Fm.	ABT08	116.00	Turbidite mud	0.64	1.73	0.27	4.92	0.26	0.92	0.34	0.36	N.D.	0.48	0.07
	ABT07	73.10	Turbidite mud	0.57	1.72	0.30	4.80	0.16	0.78	0.36	0.41	N.D.	0.36	0.06
	ABT06	72.30	Hemipelagic mud	0.57	0.71	0.12	2.95	0.77	0.66	0.29	0.43	N.D.	0.61	0.11
	ABT05	67.00	Hemipelagic mud	0.63	1.59	0.25	5.29	0.24	0.65	0.28	0.32	N.D.	0.34	0.05
	ABT04	58.80	Turbidite mud	0.4	0.23	0.06	4.08	0.28	0.96	0.36	0.46	N.D.	0.36	0.09
	ABT03	57.00	Hemipelagic mud	0.83	3.08	0.37	4.45	0.25	0.75	0.31	0.37	N.D.	0.33	0.04
	ABT02	49.20	Hemipelagic mud	0.58	1.97	0.34	4.09	0.27	0.67	0.26	0.40	N.D.	0.29	0.05
	ABT01-U	2.80	Hemipelagic mud	0.61	0.84	0.14	5.96	0.72	0.63	0.26	0.45	N.D.	0.46	0.08
	ABT01-L	2.50	Turbidite mud	0.49	1.59	0.33	3.95	0.43	0.72	0.31	0.44	N.D.	0.41	0.08

Table 3.3.3 Assignment of des-A TTs compounds in aliphatic and aromatic fractions labelled in Figs. 4 and 5, respectively.

	Trivial name	Formula	Molecular weight	Base peak (*m/z*)	Diagnostic fragment ions (*m/z*)			Retention Index #	RF	Ref.
					M^+	$M^+ - 15$	Second peak			
	Aliphatic compounds									
1	*Des*-A-bisnorhupane ?	$C_{22}H_{38}$	302	109	302	287	81	2219	0.564	--
2	Des-A-bisnorhupane ?	$C_{22}H_{38}$	302	109	302	287	81	2230	0.553	--
3	*Des*-A-oleanadiene	$C_{24}H_{38}$	326	326	326	311	173	2274	0.254	1
4	*Des*-E-D:C-friedohop-22(29)-ene	$C_{24}H_{40}$	328	313	328	313	231	2292	0.933	2
5	*Des*-E-D:C-friedohop-22(29)-ene	$C_{24}H_{40}$	328	313	328	313	231	2296	0.201	2
6	*Des*-A-olean-13(18)-ene	$C_{24}H_{40}$	328	109	328	313	313	2301	3.48	3, 4
7	*Des*-A-olean-12-ene	$C_{24}H_{40}$	328	218	328	313	205	2308	--	3, 4
8	*Des*-A-norursane ?	$C_{23}H_{40}$	316	177	316	301	109	2313	0.495	--
9	*Des*-A-urs-13(18)-ene	$C_{24}H_{40}$	328	313	328	313	177	2319	0.278	4, 5
10	*Des*-A-norhupane ?	$C_{23}H_{40}$	316	109	316	301	135	2326	0.412	--
11	*Des*-A-oleanadiene	$C_{24}H_{38}$	326	313	326	311	326	2332	0.253	1
12	*Des*-A-norhupane ?	$C_{23}H_{40}$	316	109	316	301	122	2344	0.759	--
13	*Des*-A-urs-12-ene	$C_{24}H_{40}$	328	313	328	313	95	2354	0.588	4
14	*Des*-A-oleanane	$C_{24}H_{42}$	330	191	330	315	109	2369	0.371	4, 6
15	*Des*-A-hupane	$C_{24}H_{42}$	330	123	330	315	109	2379	1.67	4, 5
16	*Des*-A-ursane	$C_{24}H_{42}$	330	109	330	315	191	2410	0.264	4, 6
17	*Des*-A-hupane isomer ?	$C_{24}H_{42}$	330	123	330	315	109	2423	0.539	--
18	*Des*-A-triterpane ?	$C_{24}H_{42}$	330	109	330	315	95	2456	0.252	--
	Aromatic compounds									
a	C-ring cleaved diaromatic *des*-A-oleanane	$C_{23}H_{30}$	306	187	306	291	308	2320	0.485	8, 9
b	Monoaromatic *des*-A-ursane / oleanane	$C_{23}H_{34}$	310	145	310	295	157	2352	0.372	--
c	Monoaromatic *des*-A-hupane	$C_{23}H_{34}$	310	295	310	295	157	2374	1.64	7
d	*Des*-E-D:C-friedo-25-norhopa-5-7-9-triene	$C_{23}H_{34}$	310	213	310	295	225	2391	0.620	2
e	*Des*-E-D:C-friedo-25-norhopa-5-7-9-triene	$C_{23}H_{34}$	310	213	310	295	225	2391	0.844	2
f	Diaromatic *des*-A-oleanane	$C_{22}H_{28}$	292	292	292	277	207	2402	0.637	7, 9
g	Diaromatic *des*-A-ursane	$C_{22}H_{28}$	292	207	292	277	292	2407	1.85	7, 9
h	Diaromatic *des*-A-hupane	$C_{22}H_{28}$	292	292	292	277	207	2424	3.10	7, 9
i	Triaromatic *des*-A-hupane	$C_{21}H_{22}$	274	231	274	259	215	2526	1.00	7, 9
j	Triaromatic *des*-A-ursane	$C_{21}H_{22}$	274	259	274	259	274	2566	2.32	7, 9
k	Triaromatic *des*-A-oleanane	$C_{21}H_{22}$	274	218	274	259	274	2588	0.493	7, 9

#: Retention index. See text.

*1: Level of identification; 1: Interpretation of mass spectral data, 2: The mass spectrum is identical to that was reported in references.

References for the identification; 1: Huang et al.(2008), 2: Hauke et al.(1993), 3: Logan and Eglington (1994), 4: Jacob et al.(2007), 5: van Bree et al.(2016), 6: Woolhouse et al.(1992), 7: Freeman et al.(1994), 8: de las Heras (1991), 9: Huang et al.(2013).

Table 3.3.4 Data of individual concentration of des-A TTs (des-E hopanoid, Oleanane type, Ursane type, Lupane type and unknown des-A TTs).

Sample No.	Depth	Lithology	TOC%	Aliphatic *des*-A TTs conc.										Aromatic *des*-A TTs conc.							
				des-E hopane type		Oneanana tyoe		Ursane tyoe		Lupane type		unknown		*des*-E hopane type		Oneanana tyoe		Ursane tyoe		Lupane type	
	(m)			(μg/g-rock)	(μg/mgC)	(μg/g-rock)	(μg/mgC)	(μg/g-rock)	(μg/mgC)	(μg/g-rock)	(μg/mgC)	(μg/g-rock)	(μg/mgC)	(μg/g-rock)	(μg/mgC)	(μg/g-rock)	(μg/mgC)	(μg/g-rock)	(μg/mgC)	(μg/g-rock)	(μg/mgC)
Somokumaisawa-gawa R.																					
SO11a-09U	32.00	Hemipelagic mud	0.52	0.065	0.013	0.24	0.045	0.13	0.024	0.58	0.11	–	–	0.064	0.012	0.34	0.066	0.044	0.0084	0.10	0.020
SO11a-09L	31.90	Turbidite mud	0.76	0.14	0.019	0.71	0.093	0.42	0.055	1.1	0.15	0.039	0.005	0.058	0.008	0.32	0.042	0.041	0.0054	0.094	0.012
SO11a-08U	29.00	Hemipelagic mud	1.77	0.15	0.0087	0.52	0.030	0.33	0.019	0.78	0.044	0.055	0.003	0.62	0.035	4.1	0.23	0.48	0.027	0.57	0.032
SO11a-08L	28.90	Turbidite mud	0.71	0.09	0.013	0.37	0.052	0.21	0.030	0.56	0.078	–	–	0.14	0.020	0.96	0.13	0.099	0.014	0.10	0.015
SO11-08U	27.50	Hemipelagic mud	0.73	0.12	0.017	0.48	0.065	0.16	0.022	0.60	0.082	–	–	0.88	0.12	5.1	0.70	0.60	0.082	0.69	0.095
SO11-08L	27.30	Turbidite mud	1.72	0.36	0.021	0.95	0.055	0.39	0.023	0.85	0.050	–	–	0.65	0.038	3.9	0.23	0.19	0.011	0.29	0.017
SO11a-07	23.90	Hemipelagic mud	0.57	0.11	0.019	0.37	0.065	0.36	0.063	0.49	0.085	0.042	0.007	0.17	0.030	1.8	0.31	–	–	0.38	0.067
SO11-06	22.30	Hemipelagic mud	0.69	0.11	0.016	0.41	0.060	0.15	0.022	0.51	0.074	–	–	0.21	0.030	0.78	0.11	–	–	0.18	0.027
SO11-05	19.10	Hemipelagic mud	0.59	0.10	0.018	0.36	0.062	0.16	0.028	0.43	0.073	–	–	0.16	0.028	0.92	0.16	0.020	0.0034	0.18	0.031
SO11-04	12.40	Hemipelagic mud	0.66	0.12	0.018	0.42	0.063	0.17	0.026	0.67	0.10	–	–	0.24	0.037	1.3	0.20	0.098	0.015	0.30	0.046
SO11-03	7.70	Hemipelagic mud	0.58	0.10	0.017	0.37	0.064	0.20	0.034	0.38	0.066	–	–	0.21	0.037	1.0	0.18	–	–	0.20	0.035
SO11-02	5.70	Hemipelagic mud	0.58	0.14	0.023	0.48	0.082	0.24	0.042	0.45	0.078	–	–	0.24	0.042	0.97	0.17	0.048	0.0083	0.089	0.015
SO11-01	2.95	Hemipelagic mud	0.70	0.11	0.015	0.56	0.079	0.29	0.042	0.68	0.097	–	–	0.17	0.024	0.63	0.090	0.021	0.0029	0.29	0.041
Horokanbesawa R.																					
NBT04	259.00	Hemipelagic mud	0.51	0.017	0.0033	0.12	0.023	0.014	0.0027	0.0087	0.0017	–	–	0.0088	0.0017	0.14	0.027	0.013	0.0025	0.028	0.0054
NBT03	236.00	Hemipelagic mud	0.73	0.039	0.0054	0.43	0.058	0.10	0.014	0.027	0.0037	–	–	0.015	0.0021	0.32	0.044	0.020	0.0027	0.049	0.0067
NBT02	215.00	Hemipelagic mud	0.49	0.0042	0.0009	0.084	0.017	0.023	0.0047	0.0066	0.0014	–	–	0.0074	0.0015	0.19	0.039	0.014	0.0028	0.046	0.0093
NBT01	213.00	Hemipelagic mud	0.69	0.041	0.0059	0.68	0.099	0.17	0.025	0.073	0.0106	–	–	0.011	0.0016	0.21	0.030	0.015	0.0022	0.046	0.0067
ABT08	116.00	Turbidite mud	0.63	0.032	0.0052	0.22	0.035	0.10	0.016	0.086	0.0136	0.0026	0.00042	0.0042	0.00066	0.059	0.009	0.021	0.0034	0.021	0.0033
ABT07	73.10	Turbidite mud	0.53	0.032	0.0061	0.094	0.018	0.021	0.0039	0.012	0.0022	0.0006	0.00012	0.0077	0.0015	0.13	0.024	0.043	0.0081	0.047	0.0088
ABT06	72.30	Hemipelagic mud	0.69	0.050	0.0072	0.24	0.034	0.081	0.012	0.029	0.0042	0.0012	0.00017	0.0043	0.00062	0.11	0.017	0.020	0.0029	0.053	0.0078
ABT05	67.00	Hemipelagic mud	0.69	0.027	0.0039	0.099	0.014	0.023	0.0033	0.033	0.0048	0.0012	0.00018	0.0038	0.00056	0.090	0.013	0.031	0.0046	0.031	0.0045
ABT04	58.80	Turbidite mud	0.67	0.012	0.0019	0.12	0.018	0.050	0.0074	0.044	0.0065	0.0008	0.00011	0.0042	0.00063	0.074	0.011	0.015	0.0022	0.022	0.0033
ABT03	57.00	Hemipelagic mud	0.72	0.023	0.0031	0.086	0.012	0.020	0.0027	0.012	0.0017	0.0005	0.00007	0.0063	0.00087	0.13	0.018	0.031	0.0043	0.035	0.0049
ABT02	49.20	Hemipelagic mud	0.65	0.012	0.0018	0.058	0.0089	0.011	0.0017	0.009	0.0013	–	–	0.0048	0.00073	0.13	0.020	0.033	0.0051	0.041	0.0063
ABT01-U	2.80	Hemipelagic mud	0.59	0.039	0.0067	0.16	0.027	0.060	0.010	0.022	0.0038	0.00047	0.00008	0.0053	0.00089	0.12	0.021	0.033	0.0055	0.061	0.010
ABT01-L	2.50	Turbidite mud	0.49	0.023	0.0046	0.093	0.019	0.044	0.0091	0.010	0.0020	0.00057	0.00012	0.0079	0.0016	0.16	0.033	0.038	0.0078	0.056	0.0114

Chapter.4. Summary and Conclusion

In this study, we analyzed organic matter in multiple event deposits and attempted to estimate the depositional processes, especially the transport, deposition, and sorting processes of organic matter in each event deposit, and examined methods for identifying event deposits from an organic geochemical perspective. Organic analysis of tsunami sediments from the eastern coast of Hokkaido, Japan.

We analyzed peat cores containing narrow tsunami sediments obtained at two sites in Akkeshi-town and Hamanaka-town Kiritappu area, and obtained the following findings. The kerogen composition of the tsunami sediments is consistent with the kerogen composition of the peat cores. The kerogen analysis of the tsunami sediments also showed a predominance of terrestrial higher plant-derived particles, but a few foraminiferal endosperms and dinoflagellate cysts were observed, strongly suggesting that the sand layers were formed by marine events. The redox (stanol/sterol ratio) using stanol, which is formed by microbial degradation of steroids in anoxic sedimentary environments, shows that the redox level in the sand layer tends to be higher for C27 steroids derived from coastal algae, and the difference with C29 steroids from terrestrial higher plants is also very large. This indicates that the tsunami transported marine and reducing organic matter from the ocean. Stanols /sterols from marine C27 steroids may provide an indicator of the effect of the tsunami on the formation of the sand layer. Triterpenoids, which are reduced components, show a characteristic tendency to increase in abundance in some sand layers, suggesting that they were transported by flood currents, but the trend is different in the Akkeshi core. The results of this study suggest that the triterpenoids were transported by the flood currents, but the results of the Akkeshi and Kiritappu cores show a different trend, which needs to be further investigated.

Samples of two typical turbidite sequences in the Kawabata Formation were analyzed by sedimentary unit and compared with the results of organic-rich sandstones reported by Furota et al.

In the analyzed turbidites, the terrestrial component is predominant in the organic-rich sedimentary unit corresponding to Tc, while the marine component tends to increase in the Ta (lower sandstone) and Td-E (upper fine-grained) sediments. Sedimentological and organic geochemical analyses were conducted on turbidite sequences of the Abetsu Formation deposited in the Hidaka Basin. Two different types of turbidite were classified into Thin/Thick OM laminations. Differences in the biomarker results may reflect the differences in sedimentary processes and may allow us to identify the origins of flood generating turbidity currents. These differences indicate that the terrigenous matter in the turbidites of the Abetsu Formation was transported from different type land area and/or different source vegetation to the deep sea. Declining triterpenoids show a high contribution throughout the sequence, suggesting possible transport by flooding, as shown by Furota et al.,2014.

Among the nodules in the Horokanbesawa nodule, the carbonate nodule contains a high percentage of ANME components, suggesting that it was formed by AOM. Among the polar fractions in the concretion (carbonate), the detection of polymeric components was lower than in the upper and lower layers, suggesting that selective fractionation may have occurred in the inflow of organic matter during concretion formation. In the Nibutani Formation, a reducing environment with ANME has existed throughout the middle Miocene, and the presence of methane-rich pore water may have been a factor in the formation of the carbonate concretion.

Alkenones were preserved 6-10Ma, no clear evidence of selective degradation of alkenone

Tectonic influence on the Haegawa outcrop is considered to be small, which may have contributed to the preservation of the alkenone-SST changing suggesting that the Hidaka sedimentary basin was influenced by both regions. Furthermore, ACL and SST showed a tendency to correlate after 6.5 Ma.

To examine the factors of variability in the degraded TTs abundances in marine turbidite sediments, we compared the degraded TTs / TOC ratios with several biomarker proxies such as the Paq, CPI, Pr/Ph, and C27/C29 sterane ratios in the mudstones from the Ishikari (Kawabata Formation) and Hidaka (Abetsu and Nibutani formations) basins. We found that the degraded TTs / TOC ratios are correlated with the Paq values in the Kawabata and Abetsu formations. The higher Paq values are interpreted to be high contribution of aquatic and submerge/floating macrophytes, and moreover, were commonly observed in lake and pond environments. The des-A TTs are formed from bio-TTs, which were derived from angiosperm leaf and bark. It therefore, is reasonable that the degraded TT abundances were closely linked to the Paq. Thus, large amounts of the degraded TTs were possibly produced by biodegradation of the transported angiospermous TTs in the dysoxic or anoxic environments such as ponds and wetlands. Furthermore, it is presumed that the organic matter deposited in the Ishikari basin was transported from wetland or marsh areas of the paleo-Hokkaido

According to the results of the degraded TTs, we comprehensively interpreted the paleoenvironments of the Ishikari and Hidaka basins These basins were thought to be formed by the arc-arc collision event and were explained as narrow and deep depressions. Therefore, many turbidites were deposited in the Abetsu and Kawabata formations with direct transport of large amounts of terrestrial plant materials by hyperpycnal flow and flood-related turbidity flow. The authors demonstrated that the floods might have accumulated terrigenous organic matter from wide areas, including marshes and wetlands, and transported these to the deep-sea floor in Ishikari and Hidaka basins during the middle Miocene. In the Ishikari basin, the remarkably large amounts of the degraded TTs imply that the lakes, ponds, marshes, and wetlands were widely distributed in hinterlands of the paleo-Hidaka Island, and the degraded TTs were efficiently formed in these areas.

Acknowledgements

First of all, I would like to thank Prof. Ken Sawada, Prof. Hideto Nakamura and Prof. Takeshi Kuritani (all of them in Hokkaido University) for reviewing this thesis and making a decision about my Ph.D research. Particularly, Prof. Sawada, who is my supervisor, helped me every time and finally gave me permission to prepare and submit this PhD thesis. I cannot thank Ken Sawada enough. And, I thank Mr. M.A.Ikeda and other members of our laboratory and group (5G) in Hokkaido University. Tsunami research used peat cores sampled by Dr. Gentaro Kawakami, Mr. Yoshihiro Kase and Keiichi. Hayashi in Hokkaido Research Organization (HRO), Prof. Yasuhiro Takashimizu and Prof. Atsushi Urabe in Niigata University. In the study of degraded triterpenoids, I used mudstone sampled by Dr. Kazuki Okano. Furthermore, Dr. Satoshi Furota (AIST/GSJ), Yoshihiro Kase (HRO) and Yuichi Nishimura (Hokkaido University) for their analytical supports and helpful comments. This study was supported by JST SPRING Grant Number JPMJSP2119. Finally, I express gratitude to my family for supporting my research life in Hokkaido University for nine years.

Reference

Alpar B., Ünlü S., Altınok Y., Özer N., Aksu A. (2012) New approaches in assessment of tsunami deposits in Dalaman (SW Turkey). *Natural Hazards* 60, 27–41.

Asahi H. and Sawada K. (2019) GC-MS analyses of ring degraded triterpenoids in event deposits. *Res. Org. Geochem.* **72**, 55–72.

Baas W.J. (1985) Naturally occurring seco-ring-A-triterpenoids and their possible biological significance. *Phytochemistry* 24, 1875–1889.

Bellanova P., Frenken M., Nishimura Y., Schwarzbauer J., Reicherter K. (2021) Tracing woody-organic tsunami deposits of the 2011 Tohoku-oki event in Misawa (Japan). *Scientific reports* 11, 8947.

Bellanova P., Frenken M., Reicherter K., Jaffe B., Szczuciński W. and Schwarzbauer, J. (2020) Anthropogenic pollutants and biomarkers for the identification of 2011 Tohoku-oki tsunami deposits (Japan). *Marine Geology* 422. 106117.

Beltran C., Flores A.J., Sicre A.M., Baudin F., Renard M. and de Rafelis M. (2011) Long chain alkenones in the Early Pliocene Sicilian sediments (Trubi Formation — Punta di Maiata section): Implications for the alkenone paleothermometry. *Paleogeography, Paleoclimatology, Paleoecology* **308** 253-263.

Bouma A. H. (1962) Sedimentology of Some Flysch Deposits. Elsevier, Amsterdam.

Bray E.E. and Evans D.E. (1961) Distribution of *n*-paraffins as a clue to recognition of source beds. *Geochim. Cosmochim. Acta* **22**, 2–15.

Chaffee A.L., Strachan G. and Johns R.B. (1984) Polycyclic aromatic hydrocarbons in Australian coals II. Novel tetracyclic components from Victorian brown coal. *Geochim. Cosmochim. Acta* 48, 2037–2043.

Chagué-Goff C., Andrew A., Szczuciński W., Goff J., Nishimura Y. (2012) Geochemical signatures up to the maximum inundation of the 2011 Tohoku-oki tsunami - Implications for the 869AD Jogan and other palaeotsunamis. *Sedimentary Geology* 282, 65–77.

Chagué-Goff C., Szczuciński W., Shinozaki T. (2017) Applications of geochemistry in tsunami research: A review. *Earth-Science Reviews* 165, 203–244.

Cleaveland C.L. and Herbert D.T. (2009) Preservation of the alkenone paleotemperature proxy in uplifted marine sequences: A test from the Vrica outcrop, Crotone, Italy. *Geology* **37**(2), 179-182.

Corbet B., Albrecht P. and Oqrisson G. (1980) Photochemical or photomimetic fossil triterpenoids in sediments and petroleum. *J. Am. Chem. Soc*. 102, 1171–1173.

de las Heras., Grimalt J. and Albaiges J. (1991) Novel C-ring cleaved triterpenoid-derived aromatic hydrocarbons in Tertiary brown coals. *Geochim. Cosmochim. Acta*. 55, 3379–3385.

Del Rio J.C., Gonzalez-Vila F.J. and Martin F. (1992) Variation in the content and distribution of biomarkers in two closely situated peat and lignite deposits. *Org. Geochem*. 18, 67–78.

Dowsett J.H., Robinson M.M., Foley M.K and Herbert D.T. (2021) The Yorktown Formation: Improved Stratigraphy, Chronology, and Paleoclimate Interpretations from the U.S. Mid-Atlantic Coastal Plain. *Geoscience* **11**, 486.

Farrimond P., Taylor A., Telnes, N. (1998) Biomarker maturity parameters: The role of generation and

thermal degradation. *Org. Geochem*. 29, 1181–1197.

Ficken K.J., Li B., Swain D.L., Eglinton G. (2000) An n-alkane proxy for the sedimentary input of submerged/floating freshwater aquatic macrophytes. *Org. Geochem*. 31, 745–749.

Freeman K.H., Boreham C.J., Summons R.E. and Hayes J.M. (1994) The effect of aromatization on the isotopic compositions of hydrocarbons during early diagenesis, *Org. Geochem*. 21, 1037-1049.

Furota S., Sawada K. and Kawakami G. (2014) Evaluation of sedimentary processes of plant particles by gravity flow using biomarkers in plant fragment-concentrated sediments of a turbiditic sequence in the Miocene Kawabata Formation distributed along the Higashiyama-gawa River, Yubari, Hokkaido, Japan. *Res. Org. Geochem*. 30, 9–21.

Furota S., Sawada K. and Kawakami G. (2021) Depositional processes of plant fragment-concentrated sandstones in turbiditic sequences recorded by plant biomarkers (Miocene Kawabata Formation, Japan). *Int. J. Coal Geol.* **233**.

Hage S., Galy V. V., Cartigny M.J.B., Acikalin S., Clare M.A., Gröcke D.R., Hilton R.G., Hunt J.E., Lintern D.G., Mcghee C.A., Parsons D.R., Stacey C.D., Sumner E.J. and Talling P.J. (2020) Efficient preservation of young terrestrial organic carbon in sandy turbidity-current deposits. *Geology* **48**, 882–887.

Hanagata S. and Hiramatsu C.(2005) Miocene-Pliocene Foraminifera from the subsurface sections in the Yufutsu Oil and Gas Field, Hokkaido. *Paleontological Research* **9**(4), 273-298.

Hauke V., Graff R., Wehrung P., Hussler G., Trendel J.M., Albrecht P., Riva A. and Connan J. (1993) Rearranged *des*-E-hopanoid hydrocarbons in sediments and petroleum. *Org. Geochem.* **20**, 415–423.

He D., Simoneit B.R.T., Cloutier J.B. and Jaffé R. (2018) Early diagenesis of triterpenoids derived from mangroves in a subtropical estuary. *Org. Geochem*. **125**, 196–211.

Hedges J.I. and Keil R.G. (1995) Sedimentary organic matter preservation: an assessment and speculative synthesis. *Mar. Chem.* **49**, 81–115.

Hoefs M.J.L., Rijpstra W.I.C., Sinninghe Damsté J.S. (2002) The influence of oxic degradation on the sedimentary biomarker record I: Evidence from Madeira Abyssal Plain turbidites. *Geochim. Cosmochim. Acta* **66**, 2719–2735.

Hong X., Tie-Guan W., Meijun L., Jian F., Youjun T., Shengbao S., Zhe Y. and Xiaolin Lu. (2018) Occurrence and Distribution of Unusual Tri- and Tetracyclic Terpanes and Their Geochemical Significance in Some Paleogene Oils from China. *Energy&fuel*. 32, 7393-7403.

Hoyanagi K. (1989) Coarse-grained turbidite sedimentation resulting from the Miocene collision event in central Hokkaido, Japan. *Sedimentary Facies in the Active Plate Margin* (Taira, A. and Masuda, F., eds.), 689–709, TERRAPUB, Tokyo.

Huang X., Xie S., Zhang C.L., Jiao D., Huang J., Yu J., Jin F. and Gu Y. (2008) Distribution of aliphatic *des*-A-triterpenoids in the Dajiuhu peat deposit, southern China. *Org. Geochem.* **39**, 1763–1769.

Huang X., Xue J., Wang X. and Meyers P.A. (2013) Paleoclimate influence on early diagenesis of plant triterpenes in the Dajiuhu peatland, central China. *Geochim. Cosmochim. Acta*. 123, 106–119.

Iijima A. and Tada R. (1990) Evolution of Tertiary sedimentary basins of Japan in reference to opening of the

Japan Sea. *Journal of the faculty of Science* **22**(2), 121-171.

Ioki K and Tanioka Y. (2016) Re-estimated fault model of the 17th century great earthquake off Hokkaido using tsunami deposit data. *Earth and Planetary Science Letters* 433, 133-138.

Jacob J., Disnar J., Boussafir M Albuquerque, ALS Sifeddine, A. and Turcq, B. (2007) Contrasted distributions of triterpene derivatives in the sediments of Lake Caco reflect paleoenvironmental changes during the last 20,000 yrs in NE Brazil. *Org. Geochem*. 38, 180–197.

Jaffé R., Elismé T. and Cabrera A.C. (1996) Organic geochemistry of seasonally flooded rain forest soils: Molecular composition and early diagenesis of lipid components. *Org. Geochem*. 25, 9–17.

Kajita H., Maeda A., Utsunomiya M., Yoshimura T., Ohkouchi N., Suzuki A. and Kawahata H. (2021) Biomarkers in the rock outcrop of the Kazusa Group reveal palaeoenvironments of the Kuroshio region. *Nature Communications Earth&Environment* **2,** 82.

Kase Y., Nishina K., Kawakami G., Hayashi K., Takashimizu Y., Hirose W., Sagayama T., Takahashi R., Watanabe T., Koshimizu K., Tajika J., Ohtsu S., Urabe A., Okazaki N., Fukami H., Ishimaru S. (2016) Tsunami deposits recognized in Okushiri Island, southwestern Hokkaido, Japan. *The Journal of the Geological Society of Japan* 122, 587–602.

Kase Y., Kawakami G. and Takano O. (2018) Depositional systems and petroleum geology of the Middle-Late Mioceneforeland basin deposits in the Hidaka coast area, central Hokkaido, Japan. J*our.Geol. Sci. Japan* **124**, 627-642

Kawakami G. (2013) Foreland basins at the Miocene arc-arc junction, central Hokkaido, northern Japan, In: Itoh, Y. (Ed.), Mechanism of sedimentary basin formation - Multidisciplinary approach on active plate margins. *InTech*. pp. 131–152.

Kawakami G., Arita K., Okada T., Itaya T. (2004) Early exhumation of the collisional orogen and concurrent infill offoredeep basins in the Miocene Eurasian –Okhotsk Plate boundary, central Hokkaido, Japan: Inferences from K-Ar dating of granitoid clasts. *Island Arc* **13**, 359–369.

Kawakami G., Shiono M., Kawamura M., Urabe A. and Koizumi I. (2002) Stratigraphy and depositional age of the Miocene Kawabata Formation, Yubari Mountains, central Hokkaido, Japan. *Jour. Geol. Soc. Japan* **108**, 186–200.

Kimura G. (1996) Collision orogeny at arc-arc junctions in the Japanese Islands. *Island Arc* **5**, 262–275.

Konechnaya O., Bellanova P., Frenken M., Reicherter K., Schwarzbauer J. (2022) Evaluation of organic indicators derived from extractable, hydrolysable and macromolecular organic matter in sedimentary tsunami deposits. *Marine Geology* 443. 106671.

Laurier F.J.G., Cossa D., Gonzalez J.L., Breviere E., Sarazin G.(2003) Mercury transformations and exchanges in a high turbidity estuary: The role of organic matter and amorphous oxyhydroxides. *Geochimica et Cosmochimica Acta.* **67**, 3329–3345.

Lina J., Xin S., Xuefa S., Marco F., Shuqing Q., Selvaraj K., Huawei W., Shengfa L., Xisheng F. and Xinqing Z. (2021) Hybrid event beds generated by erosional bulking of modern hyperpycnal flows on the Choshui River delta front, Taiwan Strait. *Sedimentology* **68**, 2500-2522.

Logan G.A.and Eglinton G.(1994) Biogeochemistry of the Miocene Lacustrine Deposit, Clarkia, Northern

Idaho, U.S.A. *Org. Geochem*. **21**, 857–870.

Lohmann F., Trendel J., Hetru, C., Albrecht, P.(1990) C-29 tritiated β-amyrin: Chemical synthesis aiming at the study of aromatization processes in sediments. *Journal of Labelled Compounds and Radiopharmaceuticals.* **28**, 377–386.

Lopes A.A., Pereira V.B., Amoranogueira L., Marotta H., Moreira L.S., Cordeiro R.C., Vanini G. and Azevedo D.A. (2021) Hydrocarbon sedimentary organic matter composition from different water-type floodplain lakes in the Brazilian Amazon. *Org. Geochem.* **159**, 104287.

Mille G., Guiliano M., Asia L., Malleret L. and Jalaluddin N.(2006) Sources of hydrocarbons in sediments of the Bay of Fort de France (Martinique). *Chemosphere.* **64**, 1062–1073.

Mathes-Schmidt M., Schwarzbauer J., Papanikolaou I., Syberberg F., Thiele A., Wittkopp F. and Reicherter K. (2013) Geochemical and micropaleontological investigations of tsunamigenic layers along the Thracian Coast (Northern Aegean Sea, Greece). *Zeitschrift fur Geomorphologie* **57**, 5–27.

Matsuzaki M. K., Itaki T., Tada R. and Kamikuri S. (2018) Paleoceanographic history of the Japan Sea over the last 9.5 million years inferred from radiolarian assemblages (IODP Expedition 346 Sites U1425 and U1430). *Progress in Earth and Planetary Science* **5**, 54.

Matsuzaki M K., Suzuki N. and Tada R. (2020) An intensified East Asian winter monsoon in the Japan Sea between 7.9 and 6.6 Ma. *Geology* **48**(9), 919-923.

Méjanelle L., Rivièrea B., Pinturier L., Khripounoff A., Baudin F., Dachs J. (2017) Aliphatic hydrocarbons and triterpenes of the Congo deep-sea fan. *Deep-Sea Research Part II* **142**, 109–124.

Milliman J.D. and Kao S.J. (2005) Hyperpycnal Discharge of Fluvial Sediment to the Ocean: Impact of Super-Typhoon Herb (1996) on Taiwanese Rivers. The Journal of Geology **113**, 503-516**.**

Miyajima Y., Watanabe Y., Goto S.A., Jenkins G.R., Sakai S., Matsumoto R., and Hasegawa T. (2020) Archaeal lipid biomarker as a tool to constrain the origin of methane at ancient methane seeps: Insight into subsurface fluid flow in the geological past. *Journal of Asian Earth Science*. **189**, 104134.

Mulder T., Migeon S., Savoye B. and Faugeres J.C. (2001) Inversely graded turbidite sequences in the deep Mediterranean: a record of deposits from flood-generated turbidity currents? *Geo-Marine Letters* **21**, 86-93.

Mulder T., Zaragosi S.,Jouanneau J.M., Bellaiche G., Guerinaud S. and Querneau J. (2009) Deposits related to the failture of the Malpasset Dam in 1959 An analogue for hyperpycnal deposits from jokulhlaups. *Marine Geology*. **260**, 81-89.

Nakakuni M., Dairiki C., Kaur G. and Yamamoto S. (2017a) Organic Geochemistry Stanol to sterol ratios in late Quaternary sediments from southern California : An indicator for continuous variability of the oxygen minimum zone. *Org. Geochem*. **111**, 126–135.

Nakakuni M., Takehara K. and Nakatomi N. (2017b) Sterol and stanol compositions in sediments from the Bungaku-no-ike pond , Tokyo , Japan : Examination of stanol sources. *Res. Org. Geochem.* **16**, 7–16.

Nanayama F., Furukawa, R., Shigeno, K., Makino, A., Soeda, Y., Igarashi, Y. (2007) Nine unusually large tsunami deposits from the past 4000 years at Kiritappu marsh along the southern Kuril Trench. *Sedimentary Geology* **200**, 275–294.

Nanayama F., Satake K., Furukawa R., Shimokawa K., Atwater B.F., Shigeno K., Yamaki S. (2003) Unusually large earthquakes inferred from tsunami deposits along the Kurile trench. *Nature* **424**, 660–663.

Nishimura M., Koyama T. (1977) The occurrence of stanols in various living organisms and the behavior of sterols in contemporary sediments. *Geochim. Cosmochim. Acta* **41**, 379–385.

Okano K. and Sawada K. (2008) Heterogeneities of hydrocarbon compositions in mudstones of a turbiditic sequence of the Miocene Kawabata Formation in Yubari, central Hokkaido, Japan. *Geochem. J.* **42**, 151–162.

Prahl G. F. and Wakeham G.S. (1987) Calibration of unsaturation patterns in long-chain ketone compositions for palaeotemperature assessment. *Nature* **330**(26), 367-369.

Prahl G. F., Muehlhausen A.L and Zahnle L.D. (1988) Further evaluation of long-chain alkenones as indicators of paleoceanographic conditions. *Geochem.Cosmochim Acta* **52,** 2303-2310.

Pruski A.M., Stetten E., Huguet A., Vétion G., Wang, H., Senyarich, C., Baudin, F.(2022) Fatty acid biomarkers as indicators of organic matter origin and processes in recent turbidites: The case of the terminal lobe complex of the Congo deep-sea fan. *Org. Geochem*. **173**, 104484.

Regnery J., Püttmann W., Koutsodendris A., Mulch A. and Pross J. (2013) Comparison of the paleoclimatic significance of higher land plant biomarker concentrations and pollen data: A case study of lake sediments from the Holsteinian interglacial. *Org. Geochem*. **61**, 73–84.

Riboulleau A., Schnyder J., Riquier L. and Lefebvre V. (2007) Environmental change during the Early Cretaceous in the Purbeck-type Durlston Bay section (Dorset , Southern England) : A biomarker approach. *Org. Geochem*. **38**, 1804–1823.

Saitoh Y., Tamura T. and Masuda F. (2005) Characteristics of Hyperpycnal Flow and its Deposits as an innovative factor for the turbidite paradigm. *Journal of Geography* **114**(5). 687-704.

Sawada K., Handa N. Shiraiwa Y. Danbara A. and Montani S. (1996) Long-chain alkenones and alkyl alkenoates in the coastal and pelagic sediments of the northwest North Pacific, with special reference to the reconstruction of Emiliania huxleyi and Gephyrocapsa oceanica ratios. *Org.Geochem*. **24**(8/9), 751-764.

Sawada K., 2006. Organic facies and geochemical aspects in Neogene neritic sediments of the Takafu syncline area of central Japan: Paleoenvironmental and sedimentological reconstructions. *Island Arc* **15**, 517–536.

Sawada K., Kaiho K., Okano K., 2012. Kerogen morphology and geochemistry at the Permian-Triassic transition in the Meishan section, South China: Implication for paleoenvironmental variation. *Journal of Asian Earth Sciences* **54–55**, 78–90.

Sawada K., Nakamura H., Arai T. and Tsukagoshi M. (2013) Evaluation of paleoenvironment using terpenoid biomarkers in lignites and plant fossil from the Miocene Tokiguchi Porcelain Clay Formation at the Onada mine, Tajimi, central Japan. *Int. J. Coal Geol*. **107**, 78–89.

Selvaraj K., Lee T.Y., Yang J.Y.T., Canuel E.A., Huang J.C., Dai M., Liu J.T., Kao S.J. (2015) Stable isotopic and biomarker evidence of terrigenous organic matter export to the deep sea during tropical storms.

Marine Geology. **364**, 32–42.

Shigeno K., Nanayama F., Sudo Y., Sagayama T., Hasegawa T., Ando H. (2013) Reconstructed Holocene sea level curve from the Akkeshi barrier system in eastern Hokkaido, Japan. *The Journal of the Geological Society of Japan* **119**, 171–189.

Shinozaki T., Fujino S., Ikehara M., Sawa, Y., Tamura T., Goto K., Sugawara D., Abe T. (2015) Marine biomarkers deposited on coastal land by the 2011 Tohoku-Oki tsunami. *Natural Hazards* **77**, 445–460.

Shinozaki T., Sawai Y., Hara J., Ikehara M., Matsumoto D., Tanigawa K. (2016) Geochemical characteristics of deposits from the 2011 Tohoku-Oki tsunami at Hasunuma, Kujukuri coastal plain, Japan. *Island Arc* **25**, 350–368.

Shinzawa M., Kamikuri S., Motoyama I. (2009) Radiolarian fossils from the Miocene Series in the Hobetsu area, southern central Hokkaido, Japan. News of Osaka Micropaleontologists, Special volume, 117–141 (in Japanese with English abstract).

Simoneit B.R.T. (2005) A review of current applications of mass spectrometry for biomarker / molecular. *Mass Spectr. Rev*. **24**, 719–765.

Simoneit B.R.T., Xu Y., Neto R.R., Cloutier J.B. and Jaffé R. (2009) Chemosphere Photochemical alteration of 3-oxygenated triterpenoids : Implications for the origin of 3, 4-seco-triterpenoids in sediments. *Chemosphere* **74**, 543–550.

Soeda Y., Nanayama F., Shigeno K., Furukawa R., Kumasaki N., Tsutsumi Y., Kurumazuka H., Sawai Y., Satake K., Nakagawa M., Yamada G., Katsuragawa M., Akamatsu M., Ishii M., Tsukuda E., Sugiyama Y. (2003) Nine tsunami sand deposits in peat layers at the historic site of Kokutaiji Temple in Akkeshi Town, eastern Hokkaido, and their correlation with regional tsunami events. *Annual Report on Active Fault and Paleoearthquake Researches* **3**, 285–296.

Stancliffe R.P.W., Matsuoka K. (1991) Marine palynomorphs found in Holocene sediments off the coast of northwestern Kyushu, Japan. Bulletin of the Faculty of Liberal Arts, Nagasaki University. *Natural Science* **31**, 661–681.

Stefanova M., Ivanov D., Yaneva N., Marinov S., Grasset L. and Amblès A.(2008) Palaeoenvironment assessment of Pliocene Lom lignite (Bulgaria) from bitumen analysis and preparative off line thermochemolysis. *Org. Geochem.* **39**, 1589–1605.

Stefanova M., Ivanov D.A., Utescher T.(2011) Geochemical appraisal of palaeovegetation and climate oscillation in the Late Miocene of Western Bulgaria. *Org. Geochem.* **42**, 1363–1374.

Summons R.E., Volkman J.K., Boreham C.J. (1987) Dinosterane and other steroidal hydrocarbons of dinoflagellate origin in sediments and petroleum. *Geochim. Cosmochim. Acta* **51**, 3075–3082.

Szczuciński W., Pawłowska J., Lejzerowicz F., Nishimura Y., Kokociński M., Majewski W., Nakamura Yugo. and Pawlowski J. (2016) Ancient sedimentary DNA reveals past tsunami deposits. *Marine Geology* **381**, 29-33.

ten Haven H.L., Peakman T.M. and Tter J.R. (1992) Early diagenetic transformation of higher-plant triterpenoids in deep-sea sediments from Baffin Bay. *Geochim. Cosmochim. Acta*. **56**, 2001–2024.

Thomsen C., Blaume F., Fohrmann H., Peeken I., Zeller U.(2001) Particle transport processes at slope

environments - Event driven flux across the Barents Sea continental margin. *Marine Geology.* **175**, 237–250.

Treignier C., Derenne S., Saliot A.(2006) Terrestrial and marine n-alcohol inputs and degradation processes relating to a sudden turbidity current in the Zaire canyon. *Org. Geochem.* **37**, 1170–1184.

Trendel J.M., Lohmann F., Kintzinger J.P., Albrecht P., Chiarone A., Riche C., Cesario M., Guilhem J., Pascard C.(1989) Identification of des-A-triterpenoid hydrocarbons occurring in surface sediments. *Tetrahedron*. **45**, 4457–4470.

Tsubakihara S. (1990) Stratigraphy and depositional environments of upper Cenozoic sediments in Kuriyama and Kurisawa towns in the eastern marginal area of the Ishikari Lowland, Hokkaido, Japan. *Chikyu Kagaku (Earth Science)* **44**, 263-278 (In Japanese with English abstract).

Van Aarssen, B.G.K., Alexander, R., Kagi, R.I.(2000) Higher plant biomarkers reflect palaeovegetation changes during Jurassic times. *Geochim. Cosmochim. Acta*. **64**, 1417–1424.

van Bree L.G.J., Islam M.M., Rijpstra W.I.C., Verschuren D., van Duin A.C.T., Sinninghe Damsté J.S. and de Leeuw J.W. (2018) Origin, formation and environmental significance of des-A-arborenes in the sediments of an East African crater lake. *Org. Geochem.* **125**, 95–108.

van Bree L.G.J. Rijpstra W.I.C., Al-Dhabi N.A., Verschuren D., Sinninghe Damsté J.S. and de Leeuw J.W. (2016) Des-A-lupane in an East African lake sedimentary record as a new proxy for the stable carbon isotopic composition of C3 plants. *Org. Geochem.* **101**, 132–139.

Venkatesan M. I. (1988) Organic geochemistry of marine sediments in Antarctic region: Marine lipids of McMurdo Sound. *Org. Geochem*. **12**, 13–27.

Venkatesan M. I. and Kaplan I. R. (1982) Distribution and transport of hydrocarbons in surface sediments of the Alaska continental shelf. *Geochim. Cosmochim. Acta* **46**, 2135–2149.

Volkman J.K., Barrerr M.S. Blackburn I.S. and Sikes L.E. (1995) Alkenones in Gephyrocapsa oceanica: Implications for studies of paleoclimate. *Geochem.Cosmochim.Acta* **59**(3), 513-520.

Volkman J.K. (2005) Sterols and other triterpenoids: source specificity and evolution of biosynthetic pathways. *Org. Geochem*. **36**, 139–159.

Wakeham S.G.(1989) Reduction of stenols to stanols in particulate matter at oxic-anoxic boundaries in sea water. *Nature* **342**, 787–790.

Wakeham S.G., Beier, J.A. (1991) Fatty acid and sterol biomarkers as indicators of particulate matter source and alteration processes in the Black Sea. *Deep-Sea Research, Part A* **38**, 943–968.

Woolhouse A.D., Oung J.-N., Philp R.P. and Weston, R.J. (1992) Triterpanes and ring-A degraded triterpanes as biomarkers characteristic of Tertiary oils derived from predominantly higher plant sources. *Org. Geochem*. **18**, 23–31.

Wyrzykiewicz E., Wrzeciono U., and Zaprutko L. (1989) Tri- terpenoids, Part IV. Mass spectrome.try of pentacyclic triterpenoids: 18β- and 18α-11-oxooleanolic acid derivatives. *Org. Mass Spec*. **24**, 105-108.

Yoshida M., Yoshiuchi Y., Hoyanagi K.(2009) Occurrence conditions of hyperpycnal flows, and their significance for organic-matter sedimentation in a Holocene estuary, Niigata Plain, Central Japan. *Island Arc*. **18**, 320–332.

Zavala C., Arcuri M., and Blanco V. L. (2012) The importance of plant remains as diagnostic criteria for the recognition of ancient hyperpycnites. *Revue de Paléobiologie*, Genève, Special Volume 11, 457–469.

Zavala C. and Arcuri M.(2016) Intrabasinal and extrabasinal turbidites : Origin and distinctive characteristics. *Sedimentary Geology*. **337**, 36–54.

Zheng Y., Zhou W., Liu Z., Chen Q., Yu X. and Liu X. (2010) Compositions of aliphatic des-A-triterpenes in the Hani peat deposit, Northeast China and its biological significance. *Chinese Sci. Bull*. **55**, 2275–2281.

Zhang Z., Zhao M., Yang X., Wang S., Jiang X., Oldfield F. and Eglinton G. (2004) A hydrocarbon biomarker record for the last 40 kyr of plant input to Lake Heqing, southwestern China. *Org. Geochem*. **35**, 595–613.